DAM BREACH MODELING and INUDATION MAPPING A CASE STUDY OF JEMA DAM, ABAY BASIN, ETHIOPIA

M.Sc. THESIS

AMDEMARIAM SHIFERIE MULU

HAWASSA, ETHIOPIA

MAY, 2018

DAM BREACH MODELING AND INUDATION MAPPING A CASE STUDY OF JEMA DAM, ABAY BASIN, ETHIOPIA

AMDEMARIAM SHIFERIE MULU

A THESIS SUBMITTED TO THE

DEPARTMENT OF WATER RESOURCE ENGINEERING AND MANAGEMENT

INSTITUTE OF TECHNOLOGY, SCHOOL OF

GRADUATE STUDIES

HAWASSA UNIVERSITY

HAWASSA, ETHIOPIA

IN PARTIAL FULFILLMENT OF THE

REQUIREMENTS FOR THE

DEGREE OF

MASTER OF SCIENCE IN WATER RESOURCES ENGINEERING AND MANAGEMENT

MAY, 2018

APPROVAL SHEET

As Thesis research advisor, we hereby certify that we have read and evaluated this thesis prepared under our guidance by AMDEMARIAM SHIFERIE entitled

Dam Breach Modeling and Inundation Mapping a Case Study of Jema Dam, Abay Basin, Ethiopia

We recommend that it be submitted as fulfillment of the thesis requirement.

________________	____________	___________
Major Advisor	Signature	Date
________________	____________	___________
Co-advisor	Signature	Date

As member of the Board of Examiners of the final open defense by **AMDEMARIAM SHIFERIE**, have read and evaluated his thesis entitled ***Dam Breach Modeling and Inundation Mapping a Case Study of Jema Dam, Abay Basin, Ethiopia*** and examined the candidate. Therefore, I certify that the thesis is accepted in partial fulfillment of the requirement for the Degree of Master of Science in Water Resources Engineering and Management.

________________	____________	___________
Chairperson	Signature	Date
________________	____________	___________
Internal Examiner	Signature	Date
________________	____________	___________
External Examiner	Signature	Date

Acknowledgement

It is a pleasure to convey my gratitude to those who helped me in making this thesis.

First I would like to thank God for being the source of my strength, Joy and success. My gratitude also goes to Dr. Moltot Zewdie for keeping me on track to finish my study. I am also sincerely grateful for staff members of Ethiopian Construction Design and Supervision Works Corporation, Especially Ato Desta, Ato Fisha, Ato Tesfa ,Ato Abdulawol ,AtoYared and W/o Amarech for giving me helpful information to finish this thesis.

My parents deserve special mention for their support and prayers. My father Shiferie Mulu and my mother Zewditu Mamay deserve special mention for showing me the joy of intellectual pursuit ever since I was a child. My deepest gratitude also goes to the rest of my family and friends for their endless support and care.

Declaration

I, **Amdemariam Shiferie**, declare that the thesis which I hereby submit for the "**Degree Of Master Of Science In Water Resource Engineering And Management At The University Of Hawassa"** is my own work and has not previously been submitted and will not be submitted by me for a degree at this or any other institution. To the best of my knowledge and belief, except as acknowledged in the text, the thesis does not contain any written work presented by other persons whether pictures, graphs or data or any other. I also declare that I have complied with the rules, requirements, procedures, and policy of the university.

Student signature: ______________________

Date: May 2018.

Dedication

I dedicate this thesis work to my father Shiferie Mulu and my mother Zewditu Mamay

Abbreviations

ASCE	American Society of Civil Engineers
DEM	Digital Elevation Model
DRO	Direct Runoff Hydrograph Ordinates
EAPs	Emergency Action Plan
ECDSWC	Ethiopian Construction Design and Supervision Works Corporation
EMA	Ethiopian Mapping Agency
FEMA	Federal Emergency Management Agency
G-B	Grubbs and Beck
GIS	Geographical Information System
HEC Geo HMS	Hydrologic Engineering Center- Geospatial Hydrologic Modeling System
HEC-Geo-RAS	Hydrologic Engineering Center - Geographic River Analysis System
HEC-RAS	Hydrologic Engineering Center - River Analysis System
ICOLD	International Committee on Large Dams
IDF	Inflow Design Flood
Masl	Mean above Sea Level
MCM	Million Cubic Meter
MoWIE	Ministry of Water, Irrigation and Energy
M-W	Mann-Whitney
PMF	Probable Maximum Flood
PMP-	Probable Maximum Precipitation
SDF	Spatial Data Format
SDF	Spillway Design Flood
UH	Unit Hydrograph

UTM	Universal Transverse Mercator
WMO	World Meteorological Organization
WWDSE	Water Works Design and Supervision Enterprise
W-W	Wald-Wolfowitz
XML	eXtensible Markup Language

Table of Contents

List of Tables

List of Figures

List of Tables in the Appendices

List of Figure in Appendices

Abstract

Preparing dam safety plans and hazard management strategies are unquestionably vital, since lots of human lives have been lost and tremendous amount of economic crisis have been recorded from dam failure events throughout the world in history. Setting out risk management, emergency action plans or evacuation planning system to protect both lives and materials during sudden dam failure phenomena and resulting flood waves is highly essential. This thesis analyzed the probable failure of a dam under a set of pre-defined scenarios, within the framework of a case study, the case subject being the Jema dam located at Amhara Region of Ethiopia. A probable maximum flood of Gilgel Abay river (tributary of Jema River) has been computed using Hershfield's technique .Breach parameters prediction, peak outflow hydrograph were determined by HEC-RAS model based on available technical and geometric data. Different maps such as flood areal extent map, flood depth map and velocity map have been produced by HEC-GeoRAS. The worst scenario was found to be scenario three (when Jema dam failed by overtopping with PMF of Gilgel Abay River). Probable maximum flood of Gilgel Abay river by Hershfield's technique was found to be 1726.28 m^3/s. The maximum breach discharge resulted from HEC-RAS model was 79,886.37m3/sec and the maximum area inundated by this flood in downstream was found to be 41.6km^2. The areal maps show that the part of command area at right side and farm in left side, Bikolo Abay Town and settlement villages to be prone to flooding. The depth and velocity of flood also depict that the downstream rural village near the river bank are under extreme hazard category and the maps reveals that Jema dam is categorized under high hazed dam.

Key words: Dam Breach, Flood Inundation Mapping, HEC-RAS, HEC –GeoRAS.

1. INTRODUCTION

1.1. General Background

The term dam breach analysis usually relates to the process of studying a dam failure phenomenon and analyzing the resulting consequences at downstream region. Dam break analysis generally deals with simulation of probable failure for existing dams and analyzing the resulting consequences (Pandya, Dixitsinh Jitaji, 2013). Dam break modeling is typically done within a larger study context that develops inflow hydrographs from various frequency storms, evaluates project spillway adequacy, estimates breach parameters, and performs routing and mapping of the resultant flood . As land pressures for human settlement and development into down land region increase, the risk of human fatality and damage to assets and infrastructure from the rapid failure of large stream blocking events (dams) increase.

The dam break can be triggered by overtopping, piping or foundation failure depending on the type of dam, its constituent construction materials, hydrodynamic movements in the reservoir and/or on the dam, magnitude of inflow, performance of the dam and its appurtenance structures, operation of gates on times of peak floods and many more. Therefore, the dam break analysis should consider these factors

In the event of failure of a dam by overtopping /or piping, a breach is formed on the dam hull, which gradually expands in terms of hours or even minutes. The water stored behind the reservoir is then set free uncontrollably in great amounts and causes damage along its route in great proportions. A flood caused by a dam breach may be much larger in magnitude and behave much differently than a natural flood (Asburry and Goodell, 2009). In the absence of preemptive measures geared towards such a risk, such as an emergency action plan, settlements and the properties located downstream of the dam and on the route of such a dam failure flood are put to great risk. Dam break analyses provide information on the consequences of a possible dam failure for risk estimation and rescue planning purposes. The development of effective emergency action plans and the design of early warning systems heavily rely on prediction results (Zagonjolli, 2007)

Dams are an important hydraulic structure, providing flood control, water supply, irrigation, hydropower, navigation, and recreation benefits. Despite their many beneficial uses and value, dams also present risks to property and life due to their potential to fail and cause catastrophic flooding. To mitigate these risks, dam owners and regulators carefully analyze and inspect dams to identify potential failure modes and protect against them. Since no program for preventing failure can ever be certain, and because the potential for loadings exceeding design limits can never be eliminated, another essential part of risk mitigation is simulating potential failures and planning for them. These plans can include public education programs, development of warning systems and procedures, and development of effective evacuation procedures. Simulations of dam failure and flooding consequences can also be used by dam owners to prioritize the risks presented by individual dams comprising a dam inventory. This prioritization process facilitates the effective use of financial and human resources to improve public safety and reduce dam failure risk.

When dams fail, property damage is certain, but loss of life can vary dramatically with the extent of the inundation area, the size of the population at risk, and the amount of warning time available. It is obvious that the average number of fatalities per dam failure is greater when there is inadequate or no warning.

In Ethiopia construction of dams is increasing both in number and type, ranging from small micro earth dams constructed to fulfill community demands such as food and water supply to mega projects as that of the Grand Ethiopian Renaissance Dam (GERD), being implemented to boost the nation’s economy.

Jema dam is one of the embankment dams planned to impounding water for irrigation purpose. The dam is a rock fill type dam with impervious clay core at the middle covered by adjacent transition fill material and sand filters on both sides with a purpose of preventing finer materials from migration (WWDSE, 2010).

1.2. Statement of the Problem

The safety of dam cannot be secured only with provision of sufficient discharging capacity of the spillway or adequate hydraulic design of the whole dam because with all the necessary arrangements made still extreme cases like dam breaching should be expected and this thesis is intended for such severe case. Breach analysis should be done for any dam in every certain period of time.

In Ethiopia construction of dams has boosted in recent years that many large dams have been built and numerous are under construction and planned. Following the establishment of dams, the downstream ecosystem is highly changed that huge area is covered with irrigation farms, new settlements and residence areas of inhabitants living on the farms will formed. All these investments and newly settled inhabitants are highly exposed to flooding and are at risk for damage and death respectively. Like most other dams in Ethiopia, dam break analysis for Jema dam is not studied yet. At downstream of Jema dam there are so many rural villages, Bikolo Abay Town and command area with irrigation structures are prone to the flood. Therefore it is apparent that a pre event analysis on Jema dam break and assessing the possible risk is crucial.

1.3. Objectives of the Study

1.3.1. General Objective

The general objective of this study is to model the dam breach process of Jema dam and map the downstream area to be inundated by the flood.

1.3.2. Specific Objectives

- To determine the maximum breach outflow at the dam site, routing the outflow through the downstream channel.
- To run the model for different catastrophic scenarios and analyze the consequences of the most hazardous one.
- Prepare different maps such as area, velocity and depth with time that can describe the nature of flood propagation and coverage.

1.4. Research Questions

The following questions can be raised to initiate this study

1. What are the different scenarios that would cause the dam break and which of these is the most catastrophic?
2. How long would it take for the breach process to complete and for the inflow flood together with the reservoir water to evacuate?
3. How much area would the emerging flood hydrograph covers in the downstream until the final cross section?
4. Which downstream areas are more prone to dam break flood?

1.5. Scope of the Study

From the known modes of failures, seismic type will not be considered in this study due to the rare chance of occurrence during reservoir full condition. Sediment transport during erosion of dam material will not be considered in HEC-RAS, since it simulates only clear water flow. The research will focus on both hydraulic failure (overtopping) and seepage failure (piping). One dimensional flood simulation model which is based on unsteady flow equations will be used for hydraulic simulation.

1.6. Significance of the Study

Preparing dam safety plans and hazard management strategies are unquestionably vital, since lots of human lives have been lost and tremendous amount of economic crisis have been recorded from dam failure events throughout the world in history. Setting out risk management, emergency action plans or evacuation planning system to protect both lives and materials during sudden dam failure phenomena and resulting flood waves is highly essential

Hence conducting pre event analysis of Jema dam break and its consequences and forwarding the hazard extent to public offices have great significances among which some are listed below:

- On time maintenance actions can be taken if the dam is susceptible to piping failure mode.

- Flood early warning system can be developed after the disastrous dam breaching flood has been identified.
- Downstream settlement of inhabitants can be planned in such a way that evacuation of the people during dam breach can be done rapidly saving as much lives as possible.
- The thesis paper can be used as a reference for further detailed researches on the study area.
- Protection dikes can be provided at both downstream banks with their top level considerably higher than the propagating flood level, especially on the stretches along residence areas and infrastructures.

2. LITERATURE REVIEW

2.1. Background

Dams are one of the most important structures in the field of water resources engineering. It is an evident historical fact that failure of dams has resulted in high casualties as indicated in the introduction part. Many dam failures have led to the inception of a new research field that deals with dam failures and its resulting consequences. There are however two basic perspectives to understand this research field that deals with dam failures. The first perspective is to answer the basic question that whether or not, a given dam will fail. This basically refers to the strength parameter of materials of dam section and this perspective basically deals with simulation of breaching process of dam section. Various parameters relating to dam failure like breach characteristics, time of formation etc. are estimated by this approach. The second perspective is to assume a given dam failure and study the resulting consequences in the downstream area. This approach helps in preparation of emergency action planning for a possible failure of dam. The final basic product of such analysis is inundation details of downstream area owing to the flood generated due to the failure of dam.

2.2. Dam Failures

In Ethiopia there is no dam breach event as far as concerned but some of the major dams are suffering from piping and structural stability problems which may lead to breach and considerable loss. To mention some among these dams Kesem is observed to have a 1m3/s flow along its left side abutment and Tendaho have a total leakage of nearly 500lts/s (Tendaho dam leakage and associated problems, 2011).

As per guidelines for dam breach analysis (Colorado dam safety office, 2010), “breach” is defined as the opening formed in the dam body that leads the dam to fail and this phenomenon causes the concentrated water behind the dam to propagate towards downstream regions.

The various causes leading to the failure of earth dams are grouped as Hydraulic failure (Overtopping, Erosion of upstream face, Erosion of downstream face and Erosion of toe of the dam), Seepage failure (Piping, Uplift, Sloughing and subsequent failure of the dam) and Structural failure (Embankment slope failures and Foundation slide) (ICOLD, 2012).

2.3. Dam Hazard Potential Classification

Hazard caused by dam failures is classified as; high Hazard Dam, Significant Hazard Dam, Low Hazard Dam and No public Hazard Dam (FEMA, 2013).

High hazard dam

High Hazard Dam is a dam for which loss of human life is expected to result from failure of the dam. Designated settlements located downstream within the bounds of possible inundation should also be evaluated for potential loss of human life. It is important to note that the potential of loss of a single life is sufficient to classify a dam as high hazard (FEMA, 2013).

Significant hazard dam

Significant Hazard Dam is a dam for which significant damage is expected to occur, but no loss of human life is expected from failure of the dam. Significant damage is defined as damage to structures where people generally live, work or recreate, or public or private facilities. Significant damage is determined to be damage sufficient to render structures or facilities uninhabitable or inoperable (FEMA, 2013).

Low hazard dam

Low Hazard Dam is a dam for which loss of human life is not expected, and significant damage to structures and public facilities as defined for a “significant Hazard” dam is not expected to result from failure of the dam (FEMA, 2013).

No public hazard dam (NPH)

No public Hazard dam is a dam for which no loss of human life is expected, and which damage only to the dam owner’s property will result from failure of the dam (FEMA, 2013).

2.4. Flood Hazard Classification

Flood severity grid prepared by FEMA is shown in Figure 2.1 in order to obtain upper limits of the depth * velocity product for each category of hazard level.

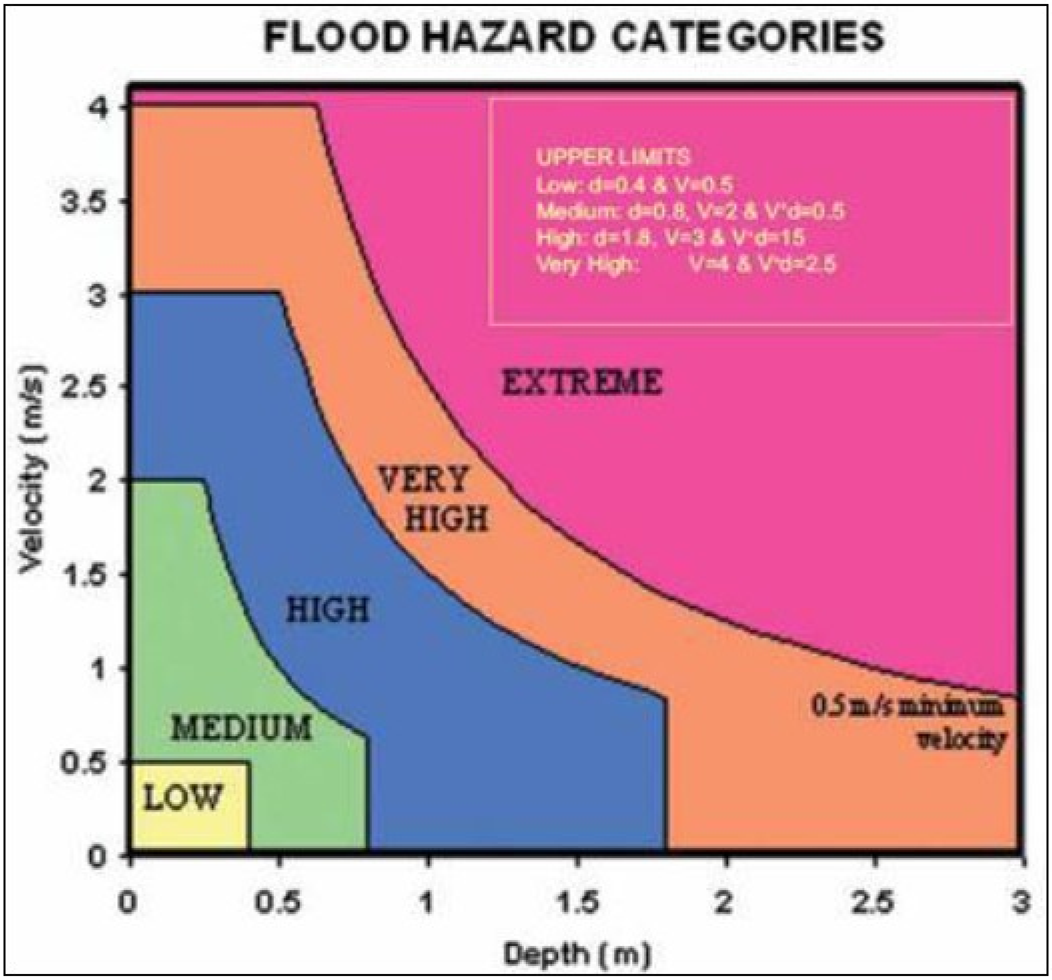

Figure 2. 1 Flood Depth and Velocity Severity Categories (FEMA (2013)

Representing the information in the figure above in a simplified table, the FEMA document states:

> "To produce a flood severity grid that exactly matches the categorization shown in the figure above, additional rules would need to be applied when calculating the depth * velocity product, to take into account the depth and velocity upper limits of each category. Additionally, the flood severity thresholds are different depending on whether they are being considered related to the impact on humans, vehicles, or buildings. As a simplified approach, the following depth * velocity categories can be applied when symbolizing the results of the dataset. However, other categorizations of this data may be used where desired."

Table 2. 1 Simplified Flood Depth and Velocity Severity Grid Categories (FEMA ,2013)

Flood Severity Category	Depth * Velocity Range (m2/sec)
Low hazard	< 0.2
Medium hazard	0.2 – 0.5
High hazard	0.5 – 1.5
Very High hazard	1.5 – 2.5
Extreme hazard	> 2.5

2.5. Dam Breach Parameters and Estimation Methods

Variation of breach parameters can affect peak discharge and inundation levels, as well as warning and evacuation time. The following are definitions of breach parameters.

A. Shape of Breach

For the hypothetical dam failures the shape of the breach is usually approximated as geometric shape such as rectangle, triangle, trapezoidal or parabola. The shape of the breach is greatly dependent on the type of dam. For embankment dams, a trapezoidal shape is common and for concrete arch dams usually the shape of the breach will be the same as the shape of the dam (Wahl, 1998).

B. Breach Size

As the dam breach advances, the dimensions of the breach keep increasing. For an earth fill dam, usually a trapezoidal breach shape, overtopping failure starts as a small breach and progresses at a linear or non- linear rate down the height of the dam as shown in Figure 2.2.

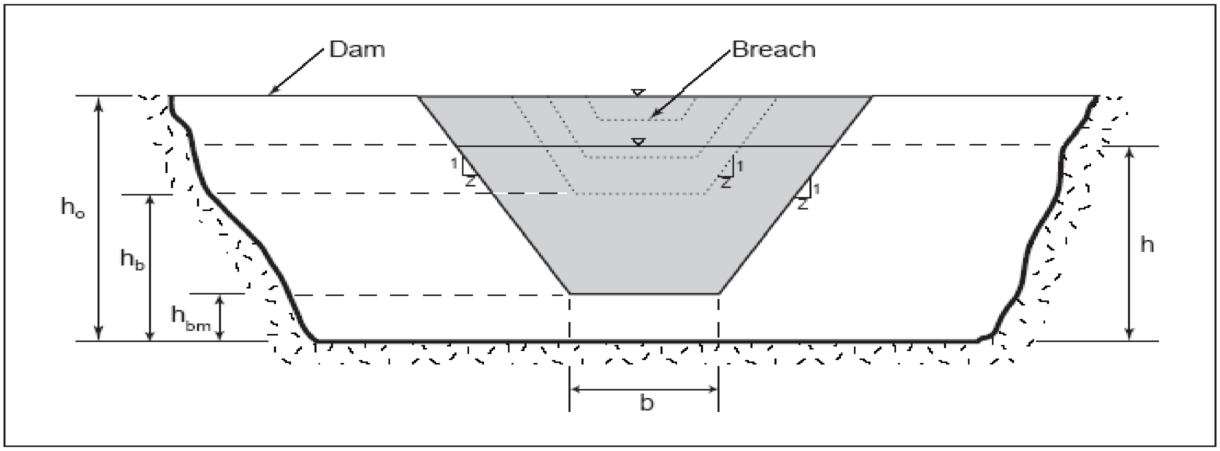

Figure 2. 2 Overtopping Breach Dimensions (Fread and Lewis, 1998)

For piping failures, the breach starts as a rectangle at some specified elevation from the crest as shown in Figure 2.3. The breach width and height grow until the elevation of the top of the breach is the same as the crest elevation, at which point the breach is identical to an overtopping failure.

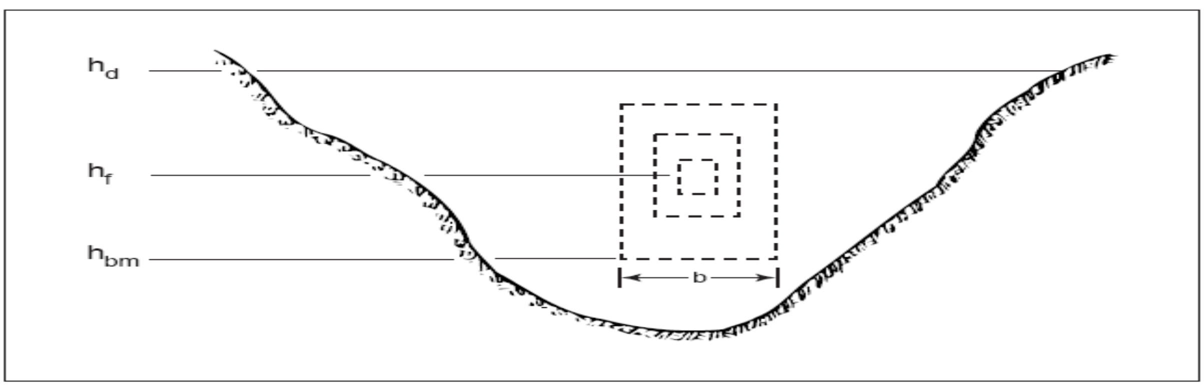

Figure 2. 3 Piping Breach Dimensions (Fread, 1991)

Where:

h_o= the breach top elevation at time t
hd= elevation at the top of the dam
hb= the breach bottom elevation at time t
hbm= lowest breach bottom elevation at time t
hf= specified center-line elevation of the pipe
b = maximum breach bottom width at time t

C. Breaching Time

Breaching time refers to the time elapsed since the initial breach formation until it reaches its terminal size. The failure time for earth dams ranges from six minutes to three hours. Concrete dam failures are much more rapid, and have a time range of six to eighteen minutes. The time of failure most commonly depends on the size of the dam, types of materials used for construction, and the structural strength of the embankment (ZAGONJOLLI, 2007).

D. Rate of Failure

The rate of breach expansion, increase in depth and width, is called rate of failure. This rate can progress at a linear or non-linear rate.

The following regression equations have been used for several dam safety studies found in the literature .These regression equations have been used on several dam break studies and have been found to give a reasonable range of values for earthen, earthen with a core wall (i.e. clay), and rock fill dams (USACE, 2014).

MacDonald and Langridge-Monopolis (1984): MacDonald and Langridge-Monopolis utilized 42 data sets (predominantly Earthfill dams, Earthfill dams with a clay core, rockfill dams) to develop a relationship for what they call the "Breach Formation Factor". The Breach Formation Factor is a product of the volume of water coming out of the dam and the height of water above the dam. MacDonald and Langridge-Monopolis (1984) then related the breach formation factor to the volume of material eroded from the dam's embankment. MacDonald and Langridge-Monopolis (1984) stated that the breach should be trapezoidal with side slope of 0.5H: 1V (USACE, 2014).

Von Thun and Gillette (1990): Von Thun and Gillette used 57 dams from both the Froehlich (1987) paper and the MacDonald and Langridge-Monopolis (1984) paper to develop their methodology. The method proposes to use breach side slopes of 1.0H: 1.0V, except for dams with cohesive soils, where side slopes should be on the order of 0.5H: 1V to 0.33H: 1V (USACE, 2014).

Froehlich (1995): Froehlich utilized 63 earthen, zoned earthen, earthen with a core wall (i.e. clay), and rock fill data sets to develop as set of equations to predict average breach width, side slopes and failure time. Froehlich states that the average side slopes should be: 1.4H: 1V for overtopping failures, 0.9H: 1V otherwise (i.e. piping/seepage) (USACE, 2014).

Froehlich, 2008: In 2008 Dr. Froehlich updated his breach equations based on the addition of new data. Dr. Froehlich utilized 74 earthen, zoned earthen, earthen with a core wall (i.e. clay), and rock fill data sets to develop as set of equations to predict average breach width, side slopes and failure time(USACE, 2014).

Xu Zhang (2009): The data base gathered by Dr.'s Xu and Zhang contained 182 earth and rockfill dams from the United States and China with nearly 50 percent of the dams greater than 15 meters in height. The Xu and Zhang paper does not provide estimates for side slopes directly. Instead they provide an equation to estimate the top width of the breach, which can then be used within the average breach width, to compute the corresponding side slopes (L.M. Zhang, M. Peng and Y. Xu, 2010)

Froehlich (2008), MacDonald and Langridge-Monopolis (1984), and Von Thun and Gillette (1990) are widely used for various dam breach modeling studies. The Three methods are selected by the researcher to predict Jema dam break parameters.

2.6. Outflow Hydrograph Prediction

The breach outflow hydrograph is crucially important for the assessment of flooding characteristics in the downstream areas. There are regression equations developed in order to predict the amount of outflow through the breach using dimensions of the dam and reservoir.

After the analysis is completed and the hydrograph developed, it is necessary to check the reasonableness of the maximum breaching outflow Qmax. There are a few commonly known techniques to check Qmax: historical predictor equations, parametric models, physically based erosion methods, direct comparison techniques, customized prediction equations and classical equations. The rule of the thumb is to check Qmax obtained in one method with the result of the other techniques (USACE, 2014).

In addition to the peak flow equations, one can also compare computed model peak outflows to envelope curves of historic failures. When comparing computed results to the envelop curve shown below keep in mind that this envelope curve was developed from only fourteen data sets, and may not be a true upper bound of peak flow versus hydraulic depth (USACE,2014).

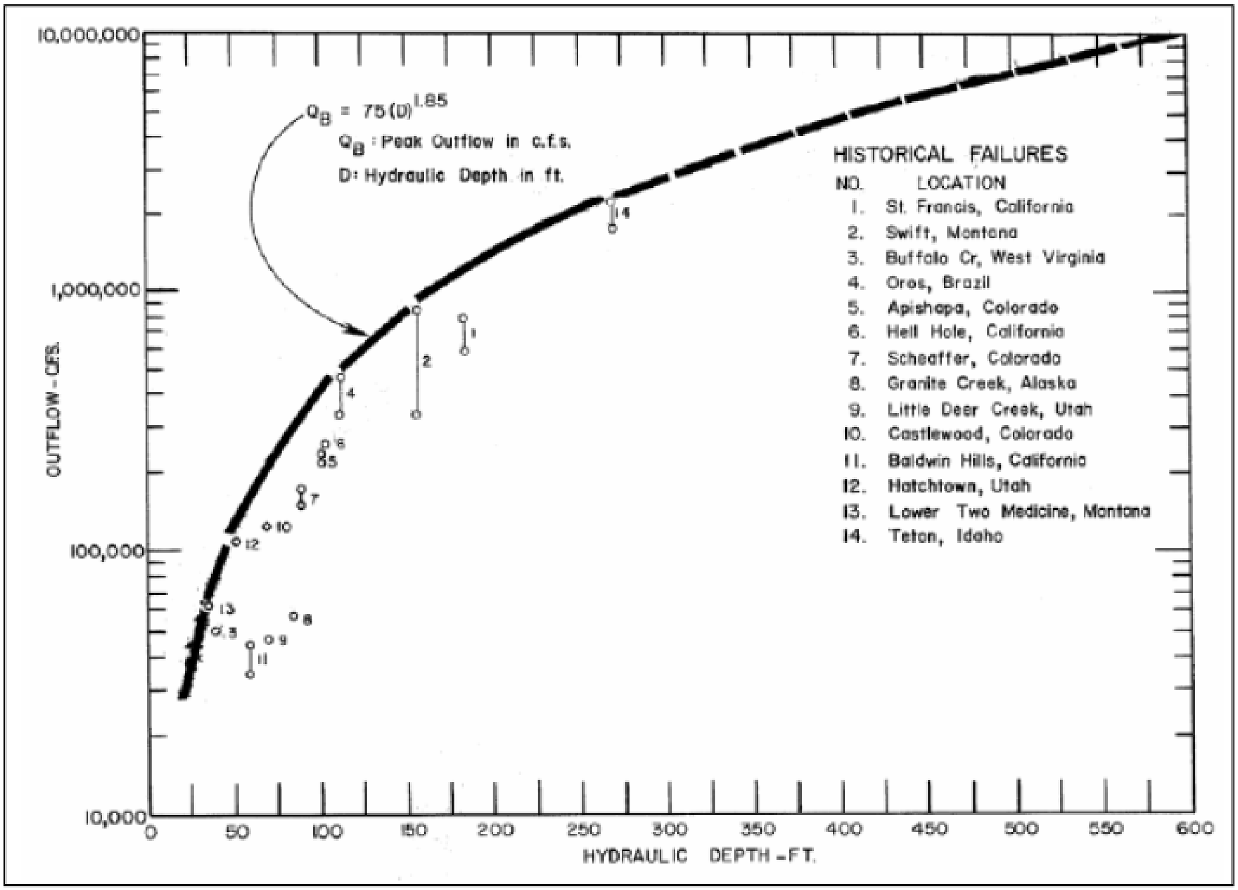

Figure 2. 4 Envelope of Experienced Outflow Rates from Breached Dams (USACE, 2014)

2.7. General Approaches to Dam Break Analysis

As per FEMA, 2013 dam break analysis approach categorized as: Event-Based approach, Risk-Based (Consequences-Based) approach and Tiered dam breach analysis.

An event-based approach is a deterministic method that requires the use of a specific or series of specific precipitation and non-precipitation events for the evaluation of dam failure and downstream inundation mapping. These events include extreme rainfall and runoff events that can lead to natural floods of variable magnitude. The maximum flood for which a dam is to be designed or evaluated is often dependent on its existing hazard potential classification or size classification (FEMA, 2013).

A risk-based approach to dam design and dam safety evaluations has been developed to account for the downstream consequences of a potential dam failure. The consequences evaluation is not based on the probability of failure, but instead on the potential loss of life or increase in economic losses caused by a potential dam failure. A benefit of the risk-based approach is that it may demonstrate, via an incremental damage assessment, that areas located downstream of a dam may be marginally affected by the reduction in the SDF or IDF design standard for a dam. By lowering the SDF or IDF requirements, limited funding for needed rehabilitation measures can be used for more dams, resulting in an overall increase in dam safety (FEMA, 2013).A disadvantage of the risk-based approach is that by reducing the SDF or IDF to less than the full PMF based on downstream consequences, new development in the downstream breach inundation zone could alter the consequences, resulting in the need for future dam rehabilitation measures to increase spillway capacity (FEMA, 2013).

A tiered approach to dam breach analyses can be used to establish an initial dam hazard potential classification and to produce dam breach inundation zone mapping for EAPs. The tiered dam breach analysis structure is not appropriate for use in dam design (FEMA, 2013). Unlike the event- and risk-based approaches discussed, the tiered approach is not used to determine the appropriate flood event to use in a dam failure analysis. Instead, the tiered approach is used to determine the appropriate level of complexity in the assessment, modeling, and mapping of a dam failure based on a dam's hazard potential, size, and the complexity of the downstream area under investigation (FEMA, 2013).

The greatest advantage to using an event-based approach is that it is a direct approach, less complicated to perform and regulate, and produces more conservative breach inundation zone mapping when compared to a risk-based approach. High-hazard potential dams are typically evaluated using a full PMF, and significant- or low-hazard potential dams are evaluated on a percentage of a PMF or some more frequent storm event (FEMA, 2013). Because of it is more advantageous than others; an event-based approach is selected by the researcher to simulate the Jema dam break floods.

2.8. Dam Breach Simulation Models

BRDAM (BReach DAM)

BRDAM (BReach DAM) was developed applying the Schoklitsch sediment transport equation to dam breach flows. It was assumed breach erosion to begin immediately upon overtopping, and to proceed until the breach reached the bottom of the dam. The model developed by Lou, Ponce and Tsivoglou (1981) links the Meyer-Peter and Müller sediment transport equation to the one-dimensional differential equations of unsteady flow and sediment conservation. The differential equations were solved with a four-point implicit finite difference scheme that was computationally complex and prone to problems of numerical instability. Flow resistance in the breach channel was represented using Manning's *n*. The breach width was empirically related to the flow through the breach. The model accounted for reservoir storage depletion in its upstream boundary condition (Ponce and Tsivoglou ,1981).

Breach Model

Fread (1988) developed the physically-based BREACH model to simulate breaches initiated by overtopping or piping. The model permits specification of three different embankment materials: an inner core, an outer portion (downstream shell), and a vegetated cover or riprap protective layer on the downstream face of the dam. Flow through the breach section is determined by orifice or weir equations, and flow down the face of the dam is modeled as a quasi-steady uniform flow with roughness determined from the Strickler equation for Manning's *n*. The model introduces two structural mechanisms that may contribute to breach formation: the breach shape may be impacted by slope stability of the breach side slopes or possible collapse of the upper portion of the dam by shear and sliding.

The release of water from reservoir through bottom outlet is not included and on the model BREACH there is no any room to enter the discharge capacity of the outlet. Hence while simulating overtopping mode of failure the water is supposed to outflow only via spillway and over the dam crest. Due to this exemption, the maximum water level of the reservoir may be overestimated and as a consequence the dam may be considered as overtopped at a certain discharge while it is still safe (Fread ,1988)

HEC-RAS

The Hydrologic Engineering Center-River Analysis System model (HEC-RAS) is a one-dimensional flow simulation model which performs both steady and unsteady flow hydraulics (Brunner, 2010). The HEC-RAS computational program has the ability to model extreme flow dynamics in the downstream of the reach due to a dam break flood waves and produce water surface profiles over the length of the modeled area (Asburry and Goodell, 2009). HEC-RAS is the most widely used hydraulic model for dam safety analyses in the United States and can be utilized for steady and unsteady flow analyses (Colorado dam safety office, 2010). Moreover, the HEC-RAS outputs like water surface profiles can easily be converted to flood inundation maps by its companion program called HEC-GeoRAS which is an Arc-GIS extension, (Sredojevic and Simonovic, 2009).

The HEC-RAS software has found wide acceptance among hydraulic engineers and researchers due to its robust channel flow analysis capabilities and its ability to simulates unsteady flood wave propagation and identifies flood prone areas as the areas where the ground is lower than the computed water elevation and allows the user to visualize the flood propagation in real time, thus making the software ideal for dam breach modeling. Because of complexity of solving routines, the output solutions were thoroughly reviewed for stability and correctness. Furthermore, many studies indicate that the solution found by HEC-RAS is stable and trustworthy (ackerman and brunner, 2006). Hence, due to its extensive capabilities and availability in USACE website; its' outputs compatibility with Arc- GIS (HEC-GeoRAS) software packages and for the other advantages stated above, HEC-RAS model is selected by the researcher to simulate the Jema dam break floods.

2.9. Modeling the Propagation of Flood

Having determined the breach parameters and peak outflow the next task is to route the most catastrophic outflow hydrograph over the downstream channel and flood plain and prepare an inundation map. Inundation maps show the flood contour for natural floods of certain return periods, in most cases up to PMF, and flood contours of potential dam break floods caused by a "sunny day failure" and a failure superimposed over certain natural "base flood conditions". (ICOLD, 1998) These inundation maps are used to control building activities, develop necessary warning and evacuation plans and conduct consequence assessments.

In spite of the timely improvements of flood routing models, the predictive accuracy of such models can be subject to significant error (2 feet or more in the crest profile) due to inaccuracy in the computed reservoir inflow, breach parameter estimation and dynamics, downstream cross section properties, flow resistance coefficients both in channels and flood plains, effect of sediment transport and flow constrictions in channel and the complex flow patterns that are not adequately described by one- dimensional flow equations (Fread D. , 1981).

To correctly estimate the consequences derived from a structural failure modeling of flood propagation should be highly accurate. Identification of the inundated areas, inundation depth, speed and duration, as well as the impact that flood water characteristics (salt, freshwater, contaminated water, etc.) can have on the inundated areas, are very important for decision making, emergency evacuation and early warning.

The De Saint-Venant equations or shallow water equations are used for modeling dam break flood propagation. These equations consist of the mass and momentum conservation equations, and assume that the vertical velocities are much smaller than the horizontal velocities, which leads to hydrostatic pressure distribution in a channel cross section (Zagonjolli, 2007).

3. MATERIALS AND METHOD

3.1. General Description of the Study Area

3.1.1. Location

Jema Project is located in Amhara National Regional State, West Gojam Zone, Mecha Woreda, about 527 kilometers from Addis Ababa. The dam axis is located in between the geographic grid ref. UTM E 37°10'58", N 11°11'32" and E 37°11'11", N 11°12'2". Both the left and right abutments rise to an elevation higher than 2133 m. The location of the river bed at the center of the dam axis (in UTM) is E = 37°11'2" m and N= 11°11'46" m with a riverbed elevation of 2063 m. The irrigation command area covers 7,559 ha. It is more-or-less flat, with an average altitude elevation of ~2020 masl (WWDSE, 2010).

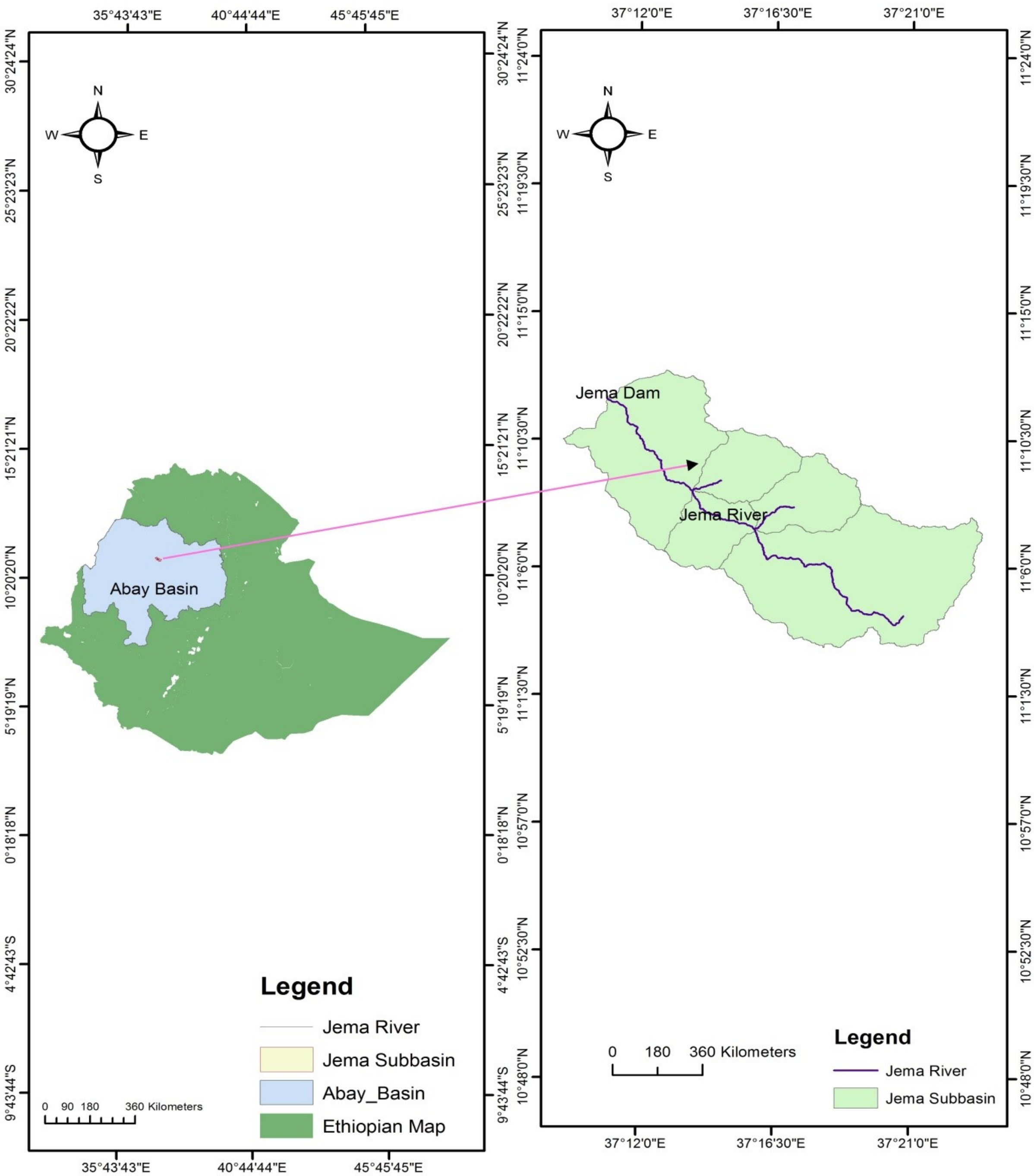

Figure 3. 1 Location Map of the Study Area

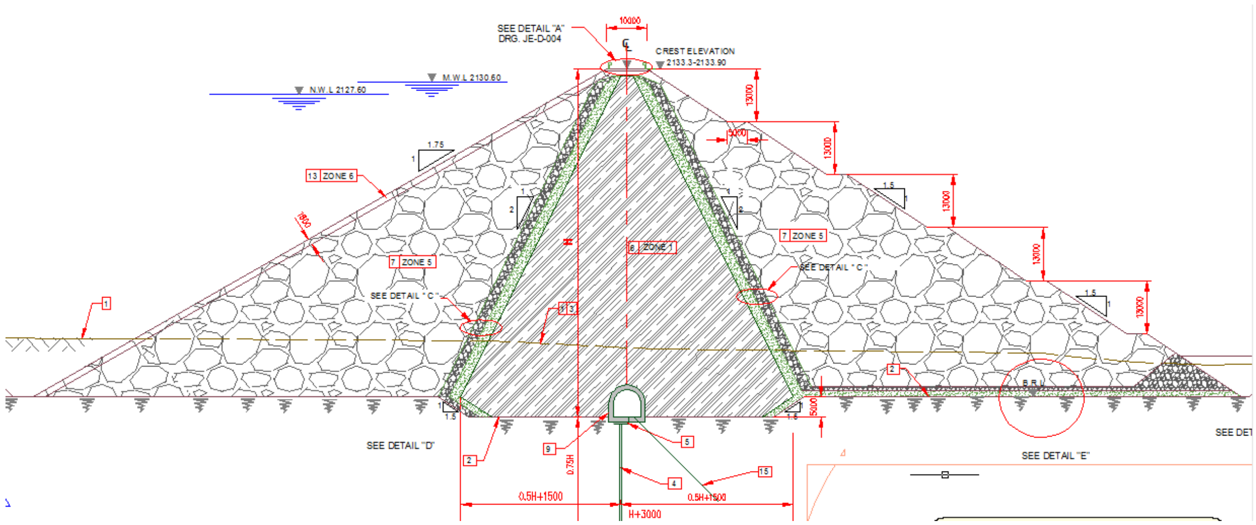

Figure 3 .2 Typical Cross Section of the Main Dam (WWDSE, 2009)

3.1.2. Description of the Dam under Study

The dam is rock fill type with crest length of 1022m and crest width of 10m. it has 70.9 m above the riverbed level and 82.9 m above general excavated foundation level; the dam crest level is at 2133.9 masl and the river bed level is at 2063m.a.s.l. the upstream and downstream slopes of the dam are 1V:1.75H of 1V:1.5H respectively. The invert level of outlet is set at 2097.5masl and it is within the body of the dam.

The reservoir is intended to accommodate a total of 124 million cubic meter of water, A free overflow spillway and chute, required for the safe passage of a 3-day half PMF flood discharge of 430 m^3/s and the passage of 1 day PMF (1469 m3/s) without dam overtopping; and Outlet pipe shall release water from the Outlet Tower of the reservoir for domestic water supply some 5.80 MCM, for downstream environmental releases, and for the 7800 to 11,615 ha irrigable area. (WWDSE, 2010).

3.1.3. Climate Characteristics

The climate of the Jema catchment is marked by a rainy season from June to September. Mean annual precipitation is about 1,836 mm. Rainfall over the Jema watershed is uni-modal with nearly 96 % of mean annual rainfall occurring in the period May to October. The dry season, from November to April, has a total rainfall of about 4% of the mean annual rainfall. Dependable rainfall (80%) varies from less than 0 mm during the dry season to 121.7-314.2 mm/month during the period of June to July/August. Temperature variations throughout the year are minor. Maximum temperatures is 27 ºC, whereas minimum temperatures 13 ºC. Humidity varies between 45% in March and 83% in August. The mean monthly wind speed varies from 0.5 to 2.5 m/sec. Sunshine duration is reduced to 4.7 – 5.8 hours during July and June, respectively (WWDSE, 2010).

3.1.4. Jema Watershed

The catchment area of Jema River at the dam site is 218 km^2 with a mean annual rainfall of 1836mm over the watershed. It is a steep catchment with an average slope of 5.5% and a river course length of 25.8 Km. About 72% of the Jema watershed soils belong to the chromic Luvisols and Euritc Nithosols units. Chromic luvisols (56% of the area) are used intensively for cultivation, while Nithosols (16% of the area) are predominantly covered with open shrub and grasslands (WWDSE, 2010).

3.1.5. Jema River

Jema River is a major tributary of Gilgel Abbay River. It originates at Adama Mountain at an altitude of 3,535 masl and joins the Gilgel Abay River at altitude about 2,100 masl upstream of the Bikolo Abay town. The intended primary source of water supply to the project under study is this Jema River. The Jema River, which is about 25.8 km long. The river flow generally in a Northern direction to joins Gilgel Abbay River (WWDSE, 2010).

3.1.6. Population Settlement

The total population residing in the project area in the year 2007 was 48,488 and the total household number – 10,424. Male and female populations are 25,803 and 22,685, respectively. The total area of the five Kebeles is about 173 km^2, giving a crude population density of 281 person per km^2, which is higher than that of the average of Amahara region and Gojjam zone - 122 and 192, respectively. Generally the Project area is one of the most populous in Amhara region almost half of the populations are residing in command area downstream of the dam (WWDSE, 2010).

3.2. Materials Used

The materials used for this research are Arc GIS and HEC -GeoRAS tools to obtain modeling reach and floodplain cross-sectional geometry and for inundation mapping, HEC- GeoHMS to delineate the watershed, Global mapper to prepare DEM data as suitable for GIS and to convert shape files to Google Earth format(KML), Google Earth for remote data of the developed infrastructures like hydraulic structures, towns and current land use information, HEC-RAS model for dam break simulation and unsteady flood routing at downstream regions and Microsoft EXCEL 2010 to do hydrology analysis including PMF hydrograph and to analyze HEC-RAS outputs.

3.3. Data Collection

In conducting the research a field visit was made on the study area to have a good perception on the catchment area, dam, other structures, river morphology and downstream flood plain area. Both primary and secondary data have been collected as listed below.

The data required for this research was collected from primary and secondary data sources.

Primary data

Physical observation and measurement made on site to visualize the dam site and downstream area and relevant photos taken on site that would be essential for the study such as Land use land cover of the area prone to flooding which is used to estimate the manning's roughness "n"

Secondary data

Different types of data such as hydrological, meteorological, important engineering and infrastructure information on the dam and overall study area were collected from Ministry of Water, Irrigation and Energy, National Meteorological Agency and from Ethiopian Construction Design and Supervision Works Corporation (ECDSWC)

These data are:

- Daily rainfall data of meteorological stations located surrounding the catchment.
- Stream flow data of Gilgele Abay and Koga River.
- Salient features of Jema dam
- Salient features of the reservoir
- Reservoir area-elevation-volume curves
- Design report of the project
- Hydrological data (full PMF inflow hydrograph for which the dam and spillway were designed.)

3.4. Data Analysis

The procedure followed to conduct this thesis is;

First hydrological study is made by Determining PMP and unit hydrograph to develop:

- PMF that flow to Gilgele Abay river at Jema river confluence 32km from the dam to downstream
- PMF of two seasonal small tributaries of Jema at right and left side of river, 10km and 11km far from dam respectively to downstream

PMF hydrographs of Jema dam were taken from ECDSWC which may overtop the dam thereby endangering the dam for failure. ECDSWC was used hershfield method to estimate The PMF hydrograph. Watershed of Gilgel Abay was delineated by HEC GeoHMS to determine the area. Dam breach analysis is then done to predict the breach size and estimate the outflow hydrograph using HEC RAS. Having determined the outflow magnitude, the flood is again routed through the downstream channel and flood plain using HEC-RAS. Results of hydraulic flow simulation are exported into HEC-GeoRAS to produce flood inundation maps in order to determine the flood prone area, so that flood early warning system can be set and emergency action plans can be made.

These procedures are depicted on the conceptual framework given in Figure 3.3

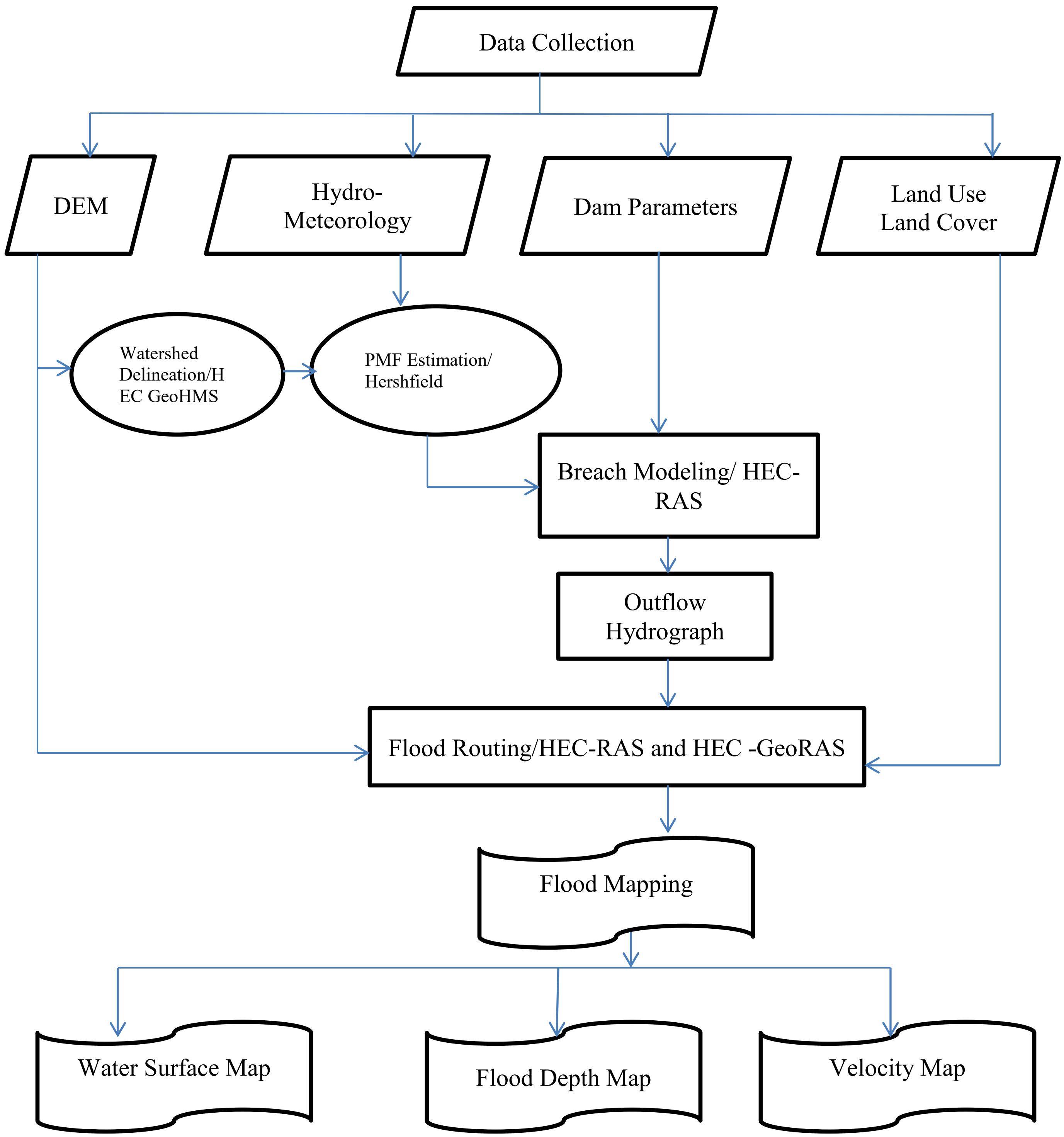

Figure 3. 3 Conceptual Framework

3.4.1. Hydrology

The general objective of this hydrology part is to compute the PMF that may come to Gilgel abay river and downstream tributaries of Jema River. In order to determine this PMF, a Probable Maximum Precipitation (PMP) is initially calculated using observed daily rainfall data from stations located nearby to the watershed. This PMP is then convoluted on the unit hydrograph representing the catchment to get the final desired PMF. This section discusses the catchment characteristics, calculation of PMP, and computation of the PMF.

3.4.1.1. Precipitation Data Analysis

3.4.1.1.1. Climatic Characteristics of the Study Area

Most of Ethiopia is characterized by tropical climate moderated by altitude with a marked wet season. Generally, in Ethiopia there are three seasons: the first is the dry season (known locally as Bega) which prevails from October to January; the second is the small rainy season (Belg) that runs from February to May and the third is the main rainy season (Kiremt) which prevails from June to September. Rainfall is above 1,000 mm a year almost everywhere in the highlands and it rises to as much as 2,000 – 3,000 mm in the wetter southwestern parts. (WWDSE, 2010)

Since Ethiopia is situated in the northeastern part of Africa, it is influenced from the northeast, to the southeast and southwest (West African) by monsoons bringing moisture from the Indian and Atlantic Oceans. In the northern hemispheric summer, moisture laden winds gradually penetrate into the countries as the African sector of the Inter-Tropical Convergence Zone (ITCZ) progresses northward. (WWDSE, 2010).

Gilgel abay watershed receives its main rainfall from June to September. The orographic influence on rainfall depth values is also marked in the mountainous area that prevails in the area under study. (WWDSE, 2010)

3.4.1.1.2. Rain Gage Stations and Availability of Data

A total of six rain gauge stations located around the periphery of the catchment are considered as a data source for the study. Table 3.1 gives geographical location and elevation of the stations. Location map of the stations is given on Figure 3.4. Daily rain fall data observed on these stations has been collected. The data obtained for all station was 30 years and all stations are outside of the catchment.

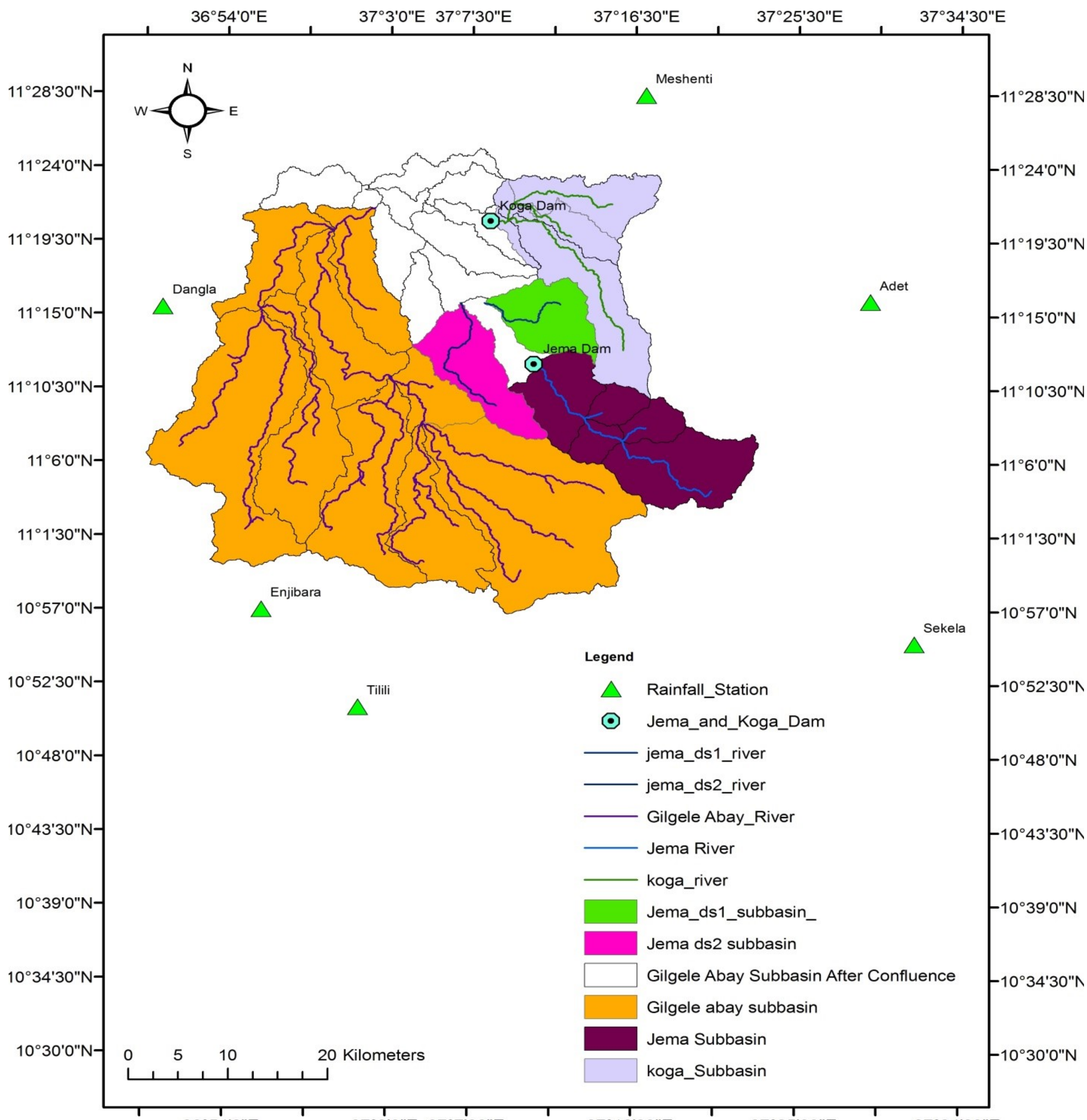

Figure 3. 4 Location of Rain Gauge Stations

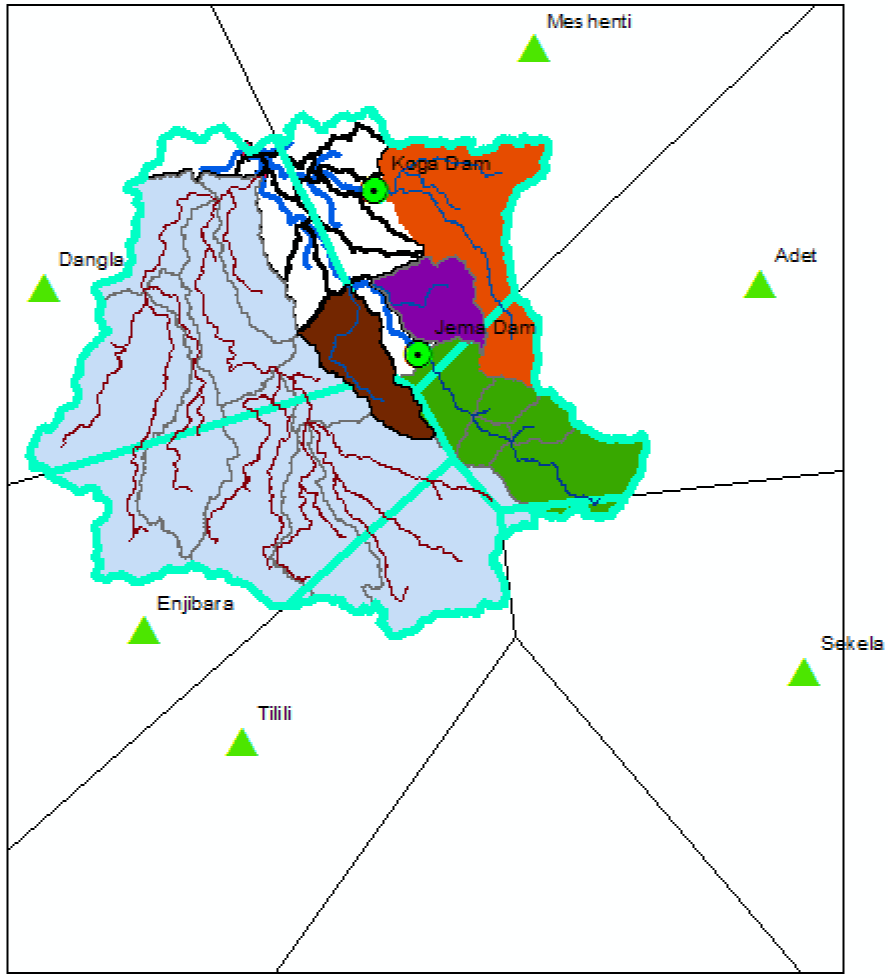

Figure 3. 5 Gilgele Abay Watershed and rainfall stations with Theisson Polygon

The rainfall stations taken for each sub basins are different based on the polygon for example meshenti rainfall station didn't considered for Gilgel Abay watershed above Bikolo Abay Town because of it doesn't has contribution.

Table 3. 1 Locations of Rain Gauge Stations

S.No.	Name	Location		
		Latitude	Longitude	Elevation
1	Adet	$33^0 53'$	$12^0 46'$	1914
2	Dangla	$26^0 43'$	$12^0 45'$	1590
3	Enjibara	$27^0 41'$	$12^0 11'$	2540
4	Meshenti	$31^0 29'$	$12^0 69'$	1748
5	Sekela	$33^0 97'$	$12^0 07'$	3034
6	Tilili	$28^0 38'$	$12^0 00'$	2429

3.4.1.1.3. Data Quality Analysis

Annual rainfall data of all the stations have been tested for independence, stationarity, homogeneity, outlier and trend using different appropriate methods. Discussions on the tests are presented on subsequent sections below and sample tables for Dangla rainfall station and Gilgel abay flow data showing the data quality analyses and results are given in Appendices section.

i. Test For Independence and Stationarity/ Wald-Wolfowitz (W-W) Test

This test is helpful to check the independence of the time series and to test the existence of trend. The hypothesis that the data is independent (no observation in the data series has any influence on any following observations) and stationary (the data series is invariant with respect to time) is confirmed at a confidence interval of 5% at all stations.

For the data set $X1,2,X3......Xn$

$$R=\sum_{i-1}^{n-1} X_iX_{i+1}+X_1X_n \quad \text{...} \quad (3.1)$$

$$\ddot{R}=\frac{X1^2-S2}{n-1} \quad \text{..} \quad (3.2)$$

$$Var(R) = =\frac{S1^2-S2}{n-1}-\ddot{R}^2+\left(\frac{S1^4-4S1^2+4S1S3+S2^2-2S4}{(n-1)(n-2)}\right) \quad \text{.............} \quad (3.3)$$

$$U=\frac{R-R^-}{var(R)^\wedge 0.5} \quad \text{..} \quad (3.4)$$

Ucritical=1.96

Where, s is the rth moment of the sample about the origin.

ii. Test for Homogeneity and Stationarity/ The Mann-Whitney (M-W) Test

The hypothesis that data set is homogenous has been checked using the M-W two tailed test and all stations are found to be homogenous at confidence interval of 5%.

In this test two samples of size *p* and *q* with $p \le q$ are compared. The combined data set of size $N = p + q$ is ranked in increasing order. The Mann-Whitney (1947) (M-W) test considers the quantities *V* and W in Equation. 3.5 and 3.6.

$$V=R-\frac{P(P+1)}{2} \quad (3.5)$$

$$W = pq - V \quad (3.6)$$

R is the sum of the ranks of the elements of the first sample (size p) in the combined series (size N), and V and W are calculated from R, p, and q. V represents the number of times an item in sample 1 follows an item in sample 2 in the ranking. Similarly, W can be computed for sample 2 following sample 1. The M-W Statistic U is defined by the smaller of V and W. When $N > 20$ and p, $q > 3$, and under the null hypothesis that the two samples came from the same population, *U* is approximately normally distributed with mean and variance.

Another method of checking stationarity of a data set is conducting a trend test on the time series. Trends are caused by gradual changes in climatic conditions or in land use such as urbanization. With the null hypothesis that the time series has no trend and fixing the level of significance α as 5%, all stations give a satisfactory result.

iii. Test for outliers/ The Grubbs and Beck (G-B) Test

Since outlying values in time series have negative impact in the detail analysis, the annual rain fall data set has been tested for such outliers using The G-B test.

The Grubbs and Beck (1972) test (G-B) may be used to detect outliers. In this test the quantities X_H and X_L are analyzed using the following equations.

$$X_H=\exp(\bar{X}+K_{NS}) \quad (3.7)$$

$$X_L=\exp(\bar{X}-K_{NS}) \quad (3.8)$$

Where, X and S are the mean and standard deviations of the logarithm of the annual rainfall peaks, respectively, and K_N, is detected and K_N, is the G-B statistic tabulated for various sample sizes and significant levels by Grubbs and Beck (1972). At 10% significant level, the following approximation proposed by Pilon et al. (1985) is used.

$$K_N= -3.62201+6.28446N^{1/4}-2.49835N^{1/2}+0.49146N^{3/4}-0.037911N \quad (3.9)$$

Where N is the sample size

iv. Mass Curve Analysis

A hydrologic time series data may be inconsistent with time due to change in physical condition of the basin, method of data collection and negligence of the observer (James et.al, 1960). In order to check the consistency of the data set as a long term data, a mass curve technique has been used. Cumulative of annual maximum daily precipitation data of the stations is used as a pattern for testing the individual station records. The mass curve for individual station is plotted against the cumulative of the pattern. If a break in slope is observed then the data of the station is adjusted by multiplying it with the ratio of the two slopes as depicted in the following formula.

$$Pa= \frac{ba}{bo} * Po \ldots\ldots\ldots\ldots\ldots\ldots\ldots\ldots\ldots\ldots\ldots \text{(3.10)}$$

Where,

Pa = adjusted precipitation

Po = observed precipitation

ba = slope of graph to which records are adjusted

bo = slope graph at time Po was observed

The annual maximum precipitation time series has been corrected using the above equation and adjusted curves are shown on Figure 3.6 below. The corrected data are used for PMP calculation on Table 3.3

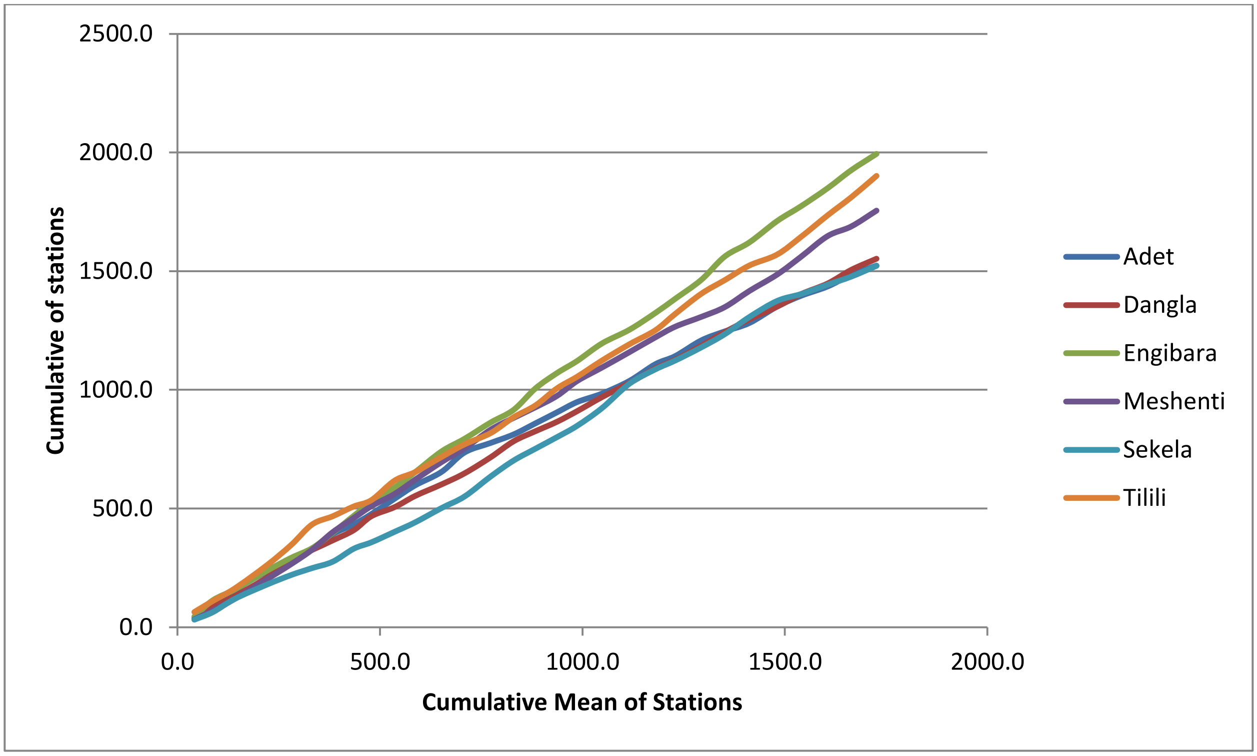

Figure 3. 6 Double mass curve of all rainfall stations

3.4.1.1.4. Data Gap Filling

The daily rainfall data collected from the National Meteorological Agency is with many data gaps. The overall missed data statistics is given on Table 3.2 below

Table 3. 2 Summary of Rainfall Missed Data

Station	Data range	Total missed days	Total days in the range	Percentage missed
Adet	1986-2015	608	10956	5.5
Dangla	1986-2015	954	10956	8.7
Enjibara	1986-2015	598	10956	5.5
Meshenti	1986-2015	1340	10956	12.2
Sekela	1986-2015	1520	10956	13.87
Tilili	1986-2015	1480	10956	13.5

For all stations, the missed data have been estimated and filled using inverse-distance weighting method.

There are many techniques used to fill data gaps and the most common are: arithmetic mean/ station average method, normal-ratio method and inverse-distance weighting method. Since the correlation matrix depicts that there is poor relation between the stations, the station average method cannot be used. The normal ratio method requires surrounding gauges to have a normal precipitation exceeding 10% of the considered gage (De Silva et.al, 2007). But as the number of data available on every station is more or less the same (with a range of 1986-2015), this method is discarded. Hence, the inverse-distance weighting method is used to fill the missed daily rainfall data. The equation of this method is:

$$Px=\frac{1}{W}\sum_{i=1}^{n} di^{-b}Pi \quad (3.11)$$

$$W=\sum_{i=1}^{n} di^{-b} \quad (3.12)$$

$$di = (xi2 + yi2) \quad (3.13)$$

Where,

Px= missing precipitation value for station X for a certain time period

Pi = precipitation values at adjacent stations for the same period

n = number of neighboring stations

b = proportionality factor 1

di = distance from gage with missing data to the neighboring gages

xi = the longitudinal distance between two stations

yi = the latitudinal distance between two stations

The following are rainfall stations and their neighbor stations which used to fill the data gap.

Dangla rainfall station was filled by Enjibara, Tilli Adet,Merawi, ,Meshenti and Bahirdar rainfall stations. Adet rainfall station was filled by Merawi,Dangla,Enjibara, Tilili,Meshenti ,Bahirdar and Sekela rainfall stations. Meshenti rainfall station was filled by bahirdar,zege, merawi and adet. Enjibara rainfall station was filled by Dangla, Merawi,Meshenti,Adet,Sekela. Tilili,Askuna,Finotselam and Bahirdar rainfall stations. Tilili rainfall station was filled by Askuna,Enjibara,Finoteselam,Sekela,Dangla, Merawi,Meshenti,Adet and Denbecha rainfall stations. Sekela rainfall station was filled by Adet,Finotselam,Denbecha,Tilli, Askuna, Engibara, Merawi and Dangla rainfall stations.

3.4.1.2. Estimation of One Day Duration Probable Maximum Flood (PMF)

The Probable Maximum Flood (PMF) is one of the ranges of conceptual flood events used in the design of hydrological structures to protect the structures from overtopping and against damage. It is computed from the Maximum Probable Precipitation (PMP) that is possible in the catchments. According to the World Meteorological Organization definition (WMO, 2009), the Probable Maximum Precipitation (PMP) is defined as theoretically the greatest depth of precipitation for a given duration that is physically possible over a given size storm area at a particular geographical location at a particular time of year. This PMP magnitude together with its spatial and temporal distributions of occurrence can be used to estimate the PMF at the dam site.

During design of dams and spillways the maximum design flood considered in fixing the height of the structures is the Maximum Probable Flood (PMF) that may occur at the dam site. Jema dam and its spillway were designed` a 3 day half PMF flood discharge of 430 m^3/s and the passage of 1 day PMF (1469 m3/s) without dam overtopping was finally selected (WWDSE, 2010)

The PMF hydrograph of Jema dam were directly taken from project report of designer organization and scaled up by 1.47 in order to breach the dam .no need to determine new PMF because the assumption of the researcher is what if the dam breach. Such type of failure may occur in such circumstances as in basin wide extreme hydrological event and the PMF may be underestimated by different reasons.

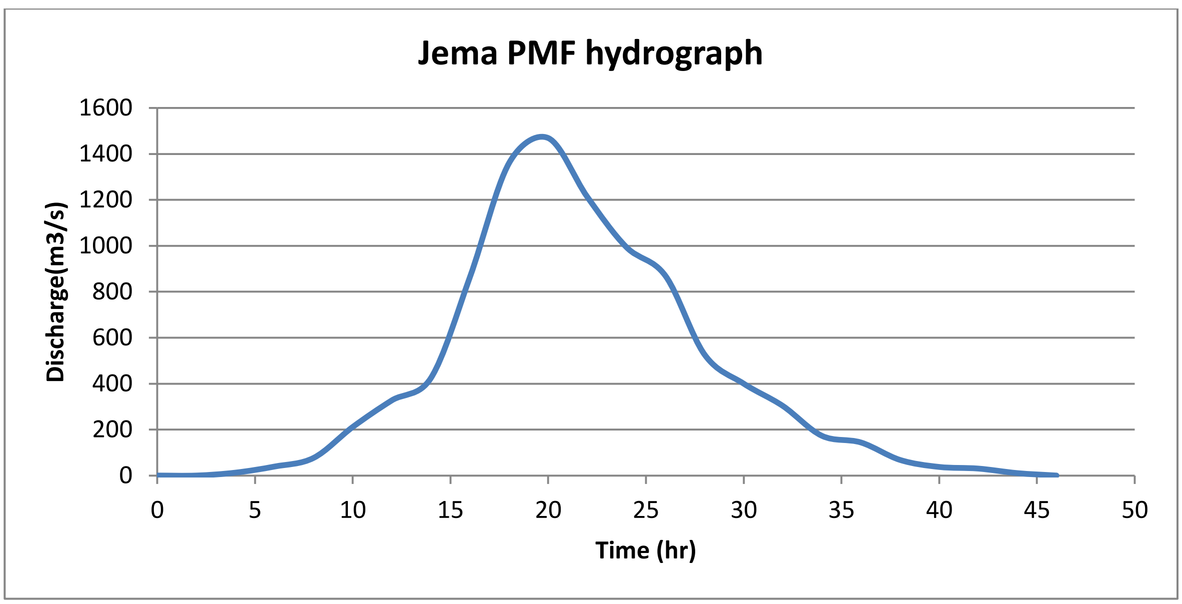

Figure 3. 7 Jema one day PMF hydrograph (WWDSE, 2010)

The PMF of Gilgele abay river and small tributaries of Jema River was computed by convoluting a Probable Maximum Precipitation (PMP) on a representative Unit Hydrograph (UH) of the watershed. In this section calculation of PMP, derivation of the UH and convolution of these two to get the PMF shall be discussed

3.4.1.2.1.1. Computing 24hr. Duration PMP

The statistical approach suggested by Hershfield (1961) can be used to estimate PMP and rainfall of different return periods. (WMO, 2009)

The procedure developed by Hershfield (1961) and later modified (1965) is based on the general flood frequency equation by Chow (1961):

$$X_T = X_{av} + \sigma K \quad \text{……………..……………............... (3.14)}$$

$$K = \frac{(X1 - Xn-1)}{\sigma n-1} \quad \text{……………..………………................. (3.15)}$$

Where X_T is the event (magnitude) at return period of T years

X_{av} the mean of the sample data

σ the standard deviation and

K =the frequency factor, which depends upon the frequency distribution representing the sample series.

X1, X n-1 and σn-1 are the highest, mean and standard deviation respectively excluding the X1 value from the series.

In a survey of more than 2700 stations world over, Km values as calculated from the above equation vary from less than 3 to a highest value of 14.5. Hershfield adopted the highest value rounded to 15 for estimating PMP,

$$PMP = X\,n + 15\,\sigma n \quad \text{…..……………..……………….............. (3.16)}$$

The frequency factor km is a very important part of the equation as it constitutes the number of standard deviations added to the mean distribution value in order to attain the largest possible precipitation value within a series (Suligowski, 2013).

The practice of design of dam spillways in Ethiopia is widely employed using the value of probable maximum flood (PMF) obtained from PMP. Apart from being extremely large flood magnitude, the procedure adapted in the country is based on Hershfield's estimation procedure.

Table 3. 3 Weighted Yearly Maximum Rainfall of Stations

S.No.	Years	Max Precipitation
1	1986	44.4
2	1987	56.2
3	1988	47.6
4	1989	81.7
5	1990	67.3
6	1991	47.1
7	1992	49.5
8	1993	55.2
9	1994	52.2
10	1995	55.5
11	1996	53.3
12	1997	67.2
13	1998	51.1
14	1999	65
15	2000	60.6
16	2001	63.9
17	2002	54.8
18	2003	48.4
19	2004	66.3
20	2005	61
21	2006	64.7
22	2007	51.5
23	2008	71.3
24	2009	74.5
25	2010	57.3
26	2011	68.1
27	2012	60.1
28	2013	64.2
29	2014	67.7
30	2015	62.5
Total		1790.3

Table 3 4 Adjustment of Parameters Mean and Standard Deviation per WMO

Parameters Adjustment	
Statistical Parameters for Observed Data	
Mean (n)	59.7
Mean (n-m)	61.7
SD (n),n-number of data	8.9
SD(n-m),m=1	8.8
Adjustment of Mean and SD for max. Observed event	
Mean (n)-Adjustment factor (Appendices Figure I-1)	1.03
SD (n)-Adjustment factor (Appendices Figure I-2)	1.1
Adjustment for Fixed Observational Interval (i.e. conversion of 1-day RF to 24-hr RF values) Recommended	
Mean (n) -Adjustment factor	1.13
SD (n) -Adjustment factor	1.13
Adjustment of Mean and Standard Deviation for Sample Size	
Mean (n) -Adjustment factor (Appendices Figure I-3)	1.01
SD (n) -Adjustment factor (Appendices Figure I-3)	1.04
Final Adjusted Values of Mean (Xn) and Standard Deviation (Sn)	
Mean (n)	70.2
SD (n)	11.6

$Fr = 1\text{-}0.02\ D^{-0.33}A^{0.5}$ ……………………..…………..……….......... (3.17)

Where

D = duration in hours (in our case D=24hrs)

A = drainage area in sq.km

Depth of rainfall at different return period was determined in table 3.6 using the general flood frequency equation Chow (1961), k value was adopted 15.

Table 3. 5 Point and Areal Rainfall of the Catchment

Point and Areal rainfall of the catchment				
Return period	Depth of PRF(mm)	Depth of RF(cm)	Areal RF(mm)	Areal RF(cm)
PMP	243.5	24.3	185.14	18.51

3.4.1.2.1.2. Derivation of Unit Hydrograph

Synthetic unit hydrograph methods usually relate time base to catchment, which is in turn, is related to the timing response characteristic of catchment, including catchment shape, length and slope. The synthetic unit hydrograph of Snyder is based on relationships found between three characteristics of standard unit hydrograph and descriptors of basin morphology. The hydrograph characteristics are the effective rainfall duration, (tr), the peak direct runoff rate (qp), and basin lag time (tp).

The standard unit hydrograph is associated with specific effective rainfall duration, tr, with basin lag time (hr.), tp. the peak discharge (m3/sec), qp and basin period (hr.).

Delineated of the catchment area of the project in sq.km, the longest path of channel, centroid of channel of the catchment have been done from DEM through ArcGIS and defined the maximum and minimum elevation of the catchment from DEM through Global mapper.

SCS developed a dimensionless hydrograph that has its ordinate values expressed as the dimensionless ratio, Ti/Tp and Qi/qp, where Qi is the discharge at any time Ti and qP is peak discharge at time Tp as shown Table 3.6 below.

Table 3. 6 Ratio of the Basic Dimensionless Hydrograph of the SCS

Ti/Tp	Qi/qp	Ti/Tp	Qi/qp	Ti/Tp	Qi/qp
0	0	1.2	0.93	2.6	0.107
0.1	0.03	1.3	0.86	2.8	0.077
0.2	0.1	1.4	0.78	3	0.055
0.3	0.19	1.5	0.68	3.2	0.04
0.4	0.31	1.6	0.56	3.4	0.029
0.5	0.47	1.7	0.46	3.6	0.025
0.6	0.66	1.8	0.39	3.8	0.015

0.7	0.82	1.9	0.33	4	0.011
0.8	0.93	2	0.28	4.5	0.011
0.9	0.99	2.2	0.207	5	0
1	1	2.4	0.147		
1.1	0.99				

Using the following formulae in table and applying conversion factors peak discharge (Qp) and lag time (Tp) was determined by synder from watershed characteristics as shown in table 3.7

Table 3. 7 Snyder's Synthetic Unit Hydrograph Parameters

Basin Name	Description	Gilgel Abay
Catchment characteristics		Dimension
A,Area (km2)	Delineated (GIS)	1169.47
L,Length (km)	Measured (GIS)	60
Lc,Centroid distance (km)	Measured (GIS)	30
Ct ,coefficient		1.4
Cp		0.75
C1		0.75
Tp (hr)	$C1Ct\,(LLc)^{0.3}$	9.95
tr (hr)	Tp/5.5	1.81
tR		2
Tpr	Tp-(tr-tR)/4 (hr)	10
qp	2.78Cp/Tpr (cumec/sq.km)	0.209
Qp	qpxA(m3/sec)	243.92

Where: A = the basin area in km2.

L = the length of the main stream in kilometers from the outlet to the upstream divide.

Lc = the distance in kilometers from the outlet to a point on the stream near the centroid of the watershed area.

Ct = is a coefficient derived from gauged watersheds in the same region and represents variations in watersheds slopes and storage characteristics.

Cp was also found to vary in the range of 0.31 to 0.93.

C1 is between 0.5 and 1.

qp = the peak discharge per unit area in m3/s/sq.km and

Qp= peak discharge of the standard unit hydrograph in m3/sec.

tr= effective rainfall duration of standard unit hydrograph

tR= effective rainfall duration of required unit hydrograph

Tp=basin lag time of standard unit hydrograph

Tpr=basin lag time of required unit hydrograph

Table 3. 8 SCS Dimensionless UH Method

SCS Dimensionless UH Method				Interpolation To 2hrs time step	
t/tp	q/qp	t=Tp*t/tp	q=Qp*q/qp	t	q
0	0	0	0	0	0
0.1	0.03	1	7.32	2	24.39
0.2	0.1	2	24.39	4	75.61
0.3	0.19	3	46.34	6	160.99
0.4	0.31	4	75.61	8	226.84
0.5	0.47	5	114.64	10	243.92
0.6	0.66	6	160.99	12	226.84
0.7	0.82	7	200.01	14	190.26
0.8	0.93	8	226.84	16	136.59
0.9	0.99	9	241.48	18	95.13
1	1	10	243.92	20	68.3
1.1	0.99	11	241.48	22	50.49
1.2	0.93	12	226.84	24	35.86
1.3	0.86	13	209.77	26	26.1
1.4	0.78	14	190.26	28	18.78
1.5	0.68	15	165.86	30	13.42
1.6	0.56	16	136.59	32	9.76
1.7	0.46	17	112.2	34	7.07
1.8	0.39	18	95.13	36	6.1
1.9	0.33	19	80.49	38	3.66
2	0.28	20	68.3	40	2.68
2.2	0.207	22	50.49	42	2.39
2.4	0.147	24	35.86	44	2.39

2.6	0.107	26	26.1	46	0.97
2.8	0.077	28	18.78	48	0.97
3	0.055	30	13.42	50	0
3.2	0.04	32	9.76	52	0
3.4	0.029	34	7.07	54	0
3.6	0.025	36	6.1	56	0
3.8	0.015	38	3.66	58	0
4	0.011	40	2.68	60	0
4.5	0.005	45	1.22	62	0
5	0	50	0	64	0

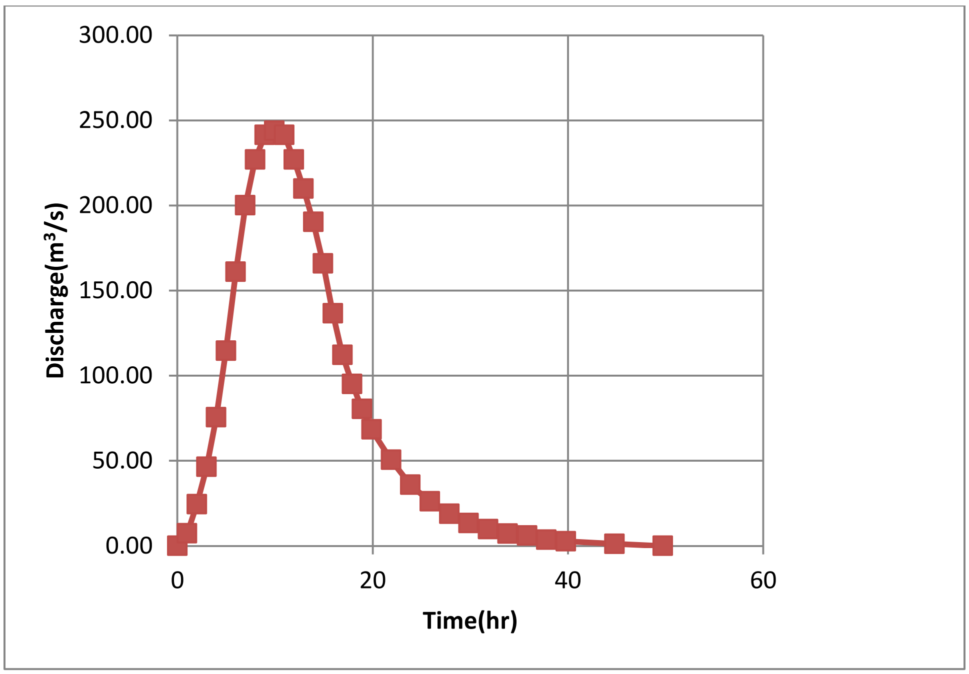

Figure 3. 8 SCS Unit Hydrograph

3.4.1.2.1.3. Convolution of PMP with UH

To convolute the PMP and UH and to obtained PMF hydrograph the following procedure were made

- ✓ Qp and Tp was determined from watershed characteristics by synder (Table 3.7) as a result SCS Dimensionless unit hydrograph was developed (Table 3.8) and interpolate the discharge in to two hour time step to make suitable for final PMF hydrograph.
- ✓ The temporal distribution of areal rainfall was prepared (Table I-9 under appendices)
- ✓ Accumulated rainfall was calculated from Table I-9(Table I-10 under appendices)
- ✓ Excess rainfall was calculated by subtract infiltration rate of 6hr/2hr (3mm/hr) (Table I-11 under appendices)
- ✓ Excess rainfall from Table I-11 was put in Reverse Critical Sequencing(Table I-12 under appendices)
- ✓ By convoluting the ordinates of the UH (Table 3.8) with the hourly values of PMP (Table I-12 in Appendices), the direct runoff hydrograph ordinates (DRO) of the PMF was obtained (Table I-13 in Appendices).

To have a complete PMF a base flow has to be added in the Direct Runoff Hydrograph (DRH). From the available a stream flow data at Gilgle Abay near merawi stations which are located on confluence of Jema River at downstream of the dam, base flow was determined using a graphical base flow separation technique. This base flow is then added to the PMF to get a full hydrograph with peak flow of 1726.28 m^3/s as shown in (Table I-13 in Appendices).

By the same procedure the PMF hydrograph of streams of jema river tributaries at downstream were prepared, their catchment characteristics is put under appendices (Table I 14 and 15) and their final PMF hydrograph is put under result section.

3.4.2. Breach Model (HEC-RAS)

3.4.2.1. HEC-RAS Model

The Hydrologic Engineering Center's River Analysis System (HEC-RAS) is a simulation software developed by the US Army Corps of Engineers and has been developed to manage rivers and other public works under their jurisdiction. The HEC-RAS system contains four one-dimensional river analysis components for: (1) steady flow water surface profile computations; (2) unsteady flow simulation; (3) movable boundary sediment transport computations; and (4) water quality analysis. A key element is that all four components use a common geometric data representation and common geometric and hydraulic computation routines (HEC, 2010).

The HEC-RAS system is comprised of a graphical user interface, separate hydraulic analysis components, data storage and management capabilities, and graphing and reporting facilities. The HEC-RAS modeling system was developed as part of the Hydrologic Engineering Centers Next Generation software and replaces several existing Corps of Engineers programs, including the HEC-2 water surface profile program (ASCE, 2014).

The dam break tool in HEC-RAS can simulate the breach of an inline structure such as dam, or a lateral structure such as a levee. The latest versions of the HEC-RAS model include algorithms to model both overtopping and piping breaches (HEC, 2010). HEC-RAS uses hydraulic principles through cross sections upstream and downstream of the dam to define how the reservoir drains during the formation of a dam breach.

The dam crest is modeled as an inline weir and either a piping failure or overtopping failure is simulated with enlargement of the breach occurring over time as defined by a specified breach progression. Flow through the piping hole is calculated as orifice flow and flow through the breach is calculated as weir flow. The water surface profile upstream of the dam is back-calculated using unsteady momentum and hydraulic principles for each time step and the resulting drawdown through the hole and/or breach produces an outflow hydrograph. Resulting water levels for each time step downstream of the dam are used to model potential backwater effects and the weir and orifice coefficients are automatically adjusted for submergence, if necessary.

HEC-RAS can also model a piping failure that does not progress to the point of collapsing the crest. In this scenario, the piping hole is simulated as a sluice gate (HEC, 2010). The simplest case that can be used for testing the coupling of breach process models with HEC-RAS is that of a single reach bounded upstream by a dam with a reservoir described by a storage-elevation function, and the next refinement that can be simulated is the same system with dynamic routing being used for flow in the reservoir. HEC-RAS gives several plots, tables, cross sections, profiles and 3D plots for evaluating the results of a dam break analysis. The hydrograph can be viewed at any desired location (Brunner, 2010)

Dam break simulations are performed with HEC-RAS for dam safety studies as well as for flood damage analyses for situations that involve possible dam breaches (D. Michael Gee, 2010).These studies usually need to address the following situations and their associated uncertainties.

Dam failure scenarios

Two scenarios were created using HEC-RAS, the first scenario is the Probable Maximum Flood (PMF) dam breach and the second is the Sunny day dam breach. These two scenarios were usually utilized by different researchers for earthen dam breach analysis using HEC-RAS model (Y. XIONG, 2011).

PMF scenario: this scenario relates to a dam's inability to cope with an extreme rain event. It is also called overtopping/rainy season failure scenario. Presumably, very heavy rainfall which causes a build-up of water capable of overwhelming a dam is not likely to be confined solely to the catchment above the dam and entirely held back until the moment of failure.

Rather, a dam-failure flood is likely to be accompanied, before and after failure actually occurs, by flooding downstream and in adjacent, possibly tributary, catchments. In such a situation it would be expected that the emergency services would already be active by the time the failure took place and that some people would already have been evacuated from low-lying areas. Equally, though, evacuation routes may have already been lost. The cutting of such routes is predictable in the case of rain-related dam failure and must be considered as part of the planning process.

Sunny day scenario: Also referred to as a "Normal Pool" failure because it occur independent of rain events, even on sunny days, is initiated by erosion of material due to piping, earthquakes, slope instabilities, foundation weaknesses, or other structural weaknesses.

Worldwide, many dams have collapsed through internal erosion (piping). Hydraulically; this type of failure is often modeled as a combination of orifice and weir flow.

A dam is modeled within HEC-RAS model by using the Inline structure editor. An inline structure is represented with a weir profile (that includes the spillway) and gates for normal low-flow operation. An example of an inline structure is given in figure.3.10

The Inline structure editor allows the user to put in an embankment, define overflow spillways and weirs, and gated openings (radial or sluice gate). The lake area upstream of the dam can either be modeled with cross sections or by using a storage area. If x-sections are used, then HEC-RAS will perform full unsteady flow routing through the reservoir pool and downstream of the dam. If a storage area is used, HEC RAS uses level pool routing through the lake, then unsteady flow routing downstream of the dam. When using a storage area to represent the reservoir pool, HEC-RAS requires x-sections inside of the reservoir pool, then the Inline structure representing the dam, and then downstream x-sections

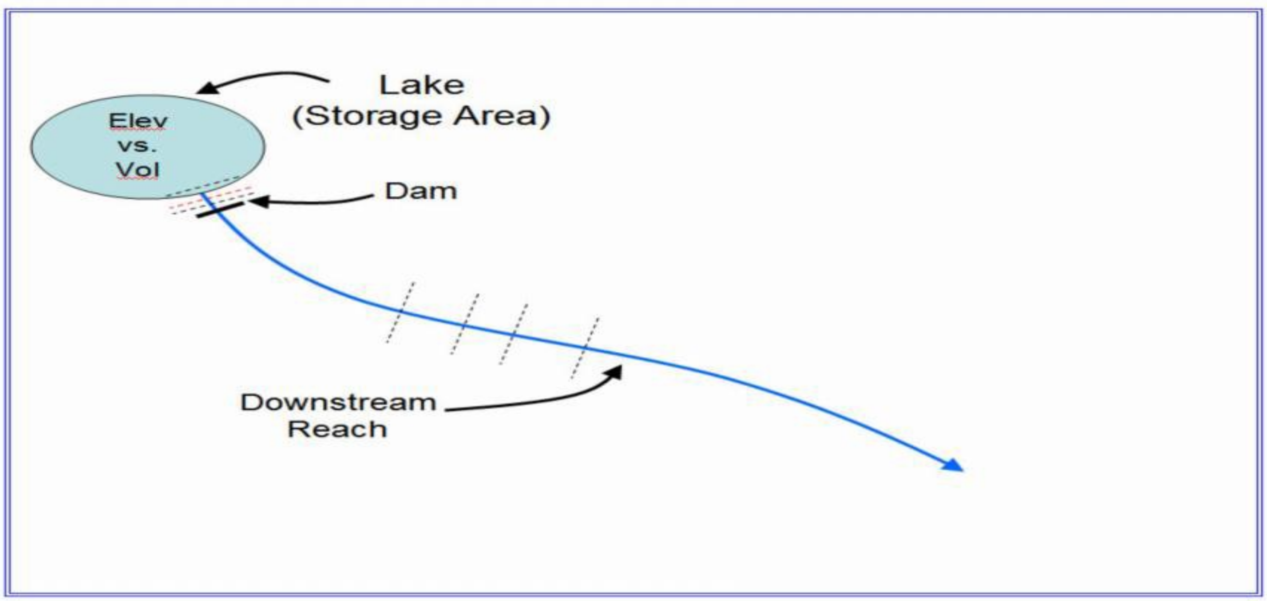

Figure 3. 9 HEC-RAS dam break module concept (HEC, 2010)

In this thesis study, cross-sections are used inside of the reservoir; therefore, HEC-RAS will perform full unsteady flow routing through the reservoir pool and downstream of the dam. The routing reach is hydraulically connected to the reservoir (storage area) with the first (most upstream) x-section. This x-section water surface is forced to the elevation of the water surface in the storage area during the unsteady flow routing. The second x-section in the pool area is required as a bounding x-section for the inline structure (the dam). Figure 3.10 summarizes an inline structure and data entry in HEC-RAS model for dam break analysis. In general, during dam break simulation, the modeler must specify the following parameters to describe a dam breach:

Failure location: transverse location of the centerline of the breach in the dam. This is selected based on many factors (type and shape of dam, failure type and mode). In general, one should consider all factors about the dam, including any historical knowledge of seepage and foundation problems, and place the breach location in the most probable location for each failure type. Commonly, the center of the breach is set to the centerline of the downstream main channel.

Failure mode: overtopping or piping failure. The HEC-RAS breach computations include both overtopping and piping failure modes. Any other failure mode can be approximated with one of those two methods. The failure mode is the mechanism by which the breach occurs. Overtopping failures start at the top of the dam and grow to maximum extents; while a piping failure can start at any elevation/location and grow to the maximum extents. The ultimate breach size and breach time are much more critical in the estimation of the outflow hydrograph than the failure mode. In general, the following data are required for overtopping and piping modes of failures (HEC, 2010).

For overtopping mode of failure: Average width of the ultimate breach configuration**,** Top and bottom elevations of the breach configuration**,** Breach side slopes**,** Time of breach formation

For piping mode of failure: Average breach width of the ultimate breach configuration**,** Top elevation of the ultimate breach configuration**,** Breach side slopes**,** Centerline elevation of initial piping location and Time of breach formation.

Trigger condition: pool elevation, pool elevation + duration, or clock time.

Weir and pipe flow coefficients: weir coefficients are used to compute overtopping/weir flow, and an orifice coefficient is used to compute piping/pressure flow.

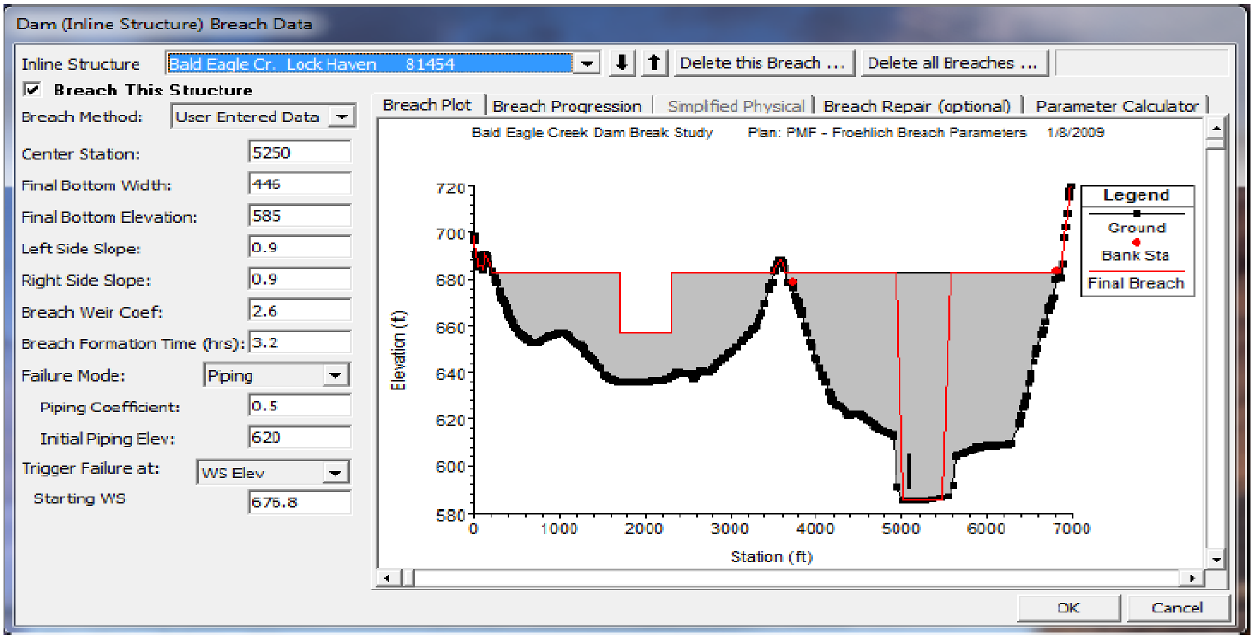

Figure 3. 10 An example of inline structure breach data editing

3.4.2.2. HEC-GeoRAS

HEC-GeoRAS is an ArcGIS extension developed by the HEC. This model contains a set of tools specifically designed to process geospatial data to support hydraulic model development and analysis of water surface profile results. It assists in creating data sets in GIS to extract information essential for hydraulic modeling. After steady or unsteady flow simulation, HEC-RAS results can be exported for processing in the GIS by GeoRAS. The user can read the HEC-RAS results into the HEC-GeoRAS and perform the flood inundation mapping.

3.4.2.3. Equations to Predict Dam Break Parameters

The most important component of a dam break analysis is the definition of reasonable breach parameters, which are highly difficult to be accurately predicted. The breach width (b), breach height (hb) and breach time (Tf) have a great influence on the forecast of the outflow and the flooded area downstream of the dam. For relatively small reservoirs, the dam break peak outflow usually occurs before the breach is completely developed, resulting from a consistent drop in reservoir levels during the formation of the rupture, while in large reservoirs the dam break peak outflow occurs as soon as the breach has extended to its maximum size (Colorado Dam Safety Office, 2010).

MacDonald and Langridge-Monopolis (1984): The data that MacDonald and Langridge-

Monopolis (1984) used for their regression analysis had the following ranges.

- Height of the dams: 4.27 - 92.96 meters
- Breach outflow volume: 0.0037 – 660.0 x $10^6 m^3$

The following is the MacDonald and Langridge-Monopolis (1984) equation for the volume of material eroded and breach formation time, as reported by Wahl (1998):

For earthfill dams:

$$V_{eroded} = 0.0261\ (V_{out} * h_w)^{0.769} \ldots\ldots\ldots\ldots\ldots (3.18)$$

$$T_f = 0.0179\ (V_{eroded})^{0.364} \ldots\ldots\ldots\ldots\ldots\ldots\ldots (3.19)$$

For earthfill with clay core or rockfill dams:

$$V_{eroded} = 0.00348\ (V_{out} * h_w)^{0.852} \ldots\ldots\ldots\ldots.... (3.20)$$

Where: V_{eroded} = volume of material eroded from the dam embankment (cubic meters)

V_{out} = volume of water that passes through the breach (cubic meters)

h_w = depth of water above the bottom of the breach (meters)

T_f = breach formation time (hours)

The base width of the breach can be computed from the dam geometry with the following equations:

$$W_b = \frac{V_{eroded} - h_b^{2}\left(CZ_b + h_b Z_b . \frac{Z_3}{3}\right)}{h_b\left(C + h_b . \frac{Z_3}{3}\right)} \ldots\ldots\ldots\ldots\ldots.... (3.21)$$

$$V_{eroded} = 0.00348\ (V_{out} * h_w)^{0.852} \ldots\ldots\ldots\ldots.... (3.22)$$

Where: - Wb = Bottom width of the breach (m)

Veroded = Volume of water eroded from the dam

Vout = Volume of water that passes through the breach

hw = depth of water above the bottom of the breach

hb = Height of the dam to the bottom of the breach

C = Crest width of the top of the dam

Z3 = Z1+Z2

Z1 = Upstream Slope of the dam

Z2 = Downstream Slope of the dam

Zb = Side Slope of the Breach

MacDonald and Langridge-Monopolis (1984) stated that the breach should be trapezoidal with side slope of 0.5H: 1V. Shown below is a peak flow equation that is developed from historic dam failures, by Mac Donald and langridge-Monopolis (1984).

$$Q = 3.85(V_w h_w)^{0.411} \text{……………………….. (3.23)}$$

Where: hw = Depth of water above the breach invert at time of breach (m)

Vw = Volume of water above breach invert at time of failure (m3)

Von Thun and Gillette (1990): The data that Von Thun and Gillette used for their regression analysis had the following ranges.

- Height of the dams: 3.66 - 92.96 meters
- Volume of water at breach time: 0.0037 – 660.0 x $10^6 m^3$

The Von Thun and Gillette equation for average breach width is:

$$Bave = 2.5hw + Cb \text{……………………... (3.24)}$$

Where: Bave = average breach width (meters)

hw = depth of water above the bottom of the breach (m)

Cb = coefficient, which is a function of reservoir size

Von Thun and Gillette developed two different sets of equations for the breach development time. The first set of equations shows breach development time as a function of water depth above the breach bottom:

$$T_f = 0.02\, h_w + 0.25 \quad \text{(erosion resistant) ……. (3.25)}$$

$$T_f = 0.015\, h_w \quad \text{(easily erodible) ……... (3.26)}$$

Where: T_f = breach formation time (hours)

h_w = depth of water above the bottom of the breach (meters)

The second set of equations shows breach development time as a function of water depth above the bottom of the breach and average breach width:

$$T_f = \frac{B_{ave}}{4h_w} \quad \text{(erosion resistant) ……... (3.27)}$$

$$T_f = \frac{B_{ave}}{4hw+61} \quad \text{(easily erodible) ………. (3.28)}$$

Where: hw = average breach width (meters)

Cb is function of reservoir size and given in table 3.9.

Table 3. 9 Values of Cb Based on Reservoir Size

Size of reservoir (m^3)	C_b (m)
$<1.23*10^6$	6.3
$1.23*10^6$-$6.17*10^6$	18.3
$6.17*10^6$-$1.23*10^7$	42.7
$>1.23*10^7$	54.9

Froehlich (2008): The data that Froehlich used for his regression analysis had the following ranges.

Height of the dams: 3.05 -92.96 meters

Volume of water at breach time: 0.0139 – 660.0 x $10^6 m^3$

Froehlich's regression equations for average breach width and failure time are:

$$B_{ave} = 0.27\, K_o\, V_w^{0.32}\, h_b^{0.04} \text{ .... } (3.29)$$

$$T_f = 63.2\sqrt{\frac{V_w}{g h_b^2}} \text{ .... } (3.30)$$

Where: Bave= average breach width (meters)

Ko= constant (1.3 for overtopping failures, 1.0 for piping)

Vw= reservoir volume at time of failure (cubic meters)

hb = height of the final breach (meters)

g = gravitational acceleration (9.80665 m/sec2)

Tf = breach formation time (seconds)

Froehlich's 2008 paper states that the average side slopes should be:

1H: 1V for overtopping failures

0.7H: 1V otherwise (i.e. piping/seepage)

While not clearly stated in Froehlich's paper, the height of the breach is normally calculated by assuming the breach goes from the top of the dam all the way down to the natural ground elevation at the breach location.

Frohelich has suggested the peak flow as follows;

$$Q = 0.607 V_w^{0.295} h_w^{1.24} \text{ .... } (3.31)$$

3.4.2.4. Approach followed to dam break analysis

An event-based approach is a deterministic method that requires the use of a specific or series of specific precipitation and non-precipitation events for the evaluation of dam failure and downstream inundation mapping. These events include extreme rainfall and runoff events that can lead to natural floods of variable magnitude. The maximum flood for which a dam is to be designed or evaluated is often dependent on its existing hazard potential classification or size classification (FEMA, 2013).

Typically, several hydrologic and non-hydrologic (fair weather) events are evaluated as part of an event-based dam safety analysis. For hydrologic failure events, an extreme flood event ranging from the 50-year event for low-hazard dams up to the PMF for high-hazard dams is selected based on the potential for loss of life due to a dam failure or for significant economic and environmental losses. Typically, the hazard potential classification of the dam is used to select the extreme hydrologic failure event. The PMF is the flood that may be expected from the most severe combination of critical meteorological and hydrologic conditions that are reasonably possible in the drainage basin under study. The Probable Maximum Precipitation (PMP) is an estimate of the maximum possible precipitation depth over a given size catchment for a given length of time (Stedinger et al. 1996).

Fair Weather (Non-Hydrologic) Failure

As defined by FEMA (2013) a fair weather (Sunny Day) breach is a dam failure that occurs during fair weather (i.e., non-hydrologic or non-precipitation) conditions. A fair weather breach is analyzed by establishing an initial reservoir water level and commencing a breach analysis without additional inflow from a storm event. A fair weather breach is typically used to model piping failures for hydrologic, geologic, structural, seismic, and human-influenced failure modes.

Base flow conditions for a fair weather failure are typically ignored because of the small discharge and volume compared to that of a dam breach. As a general guidance, base flow can be ignored if the dam breach flow is two times greater than the base flow. Where base flow is considered, the discharge is typically estimated based on reported base flows through the dam's outlet works or from stream gage records. The three most common initial water level elevations for fair weather breach analyses are;

Normal Pool Elevation: A breach at the normal pool elevation of the reservoir is used to estimate the volume and associated breach discharge that would result from a failure event during fair weather conditions. For an embankment dam, this type of event is modeled as piping/internal erosion failure, whereas for a concrete dam, this event is modeled as a monolith collapse resulting from sliding, foundation instabilities, or a seismic event (FEMA, 2013).

Invert of Auxiliary Spillway (lowest uncontrolled spillway): A breach of the dam with the reservoir water level set at the auxiliary spillway (also referred to as an emergency spillway) is common practice to simulate a breach during disoperation of the primary outlet works. Initiation of dam failure is typically the same as for the reservoir level at normal pool (FEMA, 2013).

Top of Dam / Maximum High Pool: The reservoir level set to the top of the dam to represent the maximum amount of volume that may be stored in the reservoir. This condition may be selected to evaluate the most conservative non-hydrologic event. In practice, dams without adequate spillways or pump storage facilities, where the water level during non-hydrologic events is maintained at the top of dam, are unique situations subject to this conservative assumption. A breach event when the water level is at the top of dam may be modeled as a piping / internal erosion failure or as an overtopping failure with the water level just above the top of dam invert (FEMA, 2013).

Various Federal agency publications provide guidance for establishing the initial water surface elevation of a reservoir during a fair weather failure event. Each of these specified elevations is used to characterize different failure modes as well as the potential volume of the reservoir at the time of failure. The normal pool elevation is recommended as the default volume for the fair weather failure. States should consider a larger storage volume for dams where the primary and emergency spillway systems are considered susceptible to blockage resulting in a higher water surface elevation and volume during a non-hydrologic event.

Hydrologic Failure

Hydrologic breaches that occur with extreme precipitation and runoff are termed “rainy day” or hydrologic failures. Hydrologic failures that cause dam breach events are generally analyzed based on the IDF established by the dam’s hazard potential and hazard size classification, typically a PMF for high-hazard potential dams. For significant-hazard potential dams, the breach event may include a breach of the PMF and IDF that could range from the 1-percent-annual-chance flood event (often called the 100-year flood) to a percentage of the PMF (FEMA, 2013).

3.4.2.5. Overtopping Failure

Jema Dam has been tested for overtopping failure using the model HEC RAS and applying a PMF inflow while the reservoir is at full condition i.e. when upstream water level is at Dam crest level. The following dam breach data were used in overtopping failure mode (Figure I-4 under appendices).

Table 3.10 Dam Breach Data for Overtopping Failure

Top of dam elevation :	2133.9m
Pool elevation at failure:	2133.9m
Breach bottom elevation:	2063m
Pool volume at failure:	162.9MCM
Dam crest width:	10m
Slope of upstream dam face	(H: V):1.75
Slope of downstream dam face	(H: V):1.5
Trigger failure at:	2133.9m
Breach weir coefficient:	1.44

3.4.2.6. Piping Failure

Piping through embankment body may be formed due to excessive seepage that may be triggered when the impervious core material used is poor in quality or when the construction procedure does not follow engineering standards. The Model HEC RAS simulates piping failure with elevation of piping line being defined by the user. Other geometry of the dam is as defined in the case of overtopping failure.

As explained in section 3.1, the outlet of the dam is through the body of the dam .2097.5m elevation is assumed susceptible point of start for piping. The following dam breach data were used in piping failure mode simulation (Figure I-4 under appendices).

Table 3. 11 Dam Breach Data for Piping Failure

Top of dam elevation:	2133.9m
Pool elevation at failure:	2127.6m
Breach bottom elevation:	2063m
Pool volume at failure:	124.2MCM
Dam crest width:	10m
Slope of upstream dam face :	(H: V):1.75
Slope of downstream dam face:	(H: V):1.5
Initial piping elevation:	2099.5m
Trigger failure at:	2127.6m
Breach weir coefficient:	1.44
Piping coefficient:	0.5

3.4.2.7. Analysis Scenarios

The dam break modeling was proposed to be analyzed for possible combination of events and set-ups. The analysis considers:

Gilgele Abay River 32 km from jema dam to downstream.

Jema downstream 1 tributary which join jema River10km from dam in right side.

Jema downstream 2 tributary which join Jema River 11 km from dam in left side.

Here are the scenarios set for analysis:

Jema Dam Overtopping Break with Gilgel abay mean flow (Scenario1)

Jema Dam Piping Break with Gilgel abay mean flow (Scenario2)

Jema Dam Overtopping Break with Gilgel abay PMF flow (Scenario3)

For the first and the third scenarios, a catastrophic full PMF inflow hydrograph was used as the inflow hydrographs at the upstream end (i.e. Jema dam) of the modeling reach and at lateral inflow(Gilgel Abay and the other two tributaries). But for scenario two the two tributaries were not considered because they are seasonal streams and almost no flow during sunny day.

The value of the lateral mean inflow of Gilgel Abay River were obtained from the daily observed flow data collected at Ministry of Water, Irrigation and Energy department of hydrology. The annual average flow was found 132.2m^3/s.

Mean flow of Jema river at dam for piping failure mode were taken from Koga river flow station near Merawi because Jema River is ungagged .since the two stream drain in to adjacent catchments with similar hydrological characteristics the koga flow data can represent Jema catchment flow (Figure 3.4). The annual average flow and area of Koga River at station was found 45.3m^3/s and 259 km^2 respectively.

The discharges from Koga gauge station were transferred to Jema dam outlet using the following formula. (FAO, 1997; Goldsmith, 2000)

$$Qjema = \left(\frac{\text{DA of jema}}{\text{DA of koga}}\right)n * Qkoga \qquad (3.32)$$

Where:

Qjema = discharge at Jema dam

Qkoga = discharge at koga gauge station

DAkoga = drainage area at koga gauge station

DAjema = drainage area at Jema dam

The exponent n varies between 0.6 and 1.2. If the DAsite is within 20% of the DAgauge (0.6≤DA of site divided by / DA of gauge ≤1.2), n value equal to 1 is used, otherwise the value 0.6 is used. The ratio of jema area to koga area is 0.84(218/259) therefore the exponent n was taken 1 and based on the above formula annual average average flow of jema river at the dam found to be 38.1m^3/s.

3.4.3. Downstream Flow Routing and Flood Mapping

The Outflow hydrograph resulted from the breaching dam is routed through the downstream river channel and flood plain and different maps of the resulting water surface extent, water depth and velocity are produced. The models HEC-RAS and HEC-GeoRAS are used integrally to extract topographic data, analyze the flow hydraulics and finally to generate the maps.

3.4.3.1. HEC-GeoRAS/Pre-Processing

The geo-spatial data used for hydraulic computation in HEC-RAS, can be prepared either by conducting detail surveying data or extracting from DEM. In this research, collecting land surveying data is almost impossible due to the fact that the study area is very wide to cover in a short period of time. Therefore, a DEM with 12.5x12.5m resolution has been used.

Layers Development in HEC-GeoRAS

The stream centerlines layer, bank lines layer, flow path layer, cross sectional cut line layer were created at the beginning. The development of all other layers is optional based on the data needs for the river analysis model. The layers which were created in HEC-GEORAS and their definitions are tabulated in the table 3.12 below.

Table 3. 12 Summary of RAS Layers Definition

RAS Layers	Description
Stream centerline	Used to identify the connectivity of the river network and assign river stations to computation points.
Cross-sectional cut lines	Used to extract elevation transects from the DEM at specified locations and other cross-sectional properties.
Bank lines	Used in conjunction with the cut lines to identify the main channel from overbank areas.
Flow path centerlines	Used to identify the center of mass of flow in the main channel and overbanks to compute the downstream reach lengths between cross sections.

Among these four layers the flow path layer need to be identified as being in the “left” overbank, “right” overbank or main “channel” and the stream centerline should be given river code and reach code. 98 cross sections for Jema River were taken at an approximate interval of 200m. Elevation data then were extracted from DEM and imported to HEC-RAS. As a rule each cross-section should be perpendicular to flow direction, and can intersect the main channel only once and may not intersect another cross section. The cross section cut lines should be long enough for the flood to attenuate and to include points of interest (Figure 3.11).

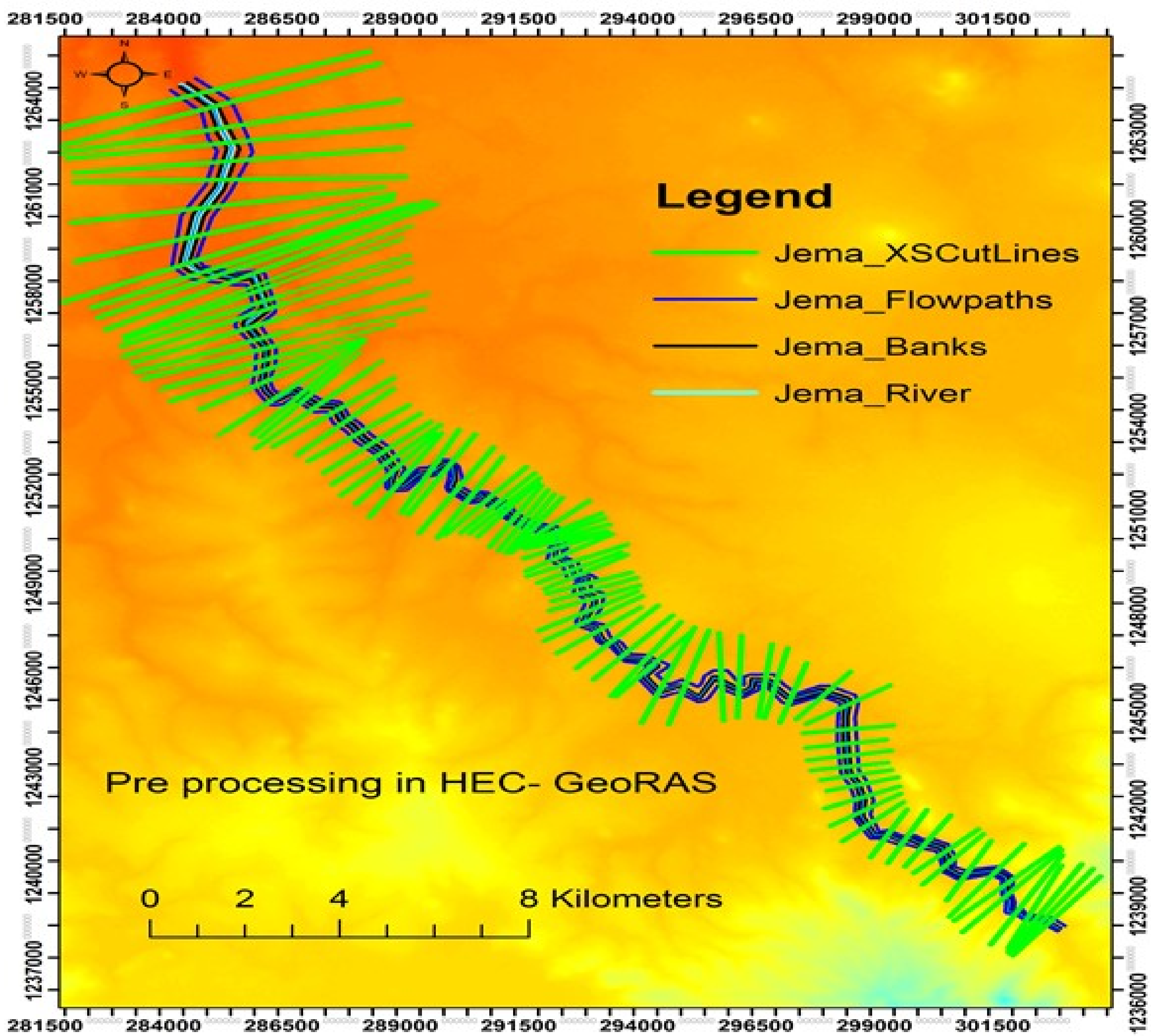

Figure 3. 11 Pre-processing stage in HEC-GeoRAS

3.4.3.2. Flood Routing on HEC-RAS/Processing

The breach outflow discharge is routed through downstream channel and flood plain using the model HEC-RAS. The model requires geometry data of downstream river channel and flood plain, boundary flow conditions at both upstream and downstream ends, and manning's roughness coefficient at different locations.

Geometry Data Setup:

The model requires detail river route, river bank lines, flow path centerlines and river channel and flood plain cross-section data for analyzing the flow. Spacing of the cross-sections is critical parameter the model stability. 30m maximum interpolation was used in this thesis. Geometry data were extracted from DEM using HEC-GeoRAS and exported into HEC-RAS. The plan view of imported river route and cross-section cut lines is shown on Figure 3.12. In HEC- RAS the cross-section spacing can further be interpolated into a minimum spacing if the model goes unstable. The river bank stations and overbank distance to immediate downstream station can also be edited here. Stationing of every point on the cut-lines is made by measuring its distance from the starting point on left bank.

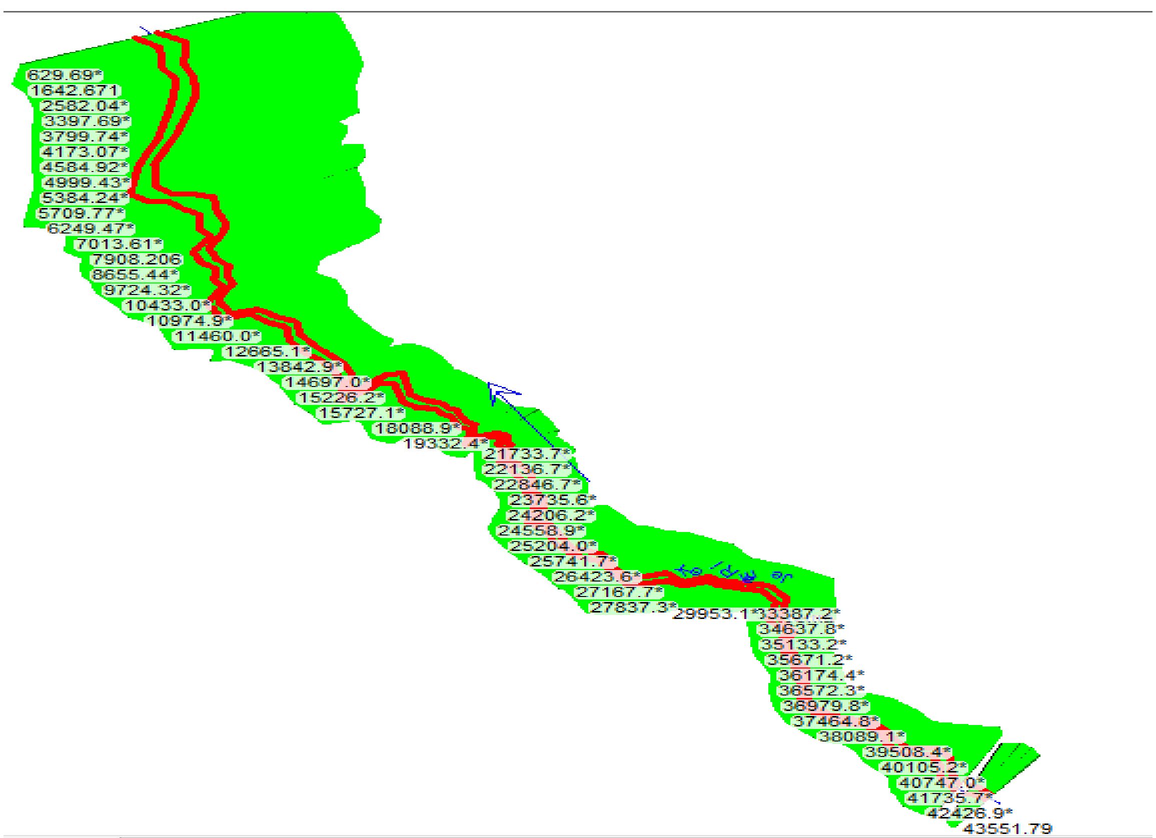

Figure 3 .12 Geometry Plan in HEC-RAS after interpolated by 30m space distance.

Manning's Roughness Coefficient

It's difficult to assign a specific representative friction value even for small areas. Especially when we come to natural channels it's possible to find a wide range of land use land cover types within small reaches. It is because of this fact that recently some dam breach analysis studies are focused on sensitivity analysis of the peak breaching flood upon increasing or decreasing the manning coefficient.

Table 3. 13 Manning roughness coefficients for various open channel surfaces (Chow, 1988)

Material	Typical Manning roughness coefficient
Concrete	0.012
Gravel bottom with concrete sides	0.020
Gravel bottom with mortared stone	0.023
Gravel bottom with riprap	0.033
Clean, straight stream	0.030
Clean, winding stream	0.040
Winding with weeds and pools	0.050
With heavy brush and timber	0.100
Pasture Flood plains	0.035
Flood plains with flood plains	0.040
Flood plains with light brush and weeds	0.050
Dense brush	0.070
Dense trees	0.100

The Manning roughness value ranges suggested by Chow (1959) for main channels and the floodplains in case of "Minor Streams" were identified as follows:

Minor streams (surface width at flood stage less than 100 feet)

Some weeds, light brush on banks……………………..0.035-0.050

Flood plains (adjacent to natural streams)

Light brush and trees:

a) Winter..0.050-0.060

b) Summer...0.060-0.080

In Jema case, the Google earth view of the downstream reaches is significantly green indicating considerable bushes and/or trees are found in downstream river banks. Based on the above justifications the researcher adopts a roughness value between 0.035-0.09.

Flow Boundary Conditions

For unsteady flow analysis, upstream boundary conditions are typically flow hydrographs; design hydrograph of particular return period, or Probable Maximum Flood (PMF) hydrograph (for hydrological induced failures), or a mean inflow which in this case is taken as base flow (for sunny day failure analyses).

Downstream boundary conditions can be set to normal depth, a rating curve, a known water surface elevation, or critical depth. Here, the downstream boundary conditions are input as a normal depth with friction slope of 0.00172. The use of this value as a downstream boundary condition is reasonable since the reach below the last cross section is somehow flat (downstream of bikolo).

Unsteady Flow Computation in HEC-RAS

Once the boundary flow conditions and manning's roughness coefficients are set, HEC-RAS simulates unsteady flow through the channel and flood plain. Simulation date and time duration is set by the modeler. Output data can be obtained at every time rate set initially before run. The model processes the flow routing in three stages. The first task is to analyze the geometry data set followed by unsteady flow simulation. Once the flow is simulated successfully, results are stored and made available for viewing, reporting and exporting to other formats like GIS.

3.4.3.3. Flood Mapping/Post-Processing

After the unsteady flow simulation is done on HEC-RAS and a reasonable water surface profile is obtained, results are exported into HEC-GeoRAS for flood mapping. HEC-GeoRAS basically compares the resulting water surface elevation with the topographic feature and wherever the water surface is higher than the ground elevation, flooding occurs and hence the model delineates the inundated area. Moreover, water depth map and velocity maps are also generated. The water surface extent and depth maps are produced for every time interval the

HEC-RAS was set to simulate.

Initially the file imported from HEC-RAS which is in SDF format is converted into XML format. A layer is then setup where new data frame is added for the map layers to be stored and either grid or raster data set is selected for the mapping task. Once the layer is setup, all the results of HEC-RAS are extracted and then water surface, depth and velocity maps for any required time of occurrence can be mapped using the Ras Mapping tool in HEC-GeoRAS.

4. RESULTS AND DISCUSSION

4.1. Hydrology

Hydrology study was conducted to estimate the probable maximum flood (PMF) of Gilgel abay river and the two Jema downstream tributaries by Hershfield's estimation technique.

Gilgel abay river and two tributaries of PMF hydrograph result by Hershfield's estimation technique

Using hershfield method peak discharge of 1726.28m^3/s was obtained for Gilgel abay as shown in figure 4.1.

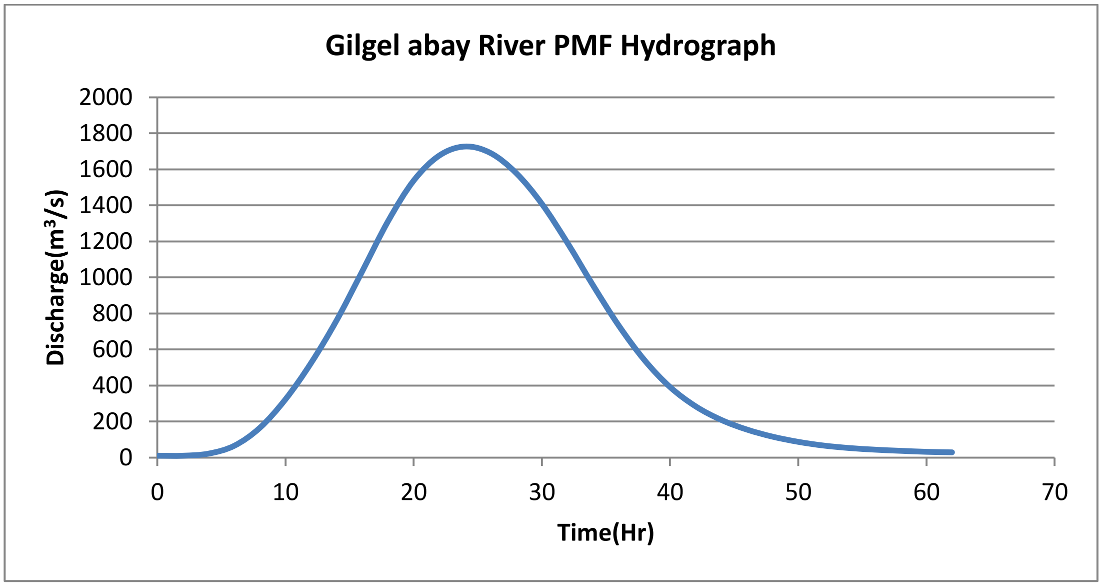

Figure 4. 1 PMF hydrograph of Gilgel Abay river by Hershfield

Using hershfield method peak discharge of Jema downstream right side tributary was 246.4m^3/s as shown in figure 4.2.

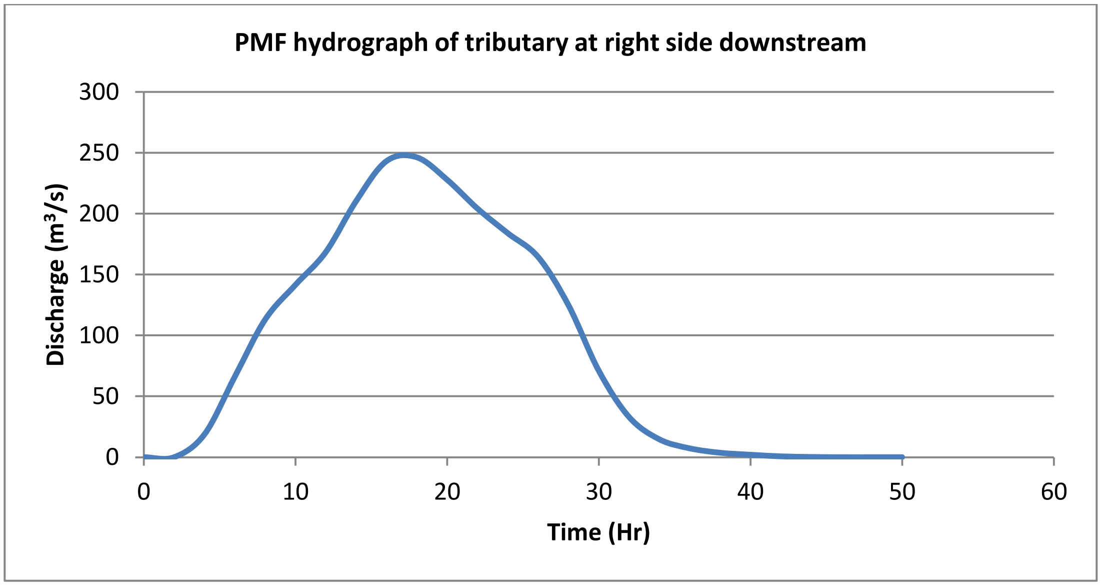

Figure 4. 2 PMF hydrograph of right side tributary 10 km from dam by Hershfield

Using hershfield method peak discharge of Jema downstream left side tributary was 161.4m^3/s as shown in figure 4.3.

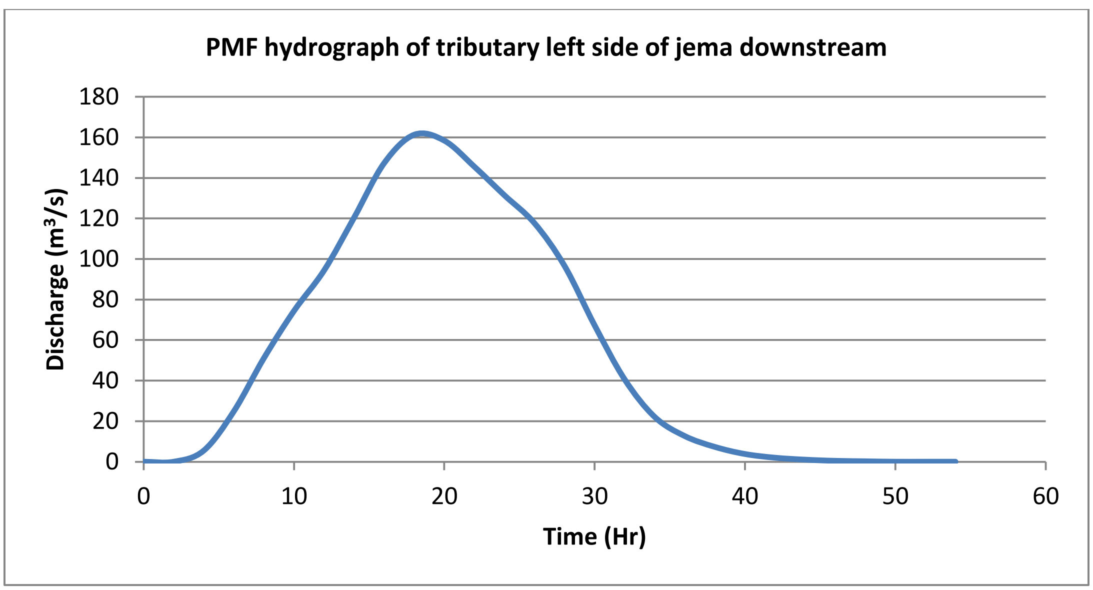

Figure 4. 3 PMF hydrograph of left side tributary 11 km from dam by Hershfield

4.2. Simulation in HEC-RAS Model

The modeling domain was tested for a set of scenarios under overtopping and piping failures. These scenarios were simulated using breach parameter results from three types of estimation methods namely; Frohelich (2008), MacDonald and Langridge-Monopolis (1984) and Von thun and Gillete (1990).

4.2.1. Jema Dam Overtopping Break with Gilgel Abay Mean Flow (Scenario1)

The dam breach peak outflow hydrograph by three estimation methods for the Jema dam resulted from the HEC-RAS dam break modeling is shown in Table 4.1 below.

Table 4. 1 PMF event breach peak outflows for Scenario one

Methods	Peak flow (m^3/s)	Time to peak, (hr) (Starting at 1/1/2025, 00:00)
MacDonald(1984)	51722.79	02/01/2025,10:00
Frohelich (2008)	66328.79	02/01/2025,09:00
Von thun and Gillete (1990)	79886.37	02/01/2025,09:00

In all cases a fictional failure is assumed to occur on 01/1/2025, 0000hr. flood routing at selected river stations in downstream from the dam has resulted the following value in table 4.2.

Table 4. 2 Maximum flow, time to peak, rate of flow and flood height for Jema river stations below the dam using Froehlich (2008)

Stations	Peak flow(m^3/s)	Velocity(m/s)	Flood height(m)	Time to peak(hr)
At Dam	66328.79	15.466	28.9	02/Jan2025,09:00
5km	63535.4	9.071	25.7	02/Jan2025,09:00
12km	38806.84	4.117	18.7	02Jan2025,09:00
20km	36430.77	4.65	22	02Jan2025,10:00
30km	28639.9	6.811	16	02Jan2025,11:00
37km	28771.9	2.253	15.7	02Jan2025,11:00
43km	24419.41	0.46	17.4	02Jan2025,12:00

NB: All distances are measured from dam location

As shown in table 4.2 the peak flow is decreasing starting from the dam downwards up to the final cross-section. The flood height shows an increased value at the dam and it continues to decrease for some distance and increases again at 43km from the dam. Flood depth and velocity is depends on the cross section of river, the amount of discharge, longitudinal slope. The time to peak at dam when analyzed by this method is found to be 09:00hr in the second day from the initial flood beginning time 00:00hr. According to this analysis the whole process i.e. the PMF event beginning upstream of the dam, the dam breach and peak flood at final cross section in the downstream regions has taken 37 hours (Figure 4.4).

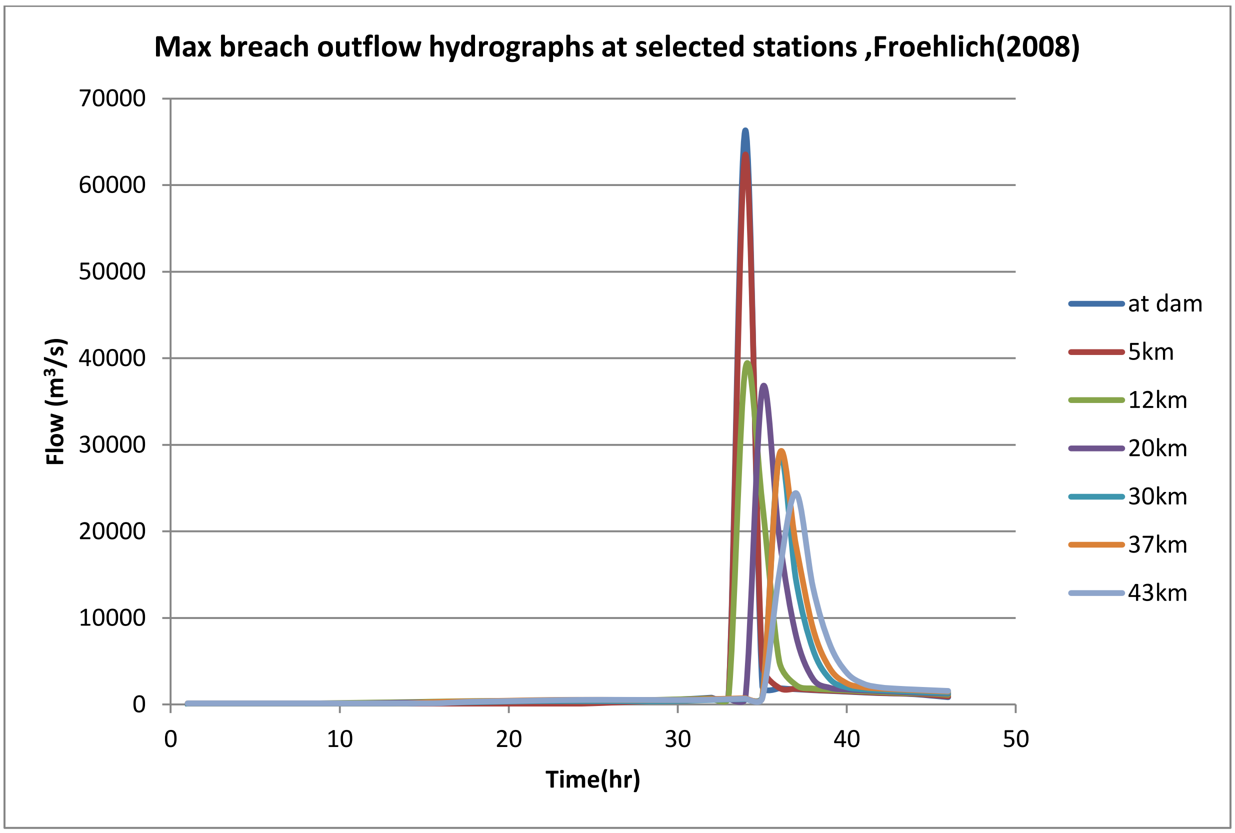

Figure 4. 4 Maximum breach outflow hydrographs at selected stations, Scenario one by Froehlich (2008)

In all cases a fictional failure is assumed to occur on 01/1/2025, 00:00hr. Flood routing at selected river stations in downstream from the dam has resulted the following value.

Table 4. 3 Maximum flow, time to peak, rate of flow and flood height for Jema river stations below the dam using (MacDonald and Langridge-Monopolis (1984)

Stations	Peak flow(m^3/s)	Velocity(m/s)	Flood height(m)	Time to peak(hr)
At Dam	51722.79	13.633	25.3	02/01/2025,10:00
5km	50419.45	7.816	22.6	02/01/2025,10:00
12km	36677.6	3.756	17.7	02Jan2025,10:00
20km	34421.78	4.572	21.6	02Jan2025,11:00
30km	28319.27	6.742	16	02Jan2025,12:00
37km	28451.27	2.244	15.3	02Jan2025,12:00
43km	24405.96	1.795	17.1	02Jan2025,13:00

NB: All distances are measured from dam location

As shown in table 4.3 the peak flow is decreasing starting from the dam downwards up to the final cross-section but the flood increase at 37km from dam this is because mean yearly flow of Gilgele Abay river join the coming flood laterally. The flood height shows an increased value at the dam and it continues to decrease for some distance and increases again at 43km from the dam actually it depends on the cross sectional area of river, discharge and bed slope of river. The flood depth and velocity increase at narrow section and decrease at wider section. The time to peak at dam when analyzed by this method is found to be 10:00hr in the second day from the initial flood beginning time 00:00hr. According to this analysis the whole process i.e. the PMF event beginning upstream of the dam, the dam breach and peak flood at final cross section in the downstream regions has taken 38 hours (Figure 4.5).

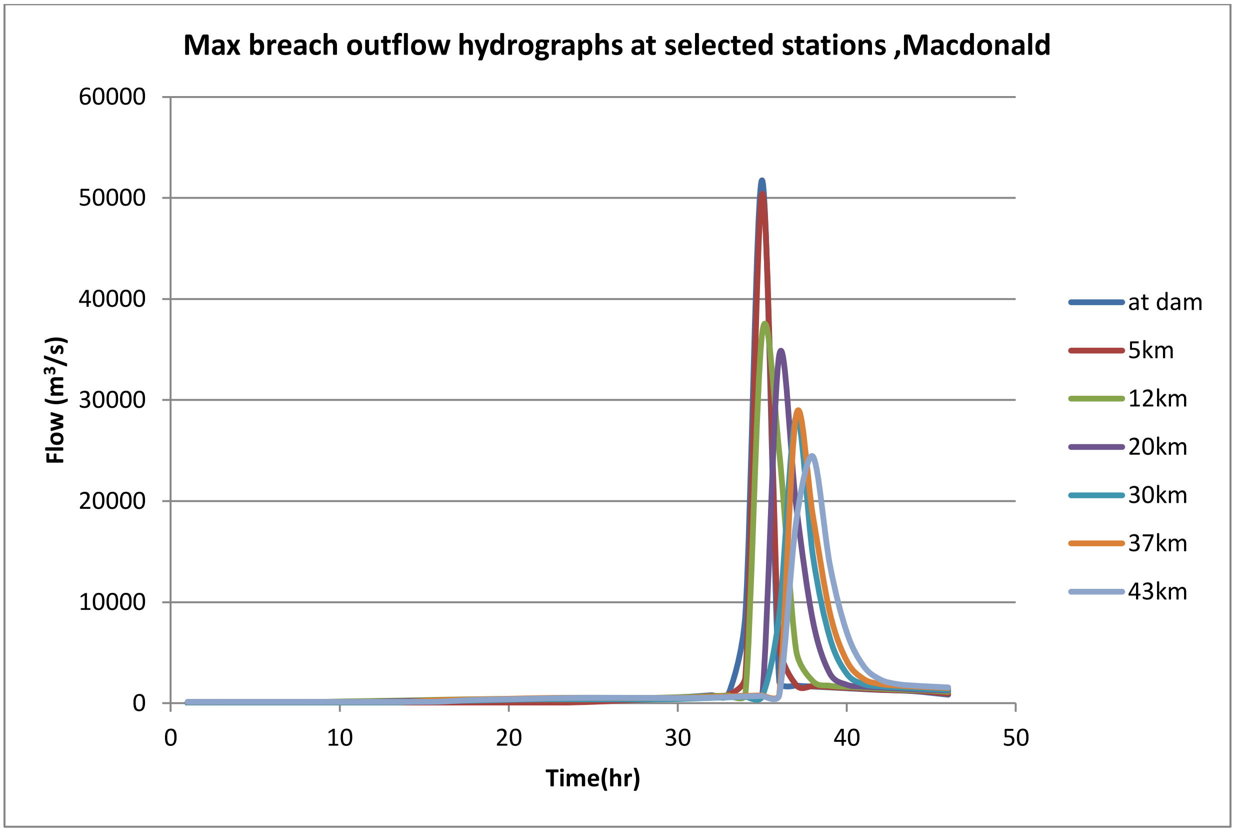

Figure 4. 5 Maximum flow hydrographs at selected stations, overtopping by Macdonald

Table 4. 4 Maximum flow, time to peak, rate of flow and flood height for Jema river stations below the dam using (Von thun and Gillete)

Stations	Peak flow(m^3/s)	Velocity(m/s)	Flood height(m)	Time to peak(hr)
At Dam	79886.37	15.042	28	02/Jan/2025,09:00
5km	77984.88	8.896	25.4	02/Jan/2025,09:00
12km	7178.23	4.174	18.9	02Jan2025,10:00
20km	37716.82	4.722	22.4	02Jan2025,10:00
30km	30609.94	6.896	16.8	02Jan2025,11:00
37km	30741.94	2.279	15.3	02Jan2025,11:00
43km	25713.01	1.751	17.1	02Jan2025,12:00

NB: All distances are measured from dam location

As shown in table 4.4 the peak flow is decreasing starting from the dam downwards up to the final cross-section but the flood increase at 37km from dam because mean yearly flow of Gilgel Abay river join the coming flood laterally. Velocity increase at narrow river cross section and at low roughness coefficient. The time to peak at dam when analyzed by this method is found to be 10:00hr in the second day from the initial flood beginning time 00:00hr.

According to this analysis the whole process i.e. the PMF event beginning upstream of the dam, the dam breach and peak flood at final cross section in the downstream regions has taken 37 hours (Figure 4.6).

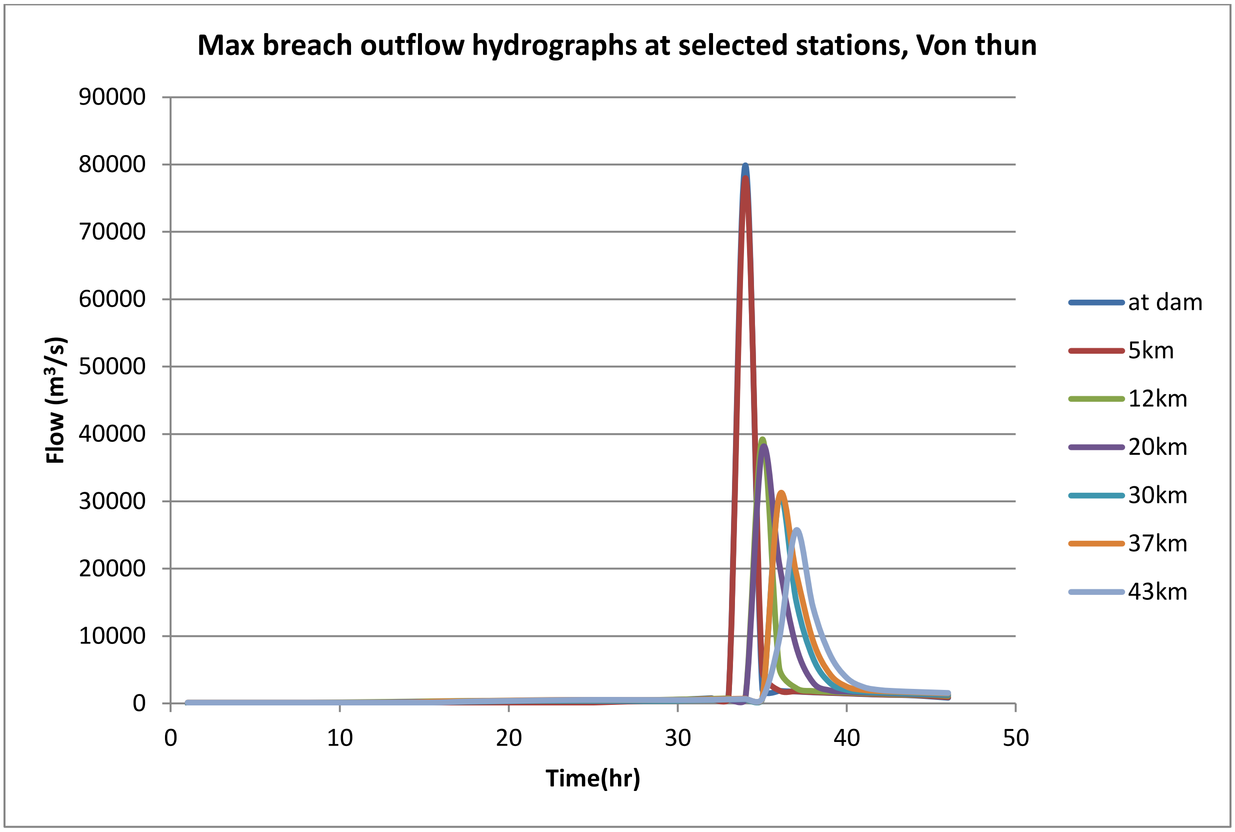

Figure 4. 6 Maximum flow hydrographs at selected stations, overtopping by Von thun and Gillete

4.2.2. Jema Dam Piping Break with Gilgel Abay Mean Flow (Scenario 2)

The dam breach peak outflow hydrograph by three estimation methods for the Jema dam resulted from the HEC-RAS dam break modeling is shown in the Table 4.5.

Table 4. 5 PMF event breach peak outflows for piping mode of failure

Methods	Peak flow (m^3/s)	Time to peak, hr (Starting at 1/1/2025, 00:00
MacDonald (1984)	27344.67	01Jan2025,02:00
Frohelich (2008)	50956.07	01Jan2005,01:00
Von thun and Gillete(1990)	48474.42	01Jan2025,01:00

In all cases a fictional failure is assumed to occur on 01/1/2025, 0000hr. piping failure mode was assumed to occur during sunny day.

Table 4. 6 Maximum flow, time to peak, rate of flow and flood height for Jema river stations below the dam during piping using Froehlich(2008).

Stations	Peak flow(m^3/s)	Velocity(m/s)	Flood height(m)	Time to peak(hr)
At Dam	50956.07	13.472	24.6	01Jan2005,01:00
5km	49851.02	7.563	21.5	01Jan2005,01:00
12km	24918.21	3.475	16.1	01Jan2005,02:00
20km	21170.35	4.038	19.3	01Jan2005,02:00
30km	21050.2	5.968	13.3	01Jan2005,03:00
37km	21180.09	1.951	13.9	01Jan2005,03:00
43km	17864.42	1.82	15.1	01Jan2025,04:00

NB: All distances are measured from dam location

As shown in table 4.6 the peak flow is decreasing starting from the dam downwards up to the final cross-section but the flood increase at 37km from dam because average flow of Gilgel Abay river join the coming flood laterally. The velocity and flood decrease at wider river cross section and increase at narrow river cross section. The time to peak at dam when analyzed by this method is found to be 01:00hr from the initial flood beginning time 00:00hr. According to this analysis the whole process i.e. the dam breach and peak flood at final cross section in the downstream regions has taken 5 hours (Figure 4.7).

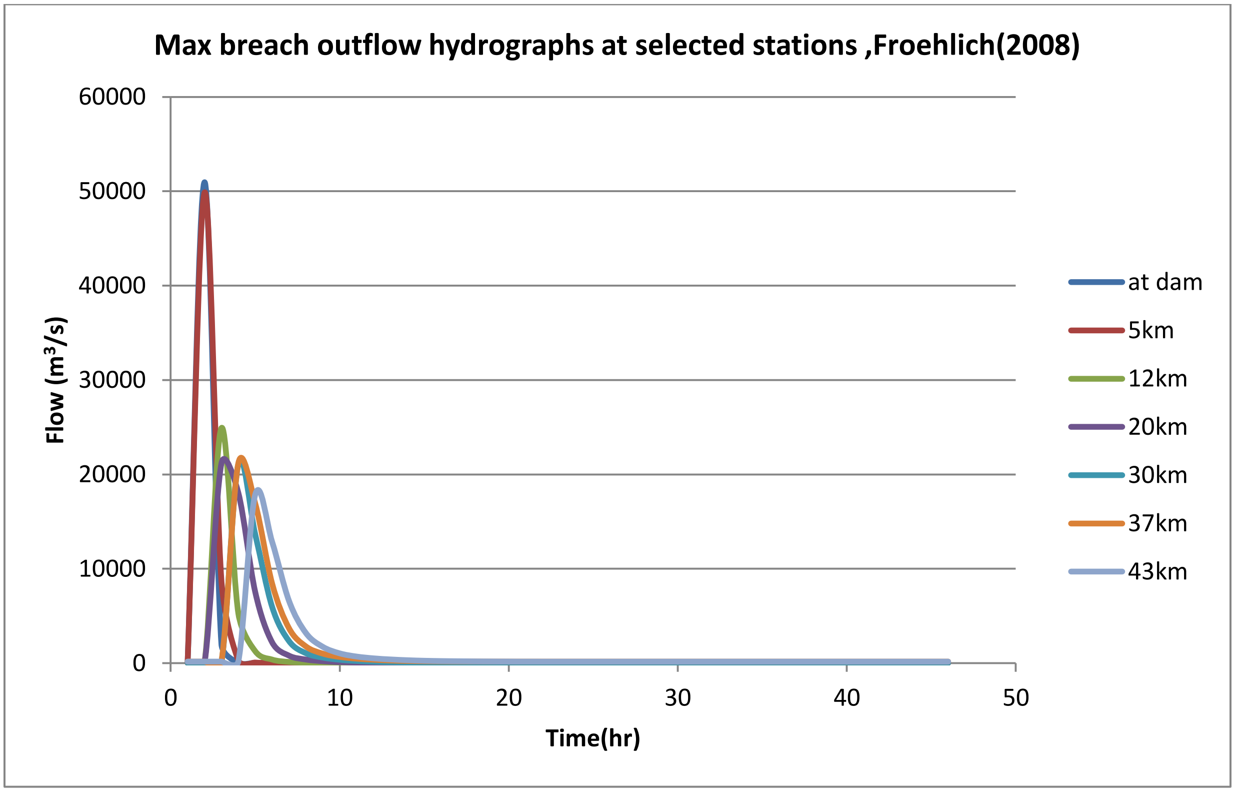

Figure 4. 7 Maximum breach outflow hydrographs at selected stations, piping by Froehlich (2008)

Table 4. 7 Maximum flow, time to peak, rate of flow and flood height for Jema river stations below the dam during piping using Macdonald.

Stations	Peak flow(m^3/s)	Velocity(m/s)	Flood height(m)	Time to peak(hr)
At Dam	27344.67	10.384	17.5	01Jan2025,02:00
5km	25567.18	5.891	17.1	01Jan2025,,02:00
12km	24897.24	2.89	14	01Jan2025,/03:00
20km	18221.48	3.692	18.3	01Jan2025,04:00
30km	17047.29	5.754	13.4	01Jan2025,04:00
37km	17174.52	1.864	13.8	01Jan2025,04;00
43km	15170.31	1.585	14.6	01Jan2025,05:00

NB: All distances are measured from dam location

As shown in table 4.7 the peak flow is decreasing starting from the dam downwards up to the final cross-section but the flood increase at 37km from dam because average flow of Gilgel Abay river join the coming flood laterally. The flood height shows an increased value at the dam and it continues to decrease for some distance and increases again at 43km from the dam actually it depends on the cross section of river. The time to peak at dam when analyzed by this method is found to be 02:00hr from the initial flood beginning time 00:00hr. According to this analysis the whole process i.e. the dam breach and peak flood at final cross section in the downstream regions has taken 6 hours (Figure 4.8).

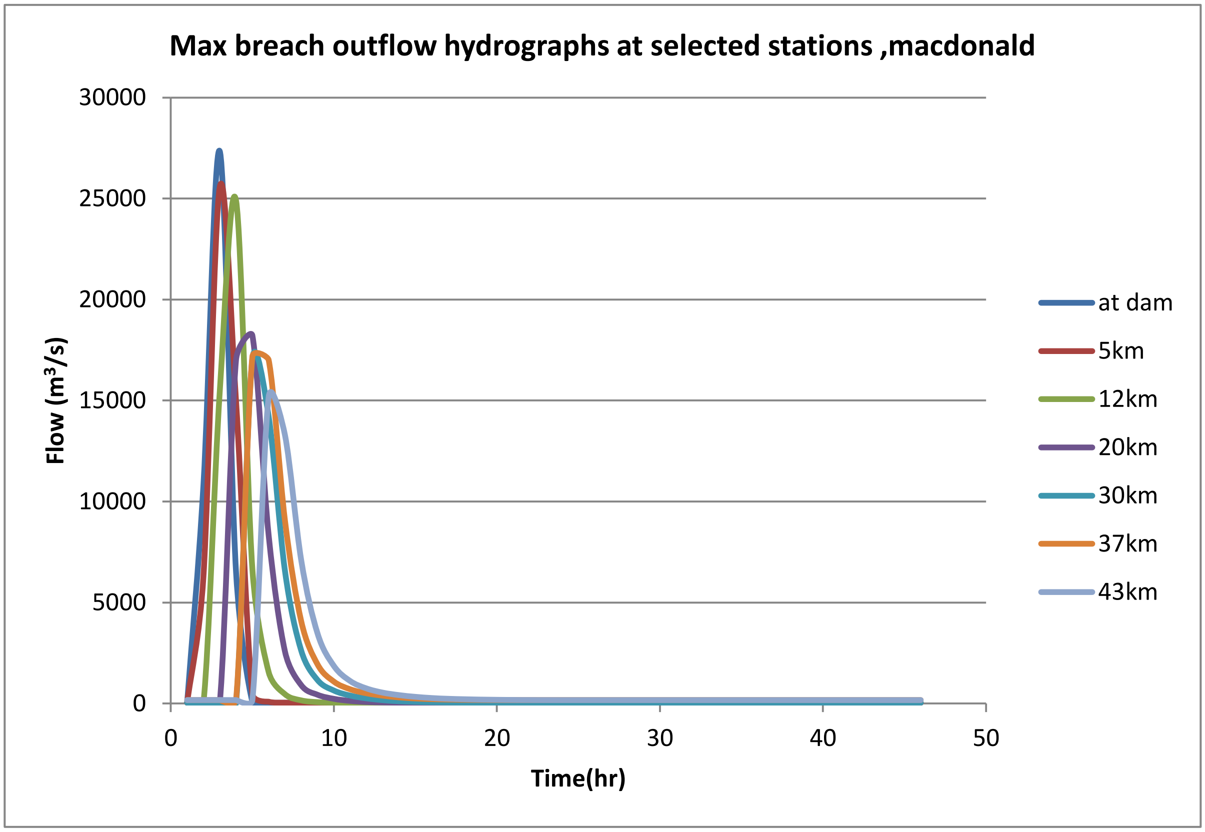

Figure 4. 8 Maximum flow hydrographs at selected stations, piping by Macdonald

Table 4. 8 Maximum flow, time to peak, rate of flow and flood height for Jema river stations below the dam during piping using Von thun and Gillete.

Stations	Peak flow(m^3/s)	Velocity(m/s)	Flood height(m)	Time to peak(hr)
At Dam	48474.42	12.613	23.88	01jan2025,01:00
5km	47281.49	7.257	20.9	01jan2025,01:00
12km	28018.14	3.512	16.4	01jan2005,02:00
20km	24383.76	4.119	19.7	01jan2005,02:00
30km	22918.36	6.049	14.5	01jan2005,03:00
37km	23045.96	1.97	14.2	01jan2005,03:00
43km	19524.72	1.51	16.2	01jan2005,04:00

NB: All distances are measured from dam location

As shown in table 4.8 the peak flow is decreasing starting from the dam downwards up to the final cross-section but the flood increase at 37km from dam because Gilgel Abay river join with mean flow the coming breach flood laterally. The time to peak at dam when analyzed by this method is found to be 01:00hr from the initial flood beginning time 00:00hr. According to this analysis the whole process i.e. the dam breach and peak flood at final cross section in the downstream regions has taken 5 hours (Figure 4.9).

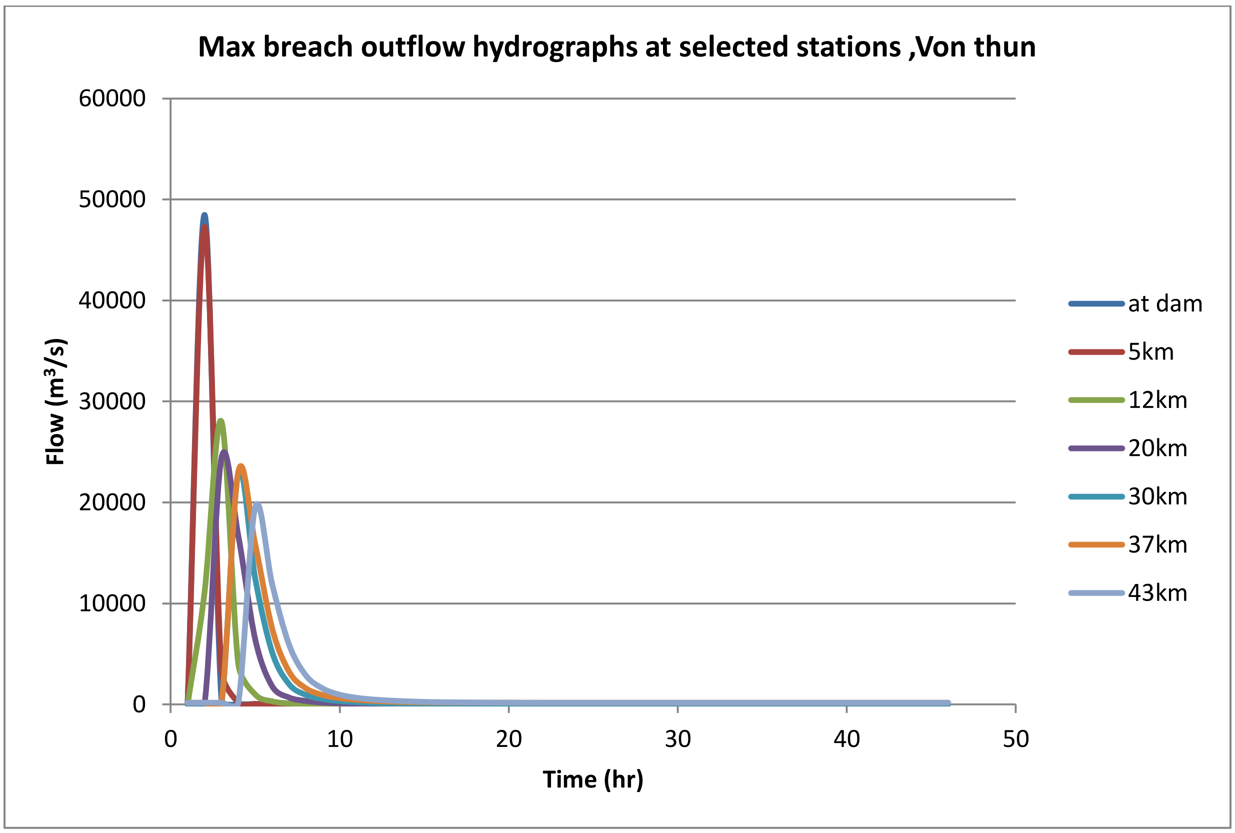

Figure 4. 9 Maximum flow hydrographs at selected stations, piping by Von thun and Gillete

4.2.3. Jema Dam Overtopping Break with Gilgel Abay PMF (Scenario 3)

Table 4. 9 PMF event breach peak outflows for overtopping mode of failure

Methods	Peak flow (m^3/s)	Time to peak, (hr) (Starting at 1/1/2025, 00:00)
MacDonald and Langridge-Monopolis (1984)	51722.79	02/01/2025,10:00
Frohelich (2008)	66328.79	02/01/2025,09:00
Von thun and Gillete(1990)	79886.37	02/01/2025,09:00

In all cases a fictional failure is assumed to occur on 01/1/2025, 00:00hr. PMF in Gilgel Abay and tributary rivers and the burst flood from the dam has resulted the following outflow hydrograph.

Table 4. 10 Maximum flow, time to peak, rate of flow and flood height for Jema river stations below the dam using Froehlich(2008).

Stations	Peak flow(m^3/s)	Velocity(m/s)	Flood height(m)	Time to peak(hr)
At Dam	66328.79	15.466	28.9	02Jan2025,09:00
5km	63535.4	9.071	25.7	02Jan2025,09:00
12km	38806.84	4.117	18.7	02Jan2025,10:00
20km	36430.77	4.65	22	02Jan2025,10:00
30km	28639.9	6.811	16	02Jan2025,11:00
37km	30339.9	2.277	15.7	02Jan2025,11:00
43km	25426.11	1.818	21.5	02Jan2025,12:00

NB: All distances are measured from dam location

As shown in table 4.10 the peak flow is decreasing starting from the dam downwards up to the final cross-section but the flood increase at 37km from dam because Gilgel Abay river join the coming breached flood laterally with PMF flow. Though two downstream tributaries are joining the incoming flood, their contribution is low that is way the flow hydrograph doesn't show any change at the confluences. The velocity and flood depth at near downstream of the dam is high because the flood is peak or not routed. The flood depth is high at 30km from the dam this is because at this river station the cross section is narrow. The time to peak at dam when analyzed by this method is found to be 09:00hr in the second day from the initial flood beginning time 00:00hr. According to this analysis the whole process i.e. the PMF event beginning upstream of the dam, the dam breach and peak flood at final cross section in the downstream regions has taken 37 hours (Figure 4.10).

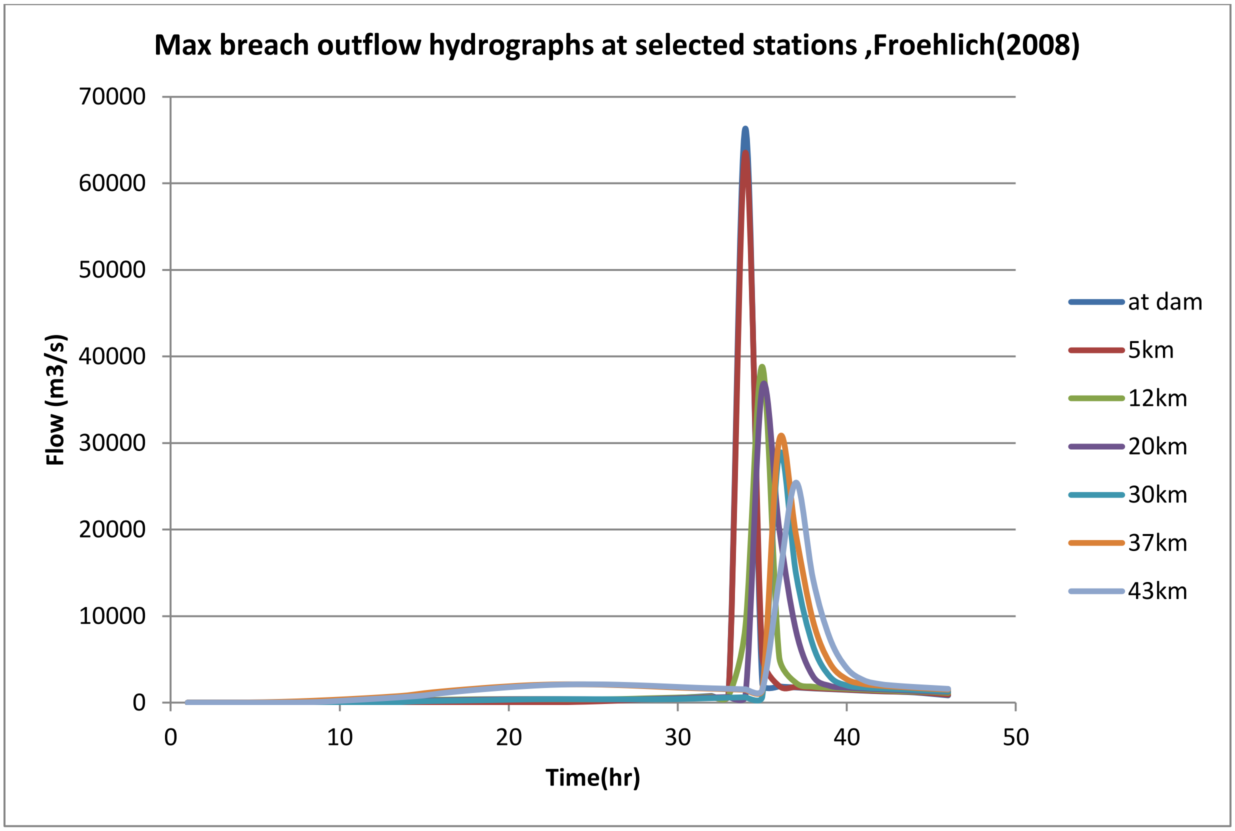

Figure 4. 10 Maximum breach outflow hydrographs at selected stations, overtopping by Froehlich (2008)

Table 4. 11 Maximum flow, time to peak, rate of flow and flood height for Jema river stations below the dam using Macdonald.

Stations	Peak flow(m^3/s)	Velocity(m/s)	Flood height(m)	Time to peak(hr)
At Dam	51722.79	13.633	25.3	02Jan2025,10:00
5km	50419.45	7.816	22.6	02Jan2025,10:00
12km	36677.6	3.756	17.7	02Jan2025,10;00
20km	34421.78	4.572	21.6	02Jan2025,11:00
30km	28319.27	6.742	16	02Jan2025,12:00
37km	30047.27	2.258	15.6	02Jan2025,12:00
43km	25313.66	1.839	20.7	02Jan2025,13;00

NB: All distances are measured from dam location

As shown in table 4.11 the peak flow is decreasing starting from the dam downwards up to the final cross-section but the flood increase at 37km from dam because Gilgel Abay river join the coming flood laterally 32 km far from the dam to downstream. The flood height shows an increased value at the dam and it continues to decrease for some distance and increases again at 43km from the dam. Flood depth depends on the cross section. The time to peak at dam when analyzed by this method is found to be 10:00hr in the second day from the initial flood beginning time 00:00hr. The whole process i.e. the PMF event beginning upstream of the dam, the dam breach and peak flood at final cross section in the downstream regions has taken 38 hours (Figure 4.11).

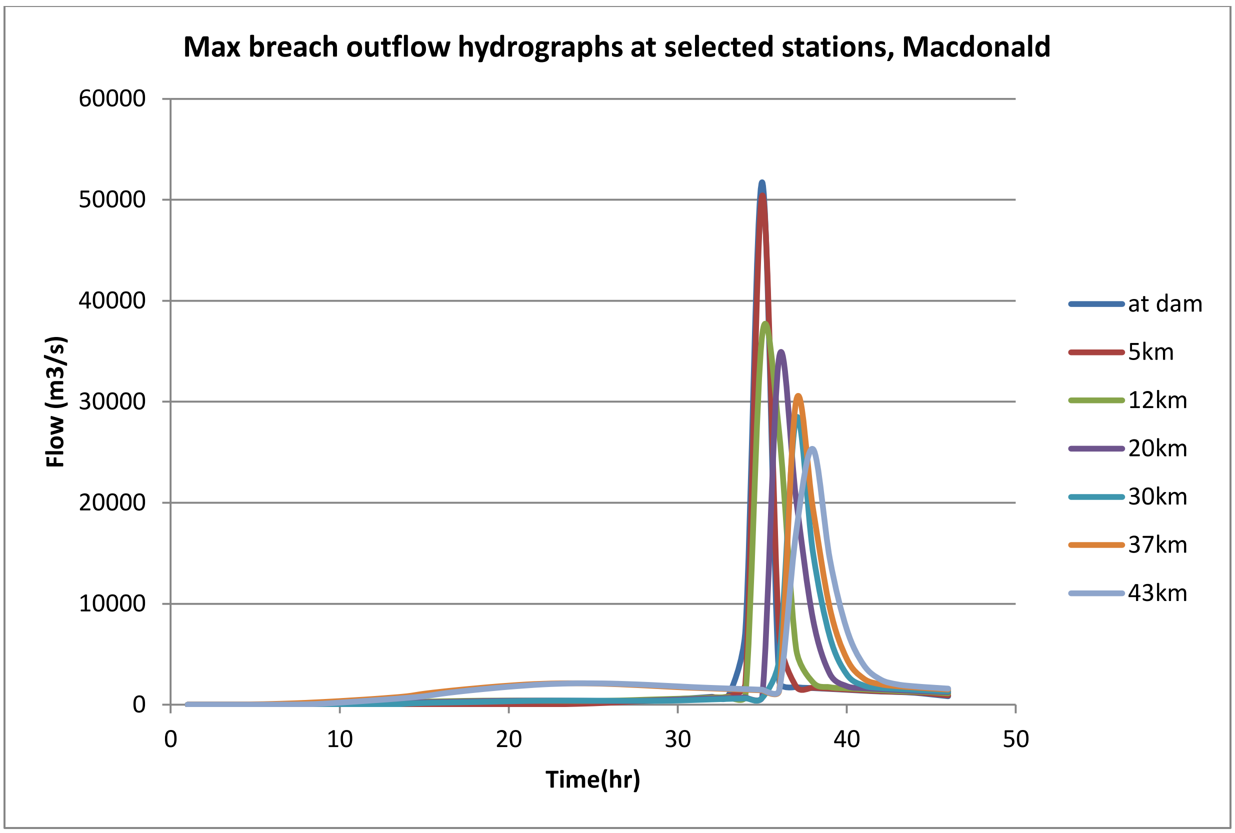

Figure 4. 11 Maximum flow hydrographs at selected stations, overtopping by Macdonald

Table 4. 12 Maximum flow, time to peak, rate of flow and flood height for Jema river stations below the dam during overtopping using Von thun and Gillete.

Stations	Peak flow(m^3/s)	Velocity(m/s)	Flood height(m)	Time to peak(hr)
At Dam	79886.37	15.042	28	02Jan2025,09:00
5km	77984.88	8.896	25.4	02Jan2025,09:00
12km	7178.23	4.174	18.9	02Jan2025,10:00
20km	37716.82	4.722	22.4	02Jan2025,10:00
30km	30609.94	6.896	16.8	02Jan2025,11:00
37km	32337.94	2.287	15.8	02Jan2025,11:00
43km	26626.22	1.921	21.2	02Jan2025,12:00

NB: All distances are measured from dam location

As shown in table 4.12 the flood velocity and depth decrease while the flood route to downstream of the river.at 30km from the dam the flood depth in crease again this is because the river cross section is narrow.

The time to peak at dam when analyzed by this method is found to be 09:00hr in the second day from the initial flood beginning time 00:00hr. The whole process i.e. the PMF event beginning upstream of the dam, the dam breach and peak flood at final cross section in the downstream regions has taken 37 hours (Figure 4.12).

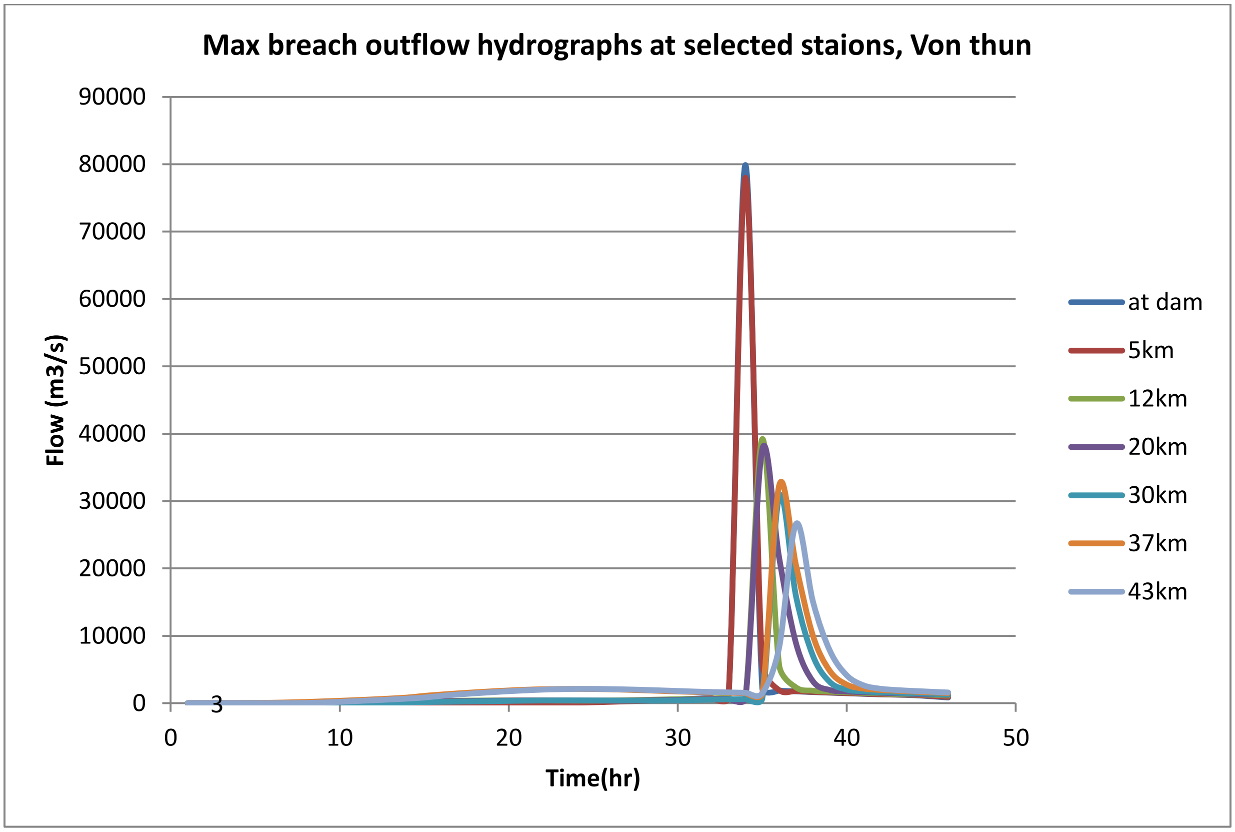

Figure 4. 12 Maximum flow hydrographs at selected points, overtopping by Von thun and Gillete

4.2.4. Breach Outflow Verification

Overtopping outflow verification

Peak overtopping outflows obtained were compared to the envelope curve as a taste of reasonableness as shown below in Figure 4-13. Closer look at the graph reveals that Macdonald's method has resulted in a more similar result when compared to the envelope curve with an error of 8.67 %. Vonthun and Gillete (1990), and Froehlich (2008)'s method are found to have 31 %, 17 % error respectively in relative to the envelope result. However this envelope curve was developed from only fourteen data sets, and may not be a true upper bound of peak flow versus hydraulic depth.

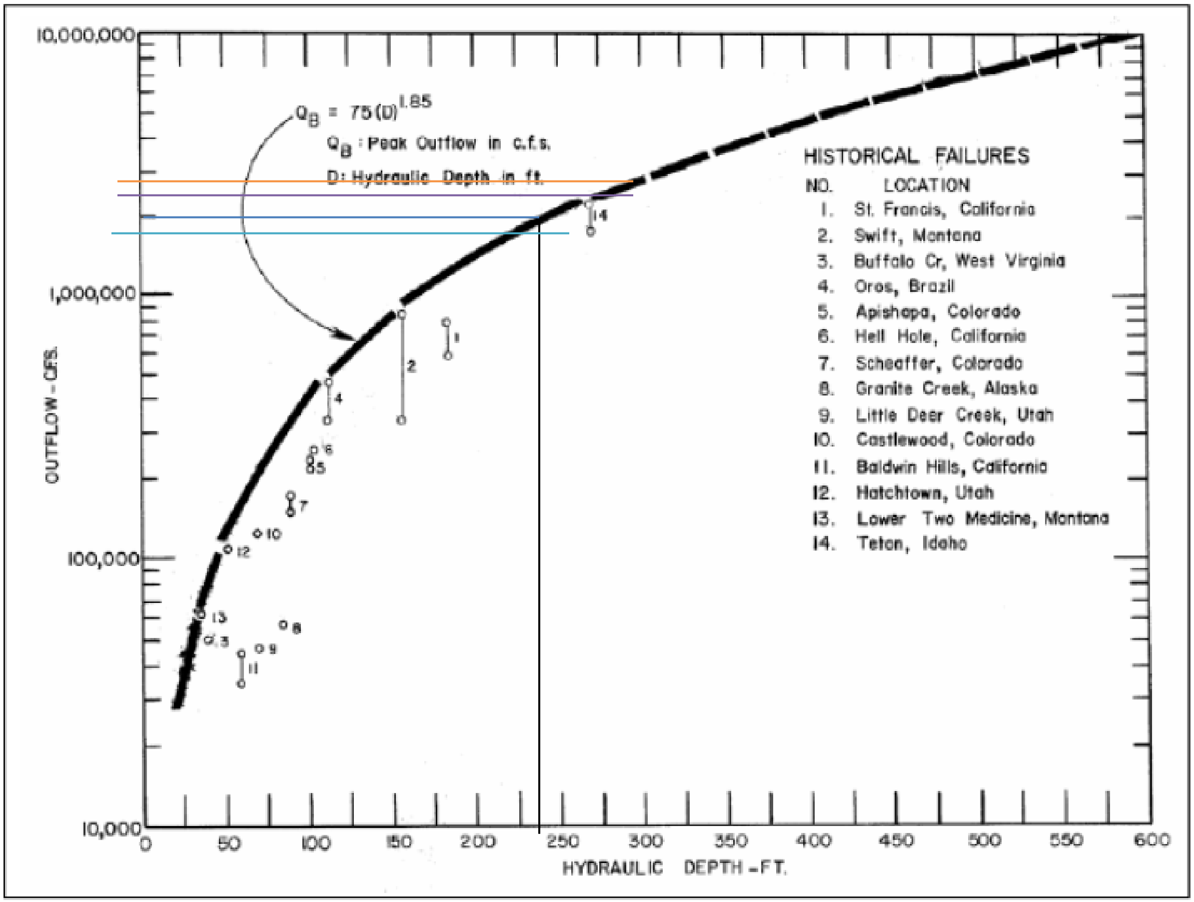

Figure 4. 13 Verification of overtopping outflows using experienced outflow rates envelope

______________________ Frohelich (2008) method 66,328.79m3/s or 2,342,379.33ft3/s

______________________ Macdonald et al method 51,722.79m3/s or 1,826,573.26 ft3/s

______________________ Vonthun and Gillete method 79,886.37m3/s or 2,821,160.794ft3/s

______________________ Hydraulic depth 232.6ft

4.2.5. Summary of Breach Parameters and Breach Outflow Results

Table 4. 13 Summary of breach parameters and breach outflow

Method	Peak flow (m^3/s)	Breach bottom width (m)	Side slopes (H:V)	Breach development time (hrs)
	Scenario Two			
Froehlich 2008	50956.07	75	0.7	0.88
MacDonald et al	27344.67	83	0.5	2.69
Von thun and Gillete	48474.42	181	0.5	1.54
	Scenario One and Three			
Froehlich 2008	66328.79	106	1	1.01
MacDonald et al	51722.79	122	0.5	3.01
Von thun and Gillete	79886.37	197	0.5	1.67

Simulating the breach by three estimation methods have resulted in the following breach outflow hydrographs as shown in the following consecutive figures.

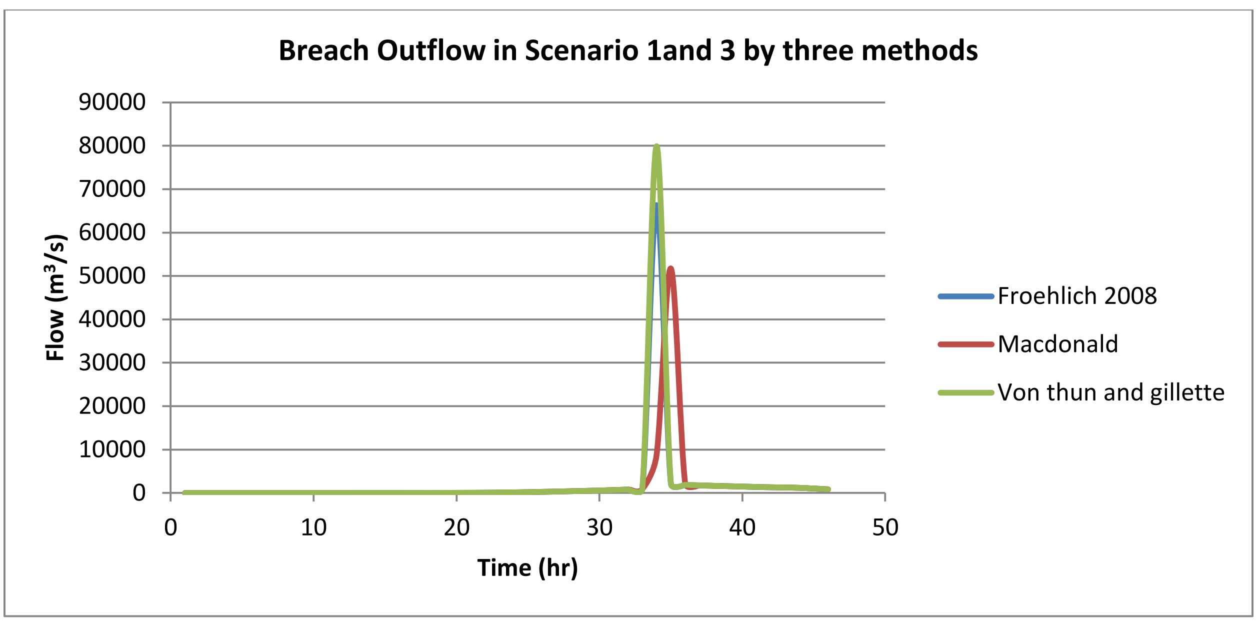

Figure 4. 14 Breach Outflow Summary in Scenario One

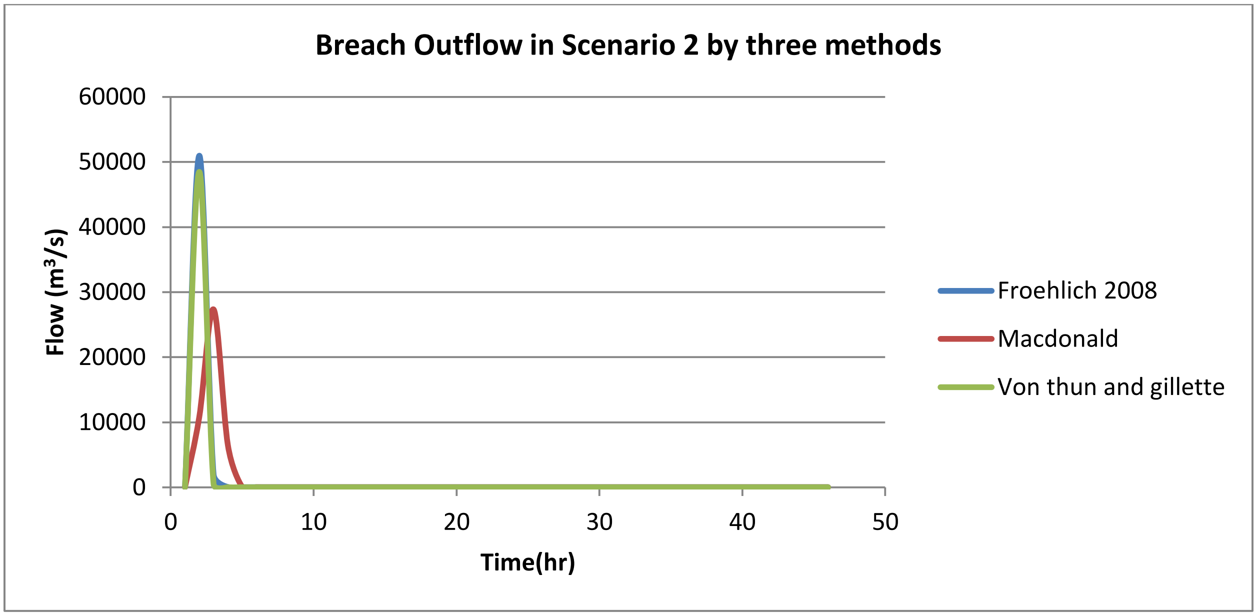

Figure 4. 15 Breach Outflow Summary in Scenario Two

Among the three estimation methods of overtopping results in all scenario Von thun and Gillete(1990) has resulted the maximum peak flow of 79886.37m^3/s and flood height of 28.9 m.and the minimum outflow hydrograph was obtained by MacDonald and Langridge-Monopolis (1984) which is 51722.79m^3/s. Froehlich(2008) resulted maximum outflow of 50956.07m^3/s for piping mode of failure.

4.3. Flood Inundation Mapping

An extended area downstream of the dam would be affected as a result of Jema dam failure. The flood inundation map for the entire study area for Jema dam failure is presented for overtopping type failure and for piping type failure. The general flood modes in low lying areas have inundated with different depth and velocity magnitudes.

Summary of the results tabulated in the above section reveals Von Thun and Gillete (1990) and Froehlich (2008) method of parameter estimation has resulted in the highest discharge values for overtopping and piping modes of failure respectively. Piping mode of failure has obviously resulted in lesser magnitudes than overtopping.

Selection of appropriate and reasonable method for emergency action plan preparation depends on the decision of the EAP preparing body but the results have a direct influence on the economy of flood hazard minimization plan.

Depth map, velocity map and area map for overtopping failure was prepared for the worst scenario (Scenario3) using Von Thun and Gillete (1990)'s result, for piping failure the maps were prepared by Froehlich (2008)'s and the result is shown in the following consecutive figures.

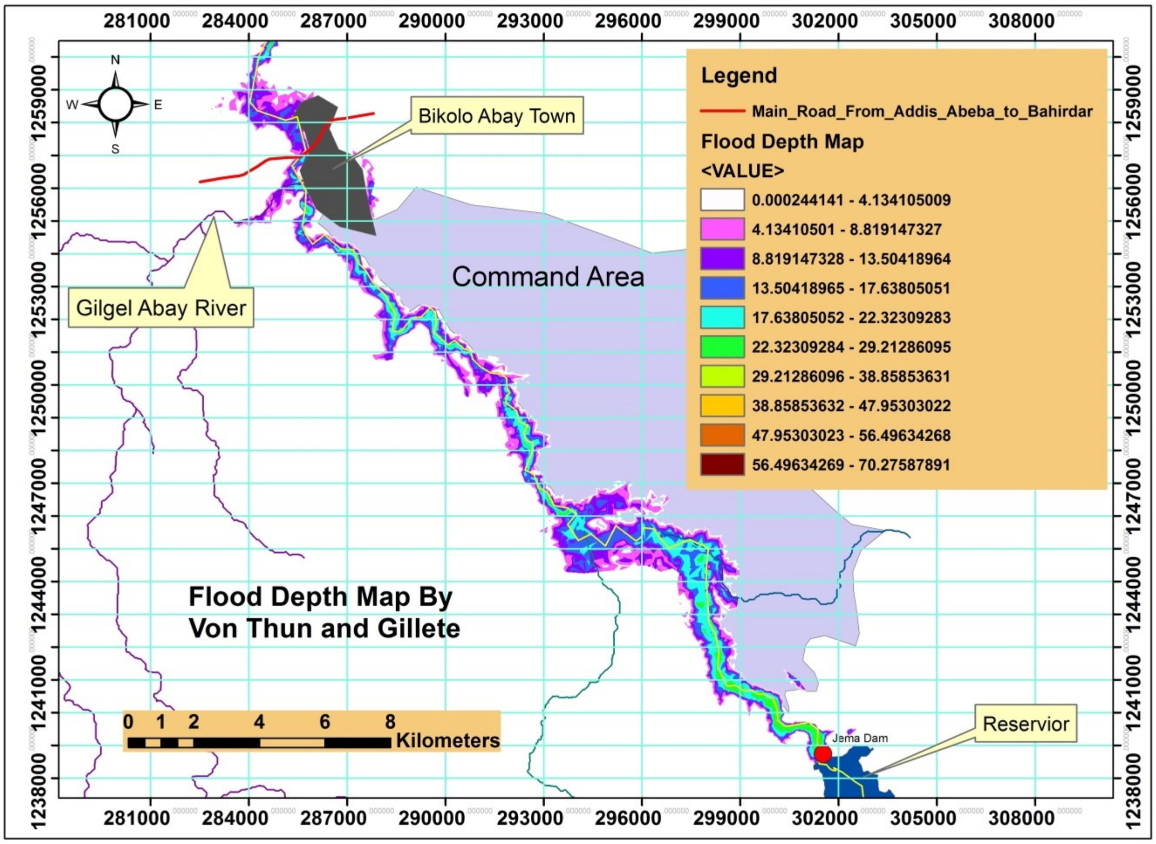

Figure 4. 16 Flood Depth Map by Von Thun and Gillete (1990) Scenario Three

The depth varies from 56m within the gorge at immediate downstream of the dam to 11m at downstream end of the study area. This is because the cross-section at upstream end is narrow and deep whereas it goes wide and shallow towards downstream end. Hence, the flood is dispersed on the flood plain gaining small depth.

Depth of flow at every location on the study area can be extracted from the produced depth map given on Figure 4.17. The depth of flood in the rural village 10km from the dam ranges from 8 to 13m. The downstream side of right command area is flooded with a maximum depth of 13m whereas the left side farm and resettlement villages are inundated with average depth of 10m. The flood continues with average depth of 13m up to a distance of 43km. The Southern part of Bikolo Abay Town will be inundated with flood water from 4m to 8 m depth.

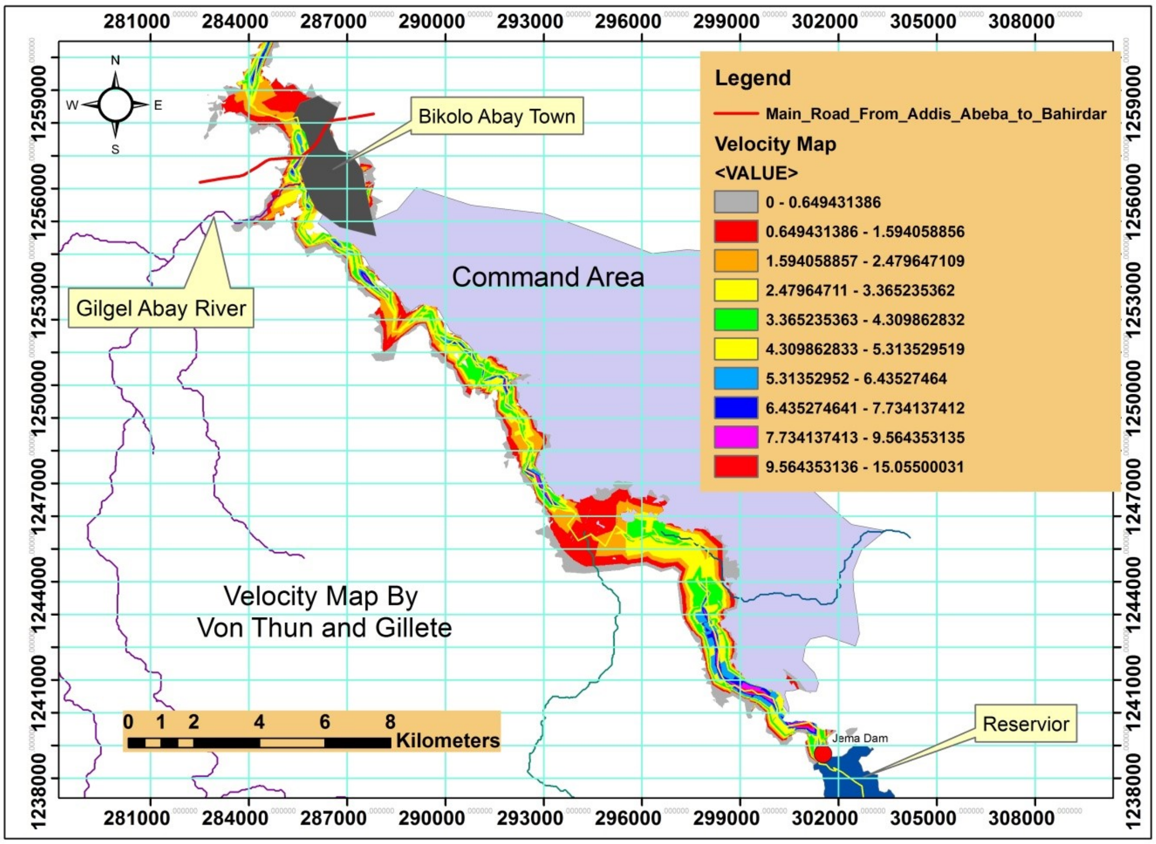

Figure 4. 17 Velocity Map by Von Thun and Gillete (1990)) Scenario Three

The velocity is high along the river channel since it is a well formed water route with less obstacles and lower value of Manning's coefficient when compared to the adjacent flood plain. From downstream of dam, left and right overbanks are covered with some dense trees and bushes where the roughness coefficient is high. The average velocity within the river channel is 6.0m/s whereas it decreases gradually up to 3.0m/s going both to left and right extremities. The velocity at any desired location can be read from Figure 4.18.

Velocity maps are also useful in understanding how fast a flood front approach to a specific area and this in turn helps in preparing Flood Emergency Action Plans. The velocity of the flood over the entire study area ranges from 0 to 15m/s.

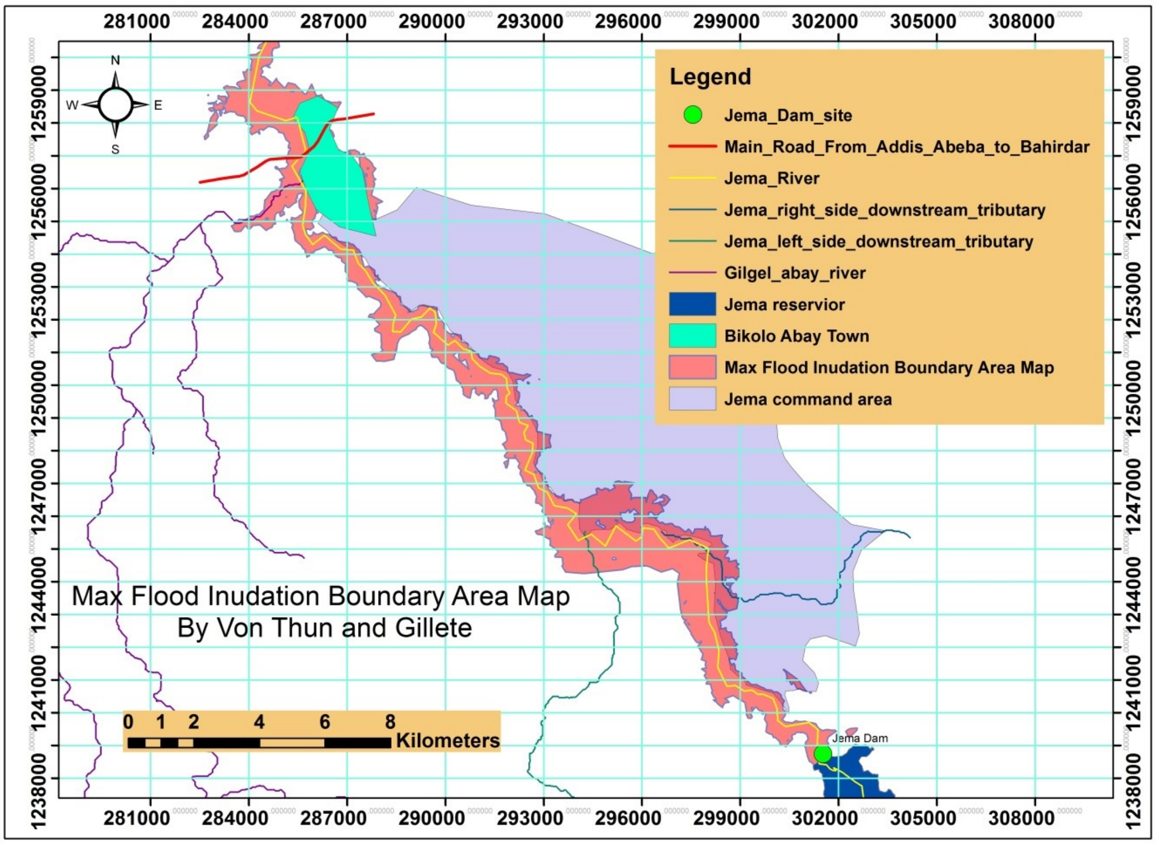

Figure 4. 18 Flood Inundation Area Map by Von Thun and Gillete (1990)) Scenario Three

Largest area in the downstream is inundated by this scenario i.e when the dam is breach by overtopping failure mode with Gilgel Abay and Jema downstream tributaries PMF flood.as shown in the figure 4.19 the command area is in the right side of the dam. The flood inundates large command area especially at the confluence of Jema River and two small tributaries, 10km far from the dam. In the left side of the river rural villages and farms are inundated. And finally after Gilgel Abay River is join Jema River the subsequent area is Bikol Abay town and the map shows that part of the towns near the river banks is inundated.

According to FEMA (2013) classification all area near the river bank is under extreme hazard Flood Severity Category i.e. product of depth and velocity is under categories of greater than 2.5, for example the rural village 10 km from the dam at confluence of small tributaries with Jema river and Bekolo Abay town are under extreme hazard category.

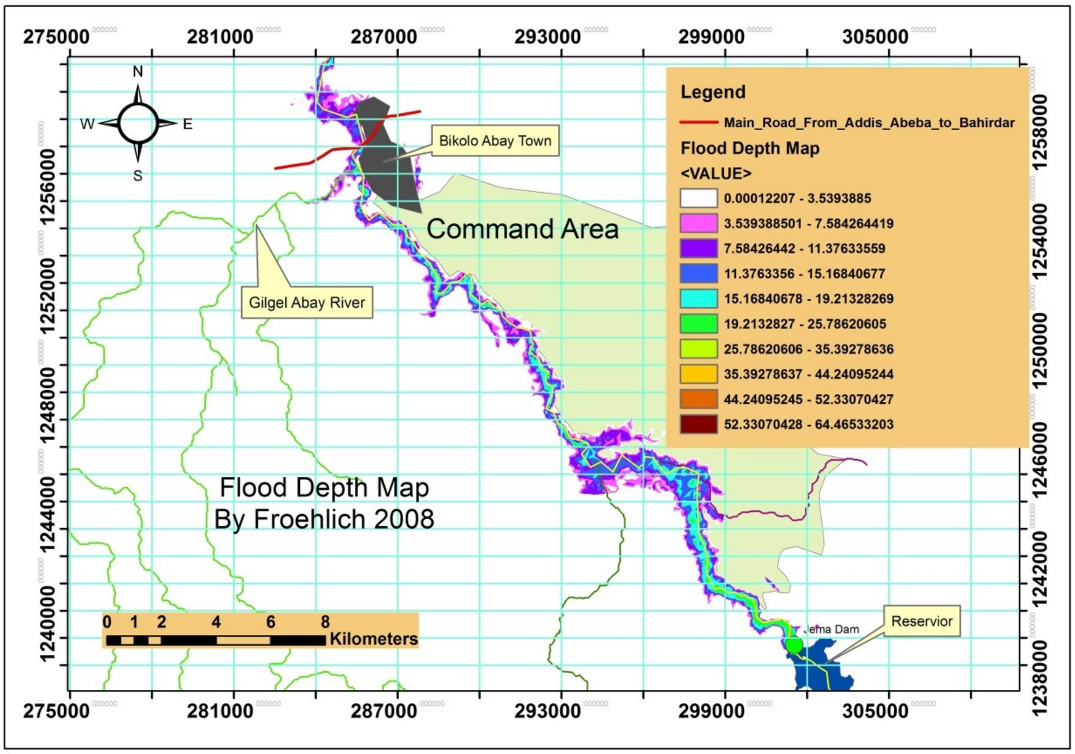

Figure 4. 19 Flood Depth Map by Froehlich (2008) Scenario Two

Depth of flow at every location on the study area can be extracted from the produced depth map given on Figure 4.20. The depth of flood in the rural village 10km from the dam ranges from 7 to 11m. The downstream side of right command area is flooded with a maximum depth of 11m whereas the left side farm and resettlement villages are inundated with average depth of 10m. The flood continues with average depth of 11m up to final cross section.

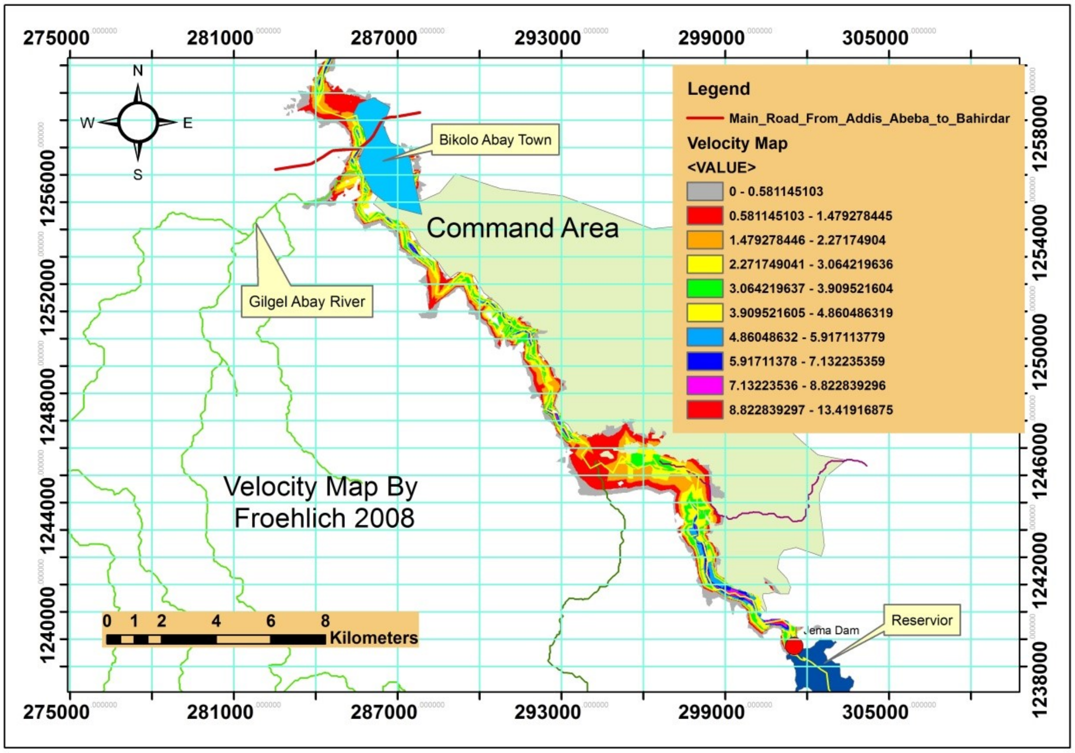

Figure 4. 20 Velocity Map by Froehlich (2008) Scenario Two

As shown in the map the velocity decrease to the downstream from the dam i.e. the velocity is high at the beginning of breach. The average velocity within the river channel is 3.5m/s whereas it decreases gradually up to 0.5m/s going both to left and right extremities. The velocity at any desired location can be read from Figure 4.21.

Velocity maps are also useful in understanding how fast a flood front approach to a specific area and this in turn helps in preparing Flood Emergency Action Plans. The velocity of the flood over the entire study area ranges from 0 to 13m/s.

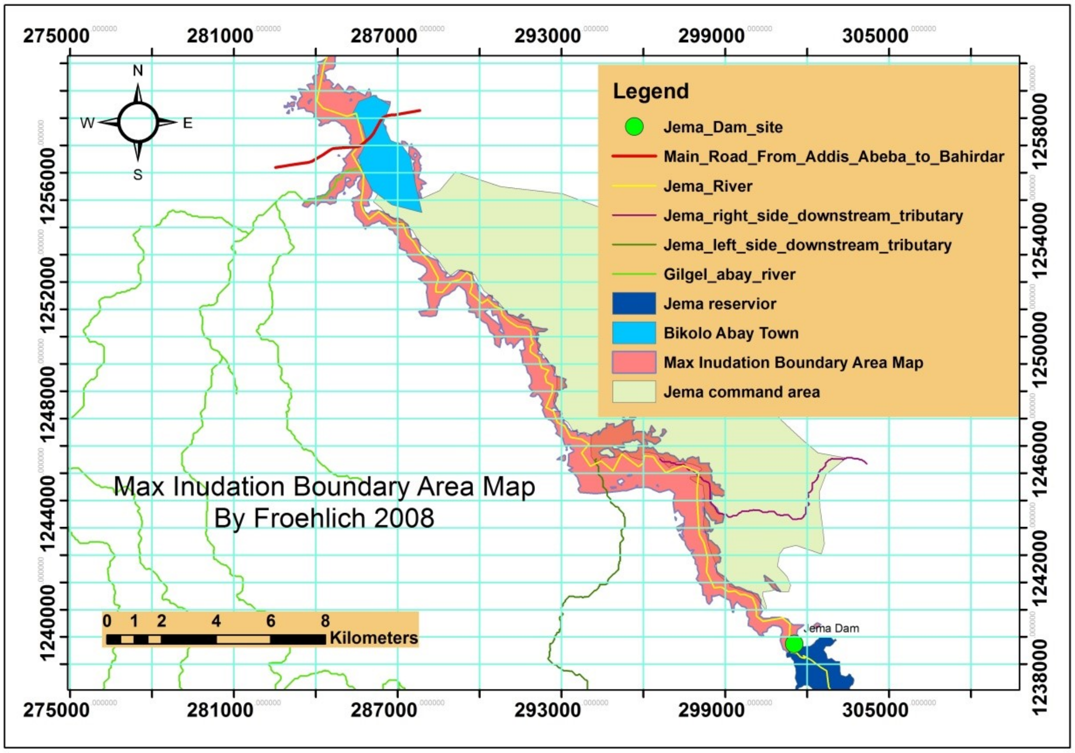

Figure 4. 21 Inundation Area Map by Froehlich (2008) Scenario Two

The flood inundates large command area especially at the confluence of Jema River and two small tributaries, 10km far from the dam. In the left side of the river many rural village and farms are inundated. And finally after Gilgel Abay river with mean flow is join Jema River the subsequent area is Bikol Abay town and the map shows that the town is inundated.

Generally, According to FEMA (2013) classification all area near the river bank is under extreme hazard Flood Severity Category i.e. product of depth and velocity is under categories of greater than 2.5.

5. CONCLUSION AND RECOMMENDATION

5.1. Conclusions

Flood management planning and implementation should consider information regarding consequential damages if a dam fails. This should involve accurate estimation of the severity and extent of dam break flood prior to the construction of a dam. Therefore, damages that could occur in the surrounding settlements, agricultural areas on both lives and infrastructure can be minimized and even controlled.

The severity level of a dam breach depends on the size of reservoir, the incoming flood, the method implied to forecast breach and the settlement magnitude and types on the downstream reaches.

In general scenario two i.e. piping modes of failures are obviously found to result in lowest values of breach parameters when compared with overtopping results. Von Thun and Gillete (1990) method of breach estimation has resulted in a peak flow of 79886.37m3/s, during overtopping

For worst scenario the flood depth, velocity and area map were prepared and in all cases part of rural villages, command area and Bikolo Abay town both side of river were inundated with considerable depth and velocity. The area where at joining of tributaries and Bikolo Abay town were found to be more prone by the flood. Based on dam hazard potential classification Jema dam is categorized under high hazard dam.

The dam breach by von thun and Gillete (1990) evacuate all water in the reservoir within one and half day. Total area of 41.6km^2 in the downstream inundate by this method.

The dam breach modeling and flood maps results in this study can adequately inform the user the extents of hydrological induced dam break and the subsequent flood. In almost all scenarios considered in this study, the flood inundation extent is not significantly different except the depth of flood.

5.2. Recommendations

- Cross-section measurements data at required River station were not available at dam owner (MoWIE) and design (WWDSE) offices. To fill this data gap cross-section geometry were generated from low resolution DEM (12.5mx12.5m details) by using HEC-GeoRAS software. There would, however, be further need to improve the generated cross-sections by taking cross-section measurements on reach or by generating cross-sectional geometry from high resolution DEM for the study area. This is because cross-sectional data generated from low resolution DEM (12.5m) might not be of sufficient span-width or maximum elevation required for the analyses. The topographic maps should be produced by actual topographic surveying or generated from finer DEM if possible.
- The results of this study can be re-checked using different dam breach and flood models with higher accuracy and strong computational algorithms, such as models considering unsteady flow and 1D-2D hybrid models.
- Further study should be continued and emergency action plan (EAP), shall be prepared in order to evacuate people potentially at risk in case the dam fails.
- The area below the dam is relatively flat and people living on this area, especially near the river banks, shall be resettled at significantly far place.
- Flood protection dykes should be designed and implemented to protect Bikolo Abay town.
- Any water resource and infrastructure development in downstream should consider the result of this thesis breach maps.
- Finally, I would like to recommend both the dam owner (Ministry of water, irrigation and Energy) and the designer (Water works design and supervision enterprise) to give special attention to the Dam break analysis and make a detail investigation by using the latest dam break software
- Further study the economic and life damage consequences in detail
- Effective dam monitoring system should be in place

References

ASCE (2014), “Technical Resources for Dam Safety”, Seminar, Dam Breach Analysis Using HEC-RAS.

Brunner, G. W. (2010). *HEC-RAS, River Analysis Systme User's Manual.* Davis: US Army Corps of Engineers Hydrologic Engineering Center (HEC).

Cameron T. Ackerman, Hydraulic Engineer, P.E. and Gary W. Brunner, Senior Technical Hydraulic Engineer, P.E. (2006), “Dam Failure Analysis Using HEC-RAS and HEC GeoRAS”, 3rd Federal Interagency Hydraulic Modeling USACE-HEC Proceedings Conference from April 2-6,2006, Reno, Nevada, USA.

Chow, V. T.,1959. Open Channel Hydraulics, Caldwell, New Jersey, USA: The Blackburn Press,

Chow, (1964). Hand Book of Applied Hydrology, A Compendium of Water Resources Technology, Mc Grew – Hill Book Company, NY, USA.

Colorado Dam Safety Office (2010), “Guidelines for Dam Breach Analysis”, Office of the State Engineer, Dam Safety Branch, Colorado, February 10, 2010.

De Silva et.al. (2007). A Comparison of Methods Used in Estimating Missing Rainfall Data . The Journal of Agricultural Sciences , 104.

D. Michael Gee, Senior Hydraulic Engineer (2010), “Use of Breach Process Models to Estimate HEC-RAS Dam Breach Parameters”, USACE-HEC 2nd Joint Federal Interagency Conference, Las Vegas

Dragan Sredojevic, Slobodan P. Simonovic (2009), “Hydraulic Modeling and Flood plain Mapping Using HEC-RAS”, Journal of Hydraulic Engineering, University of Western Ontario, ISBN 978-0-7714-2846-3, Britain.09.

FAO, 1997. Irrigation potential in Africa: A basin approach FAO Land and Water Bulletin 4

FEMA. (2013). Federal Guidelines for Inundation Mapping of Flood Risks Associated with Dam Incidents and Failures.

Fiddes D.1996: Flood estimation for small East Africa rural catchments, Proceeding Institution of Civil Engineers, Part 2.63.21-34 (1996)

Fread, D. (1981). Some Limitaions of Dam-Breach Flood Routing Models. American Society of Civil Engineers.

Fread 1988 Fread, D.BREACH: An Erosion Model for Earthen Dam Failures. Silver Spring:

Fread, D. (1991). BREACH: An Erosion Model for Earthen Dam Failures. Hydrology Laboratory, National Weather Service.

Fread, D. L. and Lewis, J. M. (1998). “NWS FLDWAV Model: Theoretical Description and User Documentation.” United Stated Department of Commerce, NWS, NOAA, Silver Springs,Maryland.

Goldsmith, P., 2000. Review note on soil erosion assessment. (Unpublished project working

paper), Zimbabwe and Tanzania.
Heirsfield, D.M., 1961: Estimating the probable maximum precipitation, ASCE, J.Hyd.Div., 87,No. HY 5, 99-116
Hershfield, D.M., 1965. Method for estimating probable maximum rainfall. Journal of the American Water Works Association, 57, 965–972.
Hydrologic Engineering Center,2014. Using HEC-RAS for Dam Break Studies, TD-39, U.S. Army Corps of Engineers, Davis, CA, Aug. 2014.
Hydrologic Engineering Center, 2010. HEC-RAS, River Analysis System Hydraulic Reference Manual, CPD-69, Version 4.1, U.S. Army Corps of Engineers, Davis, CA, Jan. 2010.
ICOLD, C. O. (1998). Dam-Break Flood Analysis. Paris: International Committee on Large Dams.
ICOLD European club,2012. working group on dam safety, [Report].
James et.al. (1960). Double - Mass Curves. Washington: United Stated Department of The Interior.
L.M. Zhang, M. Peng and Y. Xu (2010), "Assessing Risks of Breaching of Earth Dams and Natural Landslide Dams", Indian Geotechnical Conference from December 16-18, 2010, Department of Civil and Environmental Engineering, the Hong Kong University of Science and Technology, Hong Kong.
Ponce, V.M., and A.J. Tsivoglou. 1981. Modeling of gradual dam-breaches, Journal of Hydraulics Division, American Society of Civil Engineers, 107(HY6):829-838.
Purvang H. Pandya, Thakor Dixitsinh Jitaji (2013), "Brief Review of Method Available for Dam Break Analysis", Paripex-Indian Journal of Research, April 2013, Volume-2 |Issue: 4|, ISSN - 2250-1991A
Riley Asburry[1] and Christophere Goodell[2] (2009), "Dam Break Modeling Using HEC-RAS and GIS", Journal of Hydraulic Engineering, USA.
Stedinger, J., D. Heath and K. Thompson, (1996). Risk Analysis for Dam Safety Evaluation; Hydrologic Risk U.S. Army Corps of Engineers.
US Army Corps of Engineers, Hydrologic Engineering Center, HEC, (2013). HEC-GeoHMS, Users' Manual.
US Home Land Security Dams Sector (2011), "Estimating Loss of Life for Dam Failure Scenarios", USA.

Wahl, T. L. (1998). Prediction of Embankment Dam Breach Parmeters. U.S. Department of the Interior Bureau of Reclamation.

WMO, W. M. (2009). Manual on Estimation of Probable Maximum Precipitation. Geneva: World Meteorological Organization.

WMO No.168, Guid to hydrological practice, fifth edition 1994, Geneva

WWDSE. (2010). Jema Dam Final Design Report. Addis Ababa: Water Works Design and Supervision Enterprise.

WWDSE, March 2011. Tendaho dam leakage and associated problems

Y. XIONG (2011), “Dam Break Analysis Using HEC-RAS”, Journal of Water Resource and Protection, Scientific Research, Department of Civil and Environmental Engineering, Mississippi State University, MS.

Zagonjolli, M. (2007). Dam break Modelling, Risk Assessment and Uncertainty Analysis for Flood Mitigation. ISBN 9 780415 455947 (Taylor & Francis Group). London, UK: Taylor & Francis.

Appendices

Table I: 1 W-W Test on Dangla Rainfall Station

Year	Xi	Xi+1	XiXi+1	Xi^2	Xi^3	Xi^4
1986	1585.2	1581.9	2507570.0	2512873.7	3983418895.4	6314533992556.6
1987	1581.9	1786.1	2825350.7	2502277.5	3958249753.7	6261392440206.2
1988	1786.1	1646.2	2940270.2	3190136.6	5697888062.2	10176971322886.8
1989	1646.2	1559.5	2567248.9	2709974.4	4461159923.1	7343961465453.3
1990	1559.5	2001.6	3121425.4	2432040.3	3792766769.9	5914819777620.1
1991	2001.6	1422.2	2846670.2	4006223.5	8018677758.7	16049826727397.3
1992	1422.2	1715.6	2439976.3	2022735.7	2876793533.3	4091459517080.0
1993	1715.6	1317.9	2260989.2	2943283.4	5049496932.4	8662916937252.9
1994	1317.9	1184.6	1561184.3	1736860.4	2289008334.3	3016684083825.4
1995	1184.6	1654.7	1960157.6	1403277.2	1662322123.7	1969186787777.7
1996	1654.7	1667.2	2758715.8	2738032.1	4530621699.3	7496819725869.8
1997	1667.2	1577.4	2629903.1	2779555.8	4634075496.4	7725930667678.1
1998	1577.4	1959.4	3090830.2	2488307.7	3925148820.9	6191675254171.6
1999	1959.4	1895.7	3714434.6	3839248.4	7522623236.6	14739827969762.7
2000	1895.7	1411.1	2675022.3	3593678.5	6812536313.5	12914525089488.7
2001	1411.1	1349.8	1904702.8	1991203.2	2809786849.6	3964890223514.3
2002	1349.8	1369.4	1848416.1	1821960.0	2459281662.0	3319538387356.8
2003	1369.4	1627.9	2229246.3	1875256.4	2567976059.4	3516586415720.5
2004	1627.9	1405.4	2287850.7	2650058.4	4314030085.6	7022809576411.7
2005	1405.4	1869.0	2626692.6	1975149.2	2775874629.5	3901214204248.7
2006	1869.0	1478.7	2763690.3	3493161.0	6528717909.0	12202173771921.0
2007	1478.7	1858.1	2747572.5	2186553.7	3233256941.4	4781017039252.6
2008	1858.1	1454.6	2702792.3	3452535.6	6415156416.9	11920002138318.1
2009	1454.6	1404.1	2042412.3	2115861.2	3077731643.3	4476868448396.5
2010	1404.1	1599.2	2245446.0	1971513.0	2768212838.3	3886863637909.0
2011	1599.2	1640.4	2623327.7	2557440.6	4089859071.5	6540502627123.6
2012	1640.4	1945.4	3191289.5	2690912.2	4414172307.3	7241008252835.9
2013	1945.4	2008.2	3906820.0	3784712.4	7362907040.2	14324047630995.0
2014	2008.2	1716.3	3446733.1	4032867.2	8098803991.4	16264018175465.2
2015	1716.3	1600.0	2746127.4	2945787.3	5055941993.4	8677662934793.6
	48692.8		**79212868.1**	**80443476.3**	**135186497092.3**	**230909735223289.0**
	S1		**R**	**S2**	**S3**	**S4**
N	30					
R̄	78984486.31					
var (R)	63353640207					
u	0.91					
IuI	0.91					
α	5.0%					
α/2	0.025					
confidence level	0.975					
U crit.	1.96					

Ucrt.>|u|	OK
.-Ucrt.<|u|	OK

Table I: 2 M-W Test on Dangla Rainfall Station

Year		Xi	rank	J	T
1986	P	1585.2	17	1	0
1987		1581.9	18	1	0
1988		1786.1	8	1	0
1989		1646.2	13	1	0
1990		1559.5	20	1	0
1991		2001.6	2	1	0
1992		1422.2	23	1	0
1993		1715.6	10	1	0
1994		1317.9	29	1	0
1995		1184.6	30	1	0
1996	q	1654.7	12	1	0
1997		1667.2	11	1	0
1998		1577.4	19	1	0
1999		1959.4	3	1	0
2000		1895.7	5	1	0
2001		1411.1	24	1	0
2002		1349.8	28	1	0
2003		1369.4	27	1	0
2004		1627.9	15	1	0
2005		1405.4	25	1	0
2006		1869.0	6	1	0
2007		1478.7	21	1	0
2008		1858.1	7	1	0
2009		1454.6	22	1	0
2010		1404.1	26	1	0
2011		1599.2	16	1	0
2012		1640.4	14	1	0
2013		1945.4	4	1	0
2014		2008.2	1	1	0
2015		1716.3	9	1	0
				ΣT	0
p	10				
q	20				
N	30				
R	170				
V	115				
W	85				
U	85				
U(bar)	100				
Var(U)	516.67				

u	-0.66
IuI	0.66
α	0.05
α/2	0.025
confidence level	0.975
U crit.	1.959963985
Ucrt.>│u│	OK
.-Ucrt.<│u│	OK

Table I: 3 GB Test on Dangla Rainfall Station

Year	Yi	Xi=lnYi	
1986	1585.2	7.368468769	OK
1987	1581.9	7.366355928	OK
1988	1786.1	7.487787143	OK
1989	1646.2	7.406224881	OK
1990	1559.5	7.352120536	OK
1991	2001.6	7.601679792	OK
1992	1422.2	7.259980718	OK
1993	1715.6	7.447518153	OK
1994	1317.9	7.18379484	OK
1995	1184.6	7.077160444	OK
1996	1654.7	7.411375002	OK
1997	1667.2	7.418900852	OK
1998	1577.4	7.363556701	OK
1999	1959.4	7.580393583	OK
2000	1895.7	7.547343442	OK
2001	1411.1	7.252124821	OK
2002	1349.8	7.207711712	OK
2003	1369.4	7.222127967	OK
2004	1627.9	7.39504612	OK
2005	1405.4	7.248077239	OK
2006	1869.0	7.533158807	OK
2007	1478.7	7.298918602	OK
2008	1858.1	7.527309739	OK
2009	1454.6	7.282486228	OK
2010	1404.1	7.247155921	OK
2011	1599.2	7.377258783	OK
2012	1640.4	7.402695394	OK
2013	1945.4	7.573240223	OK
2014	2008.2	7.604994077	OK
2015	1716.3	7.44794334	OK
N	30.00		
$\dot{X}$	7.38		
s	0.14		
K_N	2.56		

X_H	**2284.54**
X_L	**1132.60**

Table I: 4 Man Kendall's Test Dangla Rainfall Station

Year	Xi	Sum
1986	1585.2	16
1987	1581.9	16
1988	1786.1	7
1989	1646.2	11
1990	1559.5	15
1991	2001.6	1
1992	1422.2	16
1993	1715.6	7
1994	1317.9	20
1995	1184.6	20
1996	1654.7	8
1997	1667.2	7
1998	1577.4	10
1999	1959.4	1
2000	1895.7	2
2001	1411.1	10
2002	1349.8	13
2003	1369.4	12
2004	1627.9	6
2005	1405.4	9
2006	1869.0	2
2007	1478.7	6
2008	1858.1	2
2009	1454.6	5
2010	1404.1	5
2011	1599.2	4
2012	1640.4	3
2013	1945.4	1
2014	2008.2	0
2015	1716.3	0
N	30	
S	235	
S(var.)	18850	
z	1.711639046	
IuI	1.711639046	
α	5%	
α/2	0.025	
confidence level	0.975	
U crit.	1.959963985	

Ucrt.>│u│	OK
.-Ucrt.<│u│	OK

Table I: 5 W-W Test on Gilgel Abay River Flow Data

Year	Xi	Xi+1	XiXi+1	Xi^2	Xi^3	Xi^4
1986	955.2	1077.5	1029226.7	912479.3	871634675.7	832618389982.0
1987	1077.5	1024.1	1103429.2	1160911.4	1250830987.8	1347715352799.7
1988	1024.1	1375.8	1408930.2	1048793.1	1074075305.7	1099966965005.1
1989	1375.8	1172.6	1613159.9	1892732.1	2603956452.1	3582434752235.7
1990	1172.6	1388.6	1628199.1	1374882.9	1612124423.9	1890302941735.4
1991	1388.6	1267.1	1759539.1	1928187.7	2677466073.7	3717907970188.4
1992	1267.1	1497.3	1897283.4	1605641.2	2034570642.0	2578083808676.0
1993	1497.3	1122.5	1680672.5	2241898.3	3356787608.2	5026108015382.8
1994	1122.5	1235.0	1386306.7	1259941.1	1414247397.9	1587451690983.1
1995	1235.0	1631.0	2014392.1	1525346.0	1883877092.0	2326680518561.5
1996	1631.0	1330.3	2169738.8	2660232.8	4338898164.0	7076838361234.2
1997	1330.3	1415.9	1883569.9	1769682.1	2354197514.7	3131774828627.0
1998	1415.9	1285.4	1819994.4	2004787.0	2838587893.4	4019170791172.5
1999	1285.4	1383.9	1778818.1	1652235.2	2123771514.7	2729881038641.8
2000	1383.9	1198.6	1658739.6	1915098.9	2650249891.6	3667603967765.1
2001	1198.6	987.8	1183991.4	1436697.1	1722058183.5	2064098546025.5
2002	987.8	1411.3	1394084.1	975735.0	963824213.6	952058811396.5
2003	1411.3	1242.3	1753203.7	1991801.6	2811053445.1	3967273459772.4
2004	1242.3	1059.8	1316560.0	1543187.5	1917026273.4	2381427805219.0
2005	1059.8	1059.8	1123214.2	1123214.2	1190402619.7	1261610123635.2
	25061.9		**31603053.1**	**32023484.6**	**41689640372.6**	**55241008139038.8**
	S1		**R**	**S2**	**S3**	**S4**
N	20					
R̄	31372518.06					
var (R)	17588381940					
u	1.74					
lul	1.74					
α	5.0%					
α/2	0.025					
confidence level	0.975					
U crit.	1.96					
Ucrt.>│u│	OK					
.-Ucrt.<│u│	OK					

Table I: 6 MW Test on Gilgel Abay River Flow Data

year		Xi	rank	J	T
1986	P	955.2	20	1	0
1987		1077.5	16	1	0
1988		1024.1	18	1	0
1989		1375.8	7	1	0
1990		1172.6	14	1	0
1991		1388.6	5	1	0
1992		1267.1	10	1	0
1993		1497.3	2	1	0
1994		1122.5	15	1	0
1995		1235.0	12	1	0
1996	q	1631.0	1	1	0
1997		1330.3	8	1	0
1998		1415.9	3	1	0
1999		1285.4	9	1	0
2000		1383.9	6	1	0
2001		1198.6	13	1	0
2002		987.8	19	1	0
2003		1411.3	4	1	0
2004		1242.3	11	1	0
2005		1059.8	17	1	0
				ΣT	0
p	10				
q	10				
N	20				
R	119				
V	64				
W	36				
U	36				
U(bar)	50				
Var(U)	175.00				
u	-1.06				
lul	1.06				
α	0.05				
α/2	0.025				
confidence level	0.975				
U crit.	1.959963985				
Ucrt.>|u|	OK				
.-Ucrt.<|u|	OK				

Table I: 7 GB Test on Gilgel Abay River Flow Data

Year	Yi	Xi=lnYi	
1986	955.24	6.861960315	OK
1987	1077.46	6.982357986	OK
1988	1024.11	6.931575316	OK
1989	1375.77	7.226765946	OK
1990	1172.55	7.066939555	OK
1991	1388.59	7.236045563	OK
1992	1267.14	7.144516882	OK
1993	1497.30	7.311416762	OK
1994	1122.47	7.023287784	OK
1995	1235.05	7.118865924	OK
1996	1631.02	7.396962091	OK
1997	1330.29	7.193155249	OK
1998	1415.91	7.255524182	OK
1999	1285.39	7.158819787	OK
2000	1383.87	7.232639924	OK
2001	1198.62	7.088928677	OK
2002	987.79	6.895473162	OK
2003	1411.31	7.252275047	OK
2004	1242.25	7.124680335	OK
2005	1059.82	6.965852474	OK
N	20.00		
$\dot{X}$	7.12		
s	0.15		
K_N	2.38		
X_H	**1755.32**		
X_L	**876.90**		

Table I: 8 Trend Test/ Man-Kendall Test on Gilgel Abay River Flow Data

Year	Xi	Sum
1986	955.2378	17
1987	1077.456	13
1988	1024.106	14
1989	1375.766	4
1990	1172.554	10
1991	1388.592	2
1992	1267.139	5
1993	1497.297	-1
1994	1122.471	7
1995	1235.049	5
1996	1631.022	-2
1997	1330.294	1
1998	1415.905	-2
1999	1285.393	0
2000	1383.871	-1
2001	1198.623	0
2002	987.793	1
2003	1411.312	-2
2004	1242.251	-2
2005	1059.818	-2
N	20	
S	67	
S(var.)	950	
z	2.173767	
IuI	2.173767	
α	0.025	
α/2	0.0125	
confidence level	0.9875	
U crit.	2.241403	
Ucrt.>│u│	OK	
.-Ucrt.<│u│	OK	

Table I: 9 Temporal Distribution of Rainfall

Temporal Distribution of Rainfall			
% of Rainfall and Duration		Storm Duration(hrs)	Return Periods
			PMP
Duration (%)	Accumulated RF (%)		Accumulative rainfall (CM)
0.0	0.00	0.0	0.00
2.1	1.91	0.5	0.35
4.2	2.67	1.0	0.49
6.3	4.27	1.5	0.79
8.3	5.73	2.0	1.06
10.4	7.18	2.5	1.33
12.5	8.63	3.0	1.60
14.6	10.08	3.5	1.87
16.7	11.53	4.0	2.13
18.8	12.98	4.5	2.40
20.8	15.27	5.0	2.83
22.9	17.00	5.5	3.15
25.0	18.87	6.0	3.49
27.1	20.74	6.5	3.84
29.2	22.61	7.0	4.19
31.3	24.48	7.5	4.53
33.3	26.35	8.0	4.88
35.4	28.22	8.5	5.22
37.5	30.09	9.0	5.57
39.6	31.96	9.5	5.92
41.7	33.83	10.0	6.26
43.8	35.70	10.5	6.61
45.8	37.57	11.0	6.96
47.9	39.44	11.5	7.30
50.0	41.31	12.0	7.65
52.1	43.18	12.5	7.99
54.2	45.80	13.0	8.48
56.3	47.71	13.5	8.83
58.3	49.62	14.0	9.19
60.4	51.53	14.5	9.54
62.5	53.44	15.0	9.89
64.6	55.34	15.5	10.25
66.7	57.25	16.0	10.60

68.8	59.16	16.5	10.95
70.8	61.07	17.0	11.31
72.9	63.74	17.5	11.80
75.0	66.41	18.0	12.30
77.1	69.08	18.5	12.79
79.2	71.76	19.0	13.29
81.3	74.43	19.5	13.78
83.3	77.10	20.0	14.27
85.4	79.77	20.5	14.77
87.5	82.44	21.0	15.26
89.6	85.11	21.5	15.76
91.7	87.79	22.0	16.25
93.8	90.46	22.5	16.75
95.8	93.13	23.0	17.24
97.9	95.80	23.5	17.74
100.0	100.00	24.0	18.51

Temporal Distribution of Rainfall	
Time (hrs.)	Accumulated RF (cm)
	PMP
0	0.00
2	1.06
4	2.13
6	3.49
8	4.88
10	6.26
12	7.65
14	9.19
16	10.60
18	12.30
20	14.27
22	16.25
24	18.51

Table I: 10 Calculated Accumulated Rainfall

Rainfall Increment	
Time (hrs.)	Accumulated RF (cm)
	PMP
0	0.00
2	1.06
4	1.07
6	1.36
8	1.39
10	1.39
12	1.39
14	1.54
16	1.41
18	1.70
20	1.98
22	1.98
24	2.26

Table I: 11 Calculated Excess Rainfall

Excess Rainfall	
Time (hrs.)	Accumulated RF (cm)
	PMP
0	0.00
2	0.46
4	0.47
6	0.76
8	0.79
10	0.79
12	0.79
14	0.94
16	0.81
18	1.10
20	1.38
22	1.38
24	1.66

Table I: 12 Excessed Rainfall in Reverse Critical Sequencing

Put excess Rainfall in Reverse Critical Sequencing (cm)"	
Time (hrs.)	Accumulated RF (cm)
	PMP
0	0.00
2	0.47
4	0.79
6	0.79
8	0.81
10	1.38
12	1.66
14	1.38
16	1.10
18	0.94
20	0.79
22	0.76
24	0.46

Table I: 13 Convolution of PMP Over UH

UH		Flow Hydrograph preparation (cm)							
Time(hrs)	Discharge(cms)	RF0	RF2	RF4	RF6	RF8	RF10	RF12	RF14
		0.00	0.47	0.79	0.79	0.81	1.38	1.66	1.38
0	0.000	0.00							
2	24.392	0.00	0.00						
4	75.615	0.00	11.56	0.00					
6	160.986	0.00	35.85	19.15	0.00				
8	226.844	0.00	76.33	59.36	19.15	0.00			
10	243.918	0.00	107.55	126.38	59.36	19.84	0.00		
12	226.844	0.00	115.65	178.08	126.38	61.50	33.63	0.00	
14	190.256	0.00	107.55	191.49	178.08	130.93	104.25	40.52	0.00
16	136.594	0.00	90.20	178.08	191.49	184.50	221.94	125.62	33.63
18	95.128	0.00	64.76	149.36	178.08	198.38	312.74	267.45	104.25
20	68.297	0.00	45.10	107.23	149.36	184.50	336.28	376.86	221.94
22	50.491	0.00	32.38	74.68	107.23	154.74	312.74	405.22	312.74
24	35.856	0.00	23.94	53.62	74.68	111.09	262.29	376.86	336.28
26	26.099	0.00	17.00	39.64	53.62	77.37	188.31	316.07	312.74
28	18.782	0.00	12.37	28.15	39.64	55.55	131.15	226.92	262.29
30	13.415	0.00	8.90	20.49	28.15	41.07	94.16	158.04	188.31
32	9.757	0.00	6.36	14.74	20.49	29.16	69.61	113.46	131.15
34	7.074	0.00	4.63	10.53	14.74	21.23	49.43	83.88	94.16
36	6.098	0.00	3.35	7.66	10.53	15.28	35.98	59.57	69.61
38	3.659	0.00	2.89	5.55	7.66	10.91	25.89	43.36	49.43
40	2.683	0.00	1.73	4.79	5.55	7.94	18.50	31.20	35.98
42	2.389	0.00	1.27	2.87	4.79	5.75	13.45	22.29	25.89
44	2.389	0.00	1.13	2.11	2.87	4.96	9.75	16.21	18.50
46	0.974	0.00	1.13	1.88	2.11	2.98	8.41	11.75	13.45
48	0.974	0.00	0.46	1.88	1.88	2.18	5.04	10.13	9.75
50	0.000	0.00	0.46	0.76	1.88	1.94	3.70	6.08	8.41
52	2.389	0.00	0.00	0.76	0.76	1.94	3.29	4.46	5.04
54	2.389	0.00	1.13	0.00	0.76	0.79	3.29	3.97	3.70
56	2.389	0.00	1.13	1.88	0.00	0.79	1.34	3.97	3.29
58	0.974	0.00	1.13	1.88	1.88	0.00	1.34	1.62	3.29
60	0.974	0.00	0.46	1.88	1.88	1.94	0.00	1.62	1.34
62	0.974	0.00	0.46	0.76	1.88	1.94	3.29	0.00	1.34
Maximum flood									

RF16	RF18	RF20	RF22	RF24	Cumulated DRH	Base flow (cms)	Flood Hydrograph ordinates (cms)
1.10	0.94	0.79	0.76	0.46			
					0.00	10.00	10.00
					0.00	10.00	10.00
					11.56	10.00	21.56
					55.00	10.00	65.00
					154.84	10.00	164.84
					313.13	10.00	323.13
					515.24	10.00	525.24
					752.82	10.00	762.82
0.00					1025.46	10.00	1035.46
26.73	0.00				1301.75	10.00	1311.75
82.87	22.88	0.00			1527.02	10.00	1537.02
176.44	70.94	19.15	0.00		1666.25	10.00	1676.25
248.62	151.03	59.36	18.52	0.00	1716.28	10.00	1726.28
267.33	212.82	126.38	57.40	11.22	1679.89	10.00	1689.89
248.62	228.83	178.08	122.21	34.78	1568.60	10.00	1578.60
208.52	212.82	191.49	172.21	74.05	1398.19	10.00	1408.19
149.70	178.49	178.08	185.17	104.34	1180.76	10.00	1190.76
104.26	128.15	149.36	172.21	112.20	944.77	10.00	954.77
74.85	89.25	107.23	144.43	104.34	722.08	10.00	732.08
55.34	64.07	74.68	103.69	87.52	531.00	10.00	541.00
39.30	47.37	53.62	72.22	62.83	381.02	10.00	391.02
28.60	33.64	39.64	51.85	43.76	273.80	10.00	283.80
20.58	24.49	28.15	38.33	31.42	198.49	10.00	208.49
14.70	17.62	20.49	27.22	23.23	144.96	10.00	154.96
10.69	12.59	14.74	19.81	16.49	105.65	10.00	115.65
7.75	9.15	10.53	14.26	12.01	76.93	10.00	86.93
6.68	6.64	7.66	10.18	8.64	56.07	10.00	66.07
4.01	5.72	5.55	7.41	6.17	42.51	10.00	52.51
2.94	3.43	4.79	5.37	4.49	33.42	10.00	43.42
2.62	2.52	2.87	4.63	3.25	27.03	10.00	37.03
2.62	2.24	2.11	2.78	2.80	21.67	10.00	31.67
1.07	2.24	1.88	2.04	1.68	18.59	10.00	28.59
							1726.28

Table I: 14 Watershed characteristics of Jema left side tributary in the downstream

Basin Name	Description	Jema left side tributary
Catchment characteristics		Dimension
A,Area (km2)	Delineated (GIS)	80.1
L,Length (km)	Measured (GIS)	17.9
Lc,Centroid distance (km)	Measured (GIS)	9
Ct ,coefficient		1.62
Cp		0.6
Tp (hr)	C1Ct (LLc)0.3	3.31
tr (hr)	Tp/5.5	5.58
tR		1.01
Tpr	Tp-(tr-tR)/4 (hr)	2
qp	2.78Cp/Tpr (cumec/sq.km)	5.83
Qp	qpxA(m3/sec)	0.286

Table I: 15 Watershed characteristics of Jema left side tributary in the downstream

Basin Name	Description	Jema right side tributary
Catchment characteristics		Dimension
A,Area (km2)	Delineated (GIS)	65.3
L,Length (km)	Measured (GIS)	11.6
Lc,Centroid distance (km)	Measured (GIS)	5.5
Ct ,coefficient		1.62
Cp		0.6
Tp (hr)	C1Ct (LLc)0.3	3.12
tr (hr)	Tp/5.5	4.21
tR		0.77
Tpr	Tp-(tr-tR)/4 (hr)	2
qp	2.78Cp/Tpr (cumec/sq.km)	4.52
Qp	qpxA(m3/sec)	0.369

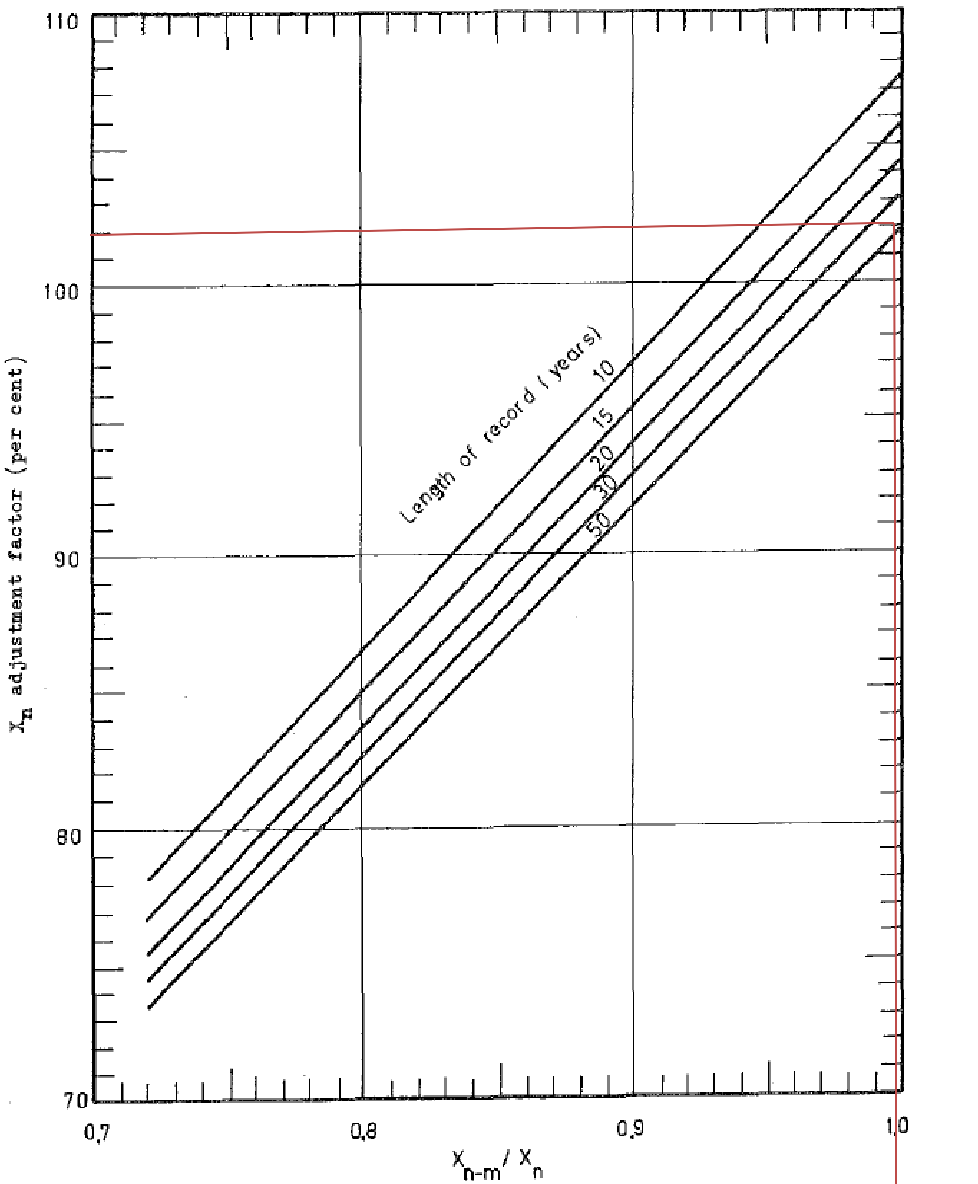

Figure 4.2-Adjustment of mean of annual series for maximum observed rainfall [Hershfield,1961b]

Figure I. 1 Adjustment of Mean for maximum. Observed event

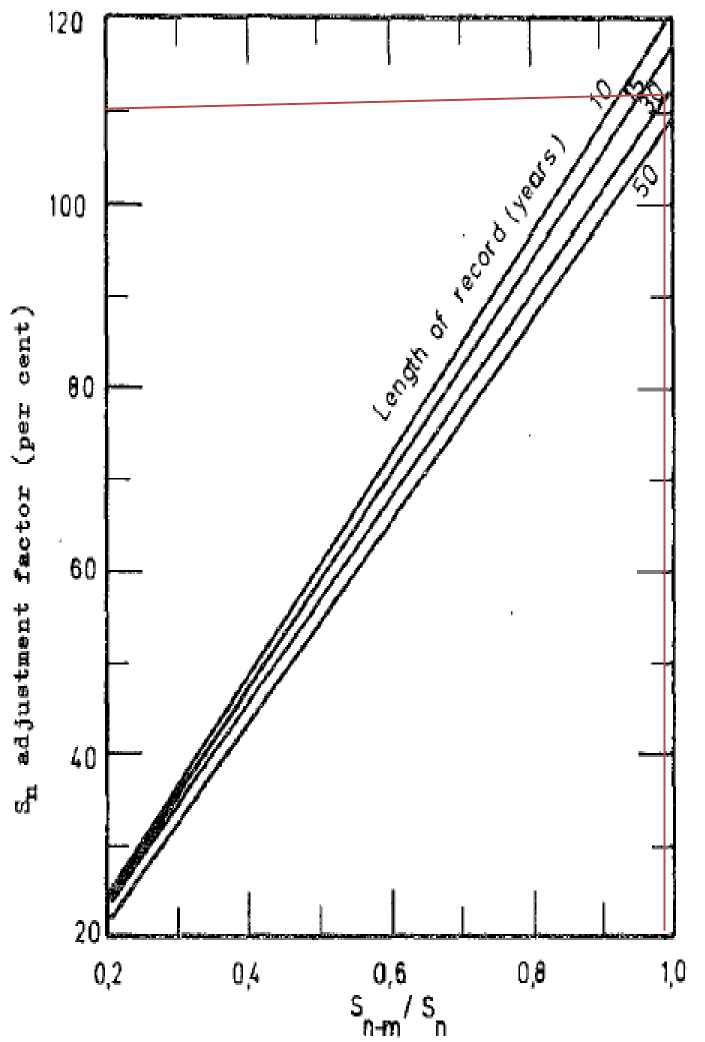

Figure 4.3-Adjustment of standard deviation of annual series for maximum observed rainfall [Hershfield,1961b]

Figure I. 2 Adjustment of Standard Deviation for maximum Observed Event

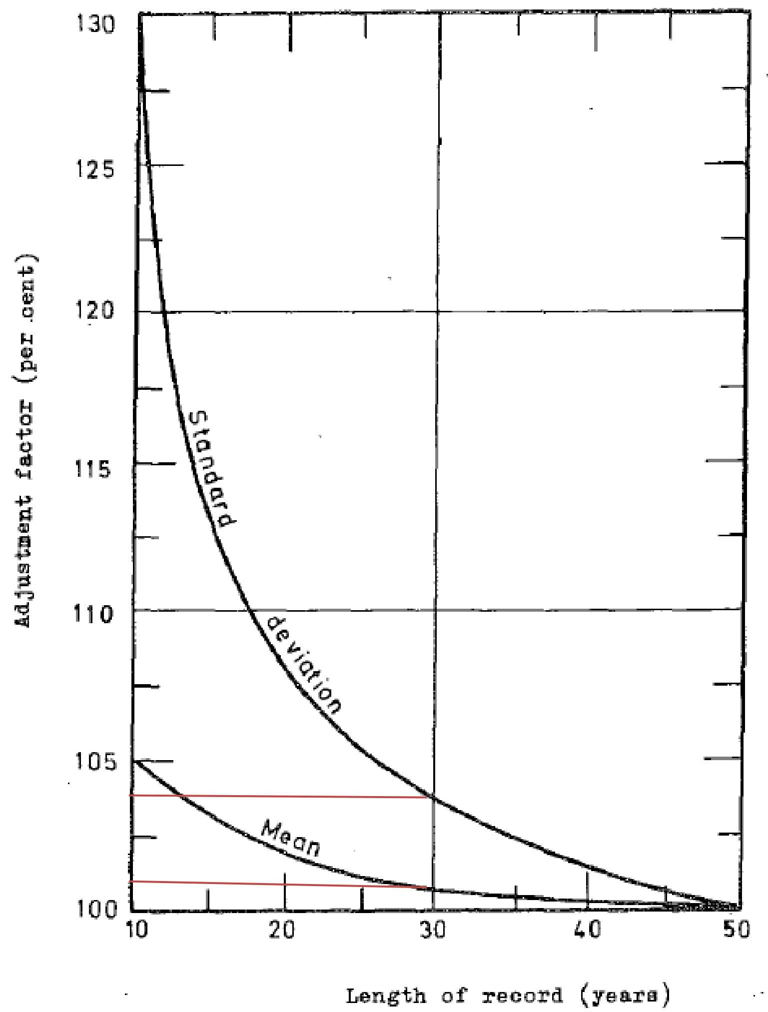

Figure 4.4-Adjustment of mean and standard deviation of annual series for length of record [Hershfield,1961b]

Figure I. 3 Adjustment of Mean and Standard Deviation for Sample Size

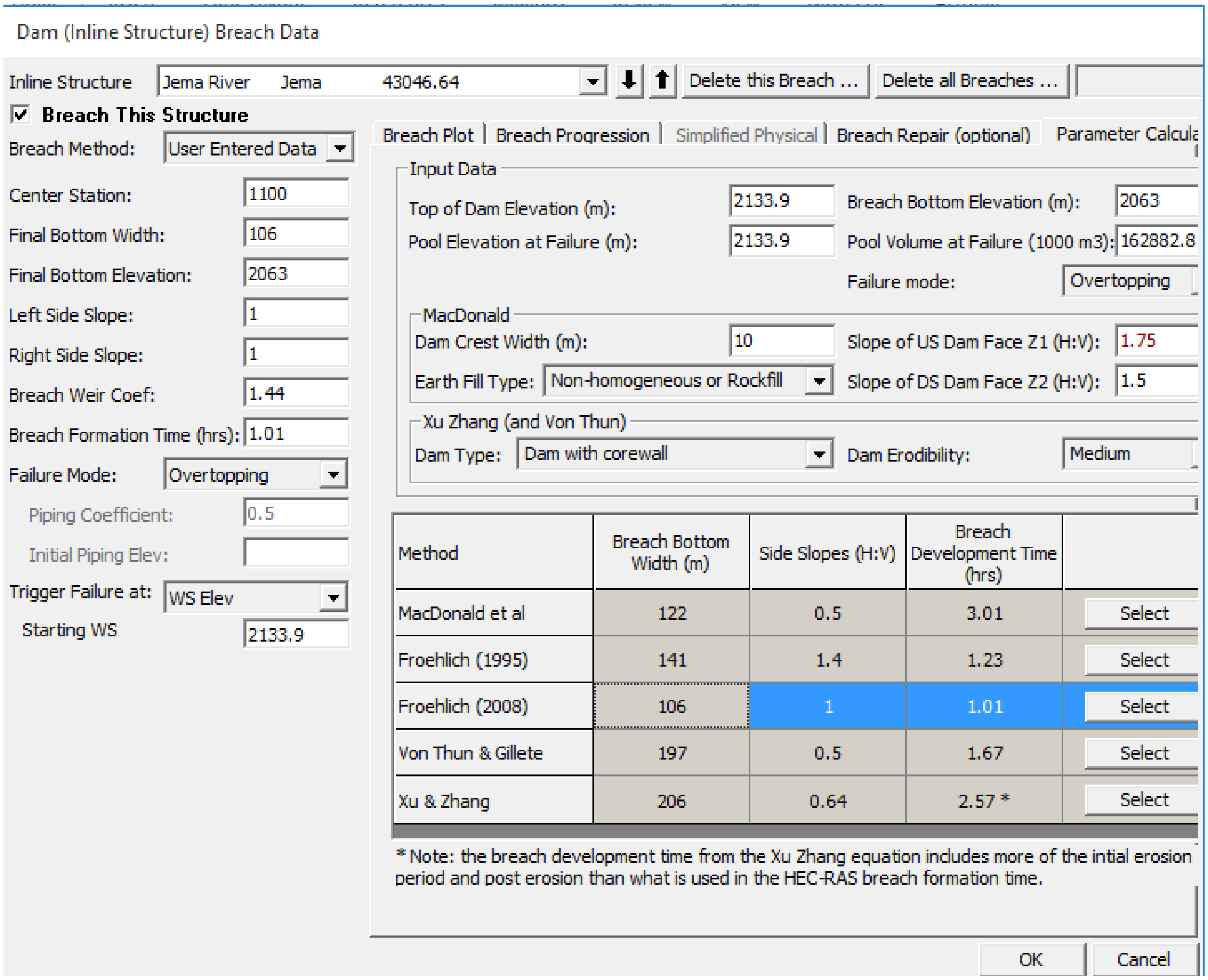

Figure I. 4 Jema Dam breach data for overtopping failure mode

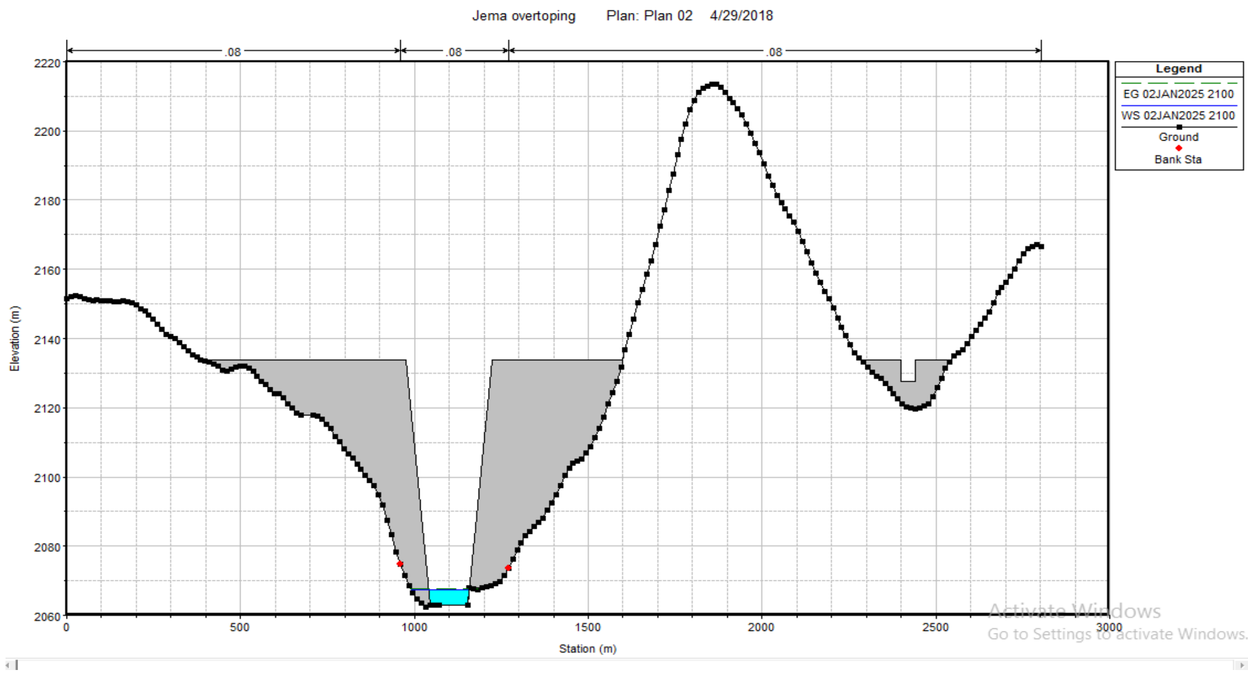

Figure I. 5 Jema dam geometry in HEC-RAS after Breach

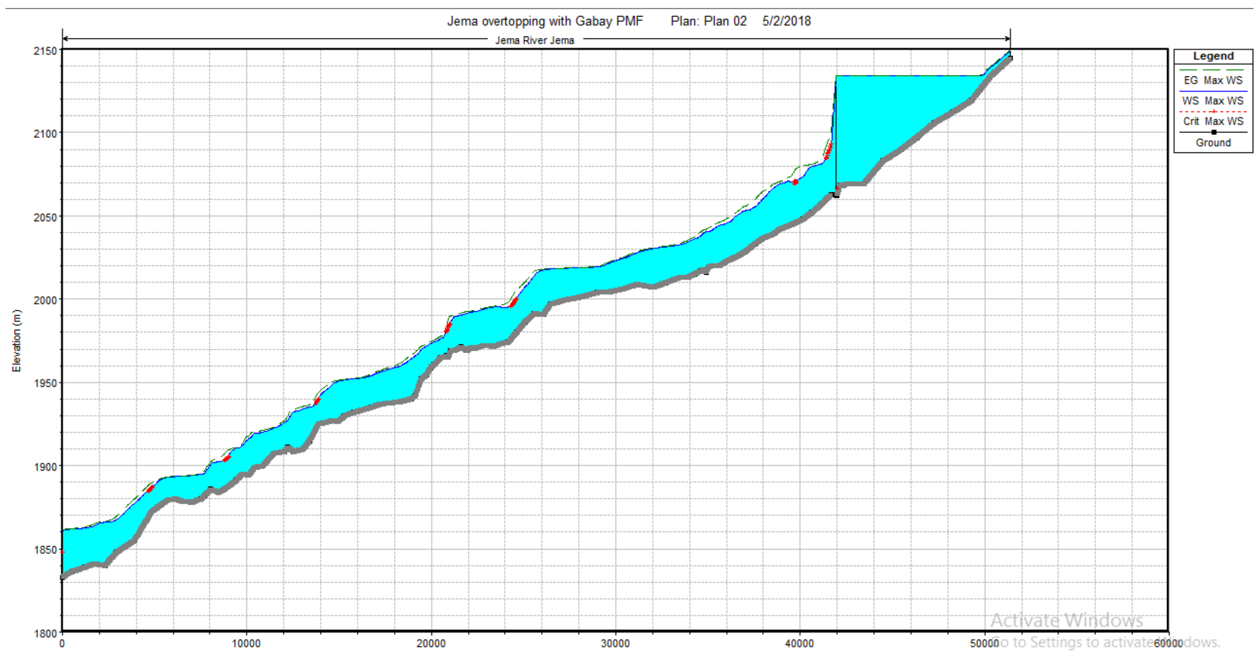

Figure I. 6 Jema water surface profile in HEC-RAS